

The Messenger



No. 190 | 2023

The 4MOST Community Surveys
First Results of Distributed Peer Review at ESO



ESO, the European Southern Observatory, is the foremost intergovernmental astronomy organisation in Europe. It is supported by 16 Member States: Austria, Belgium, the Czech Republic, Denmark, France, Finland, Germany, Ireland, Italy, the Netherlands, Poland, Portugal, Spain, Sweden, Switzerland and the United Kingdom, along with the host country of Chile and with Australia as a Strategic Partner. ESO's programme is focussed on the design, construction and operation of powerful ground-based observing facilities. ESO operates three observatories in Chile: at La Silla, at Paranal, site of the Very Large Telescope, and at Llano de Chajnantor. ESO is the European partner in the Atacama Large Millimeter/submillimeter Array (ALMA). Currently ESO is engaged in the construction of the Extremely Large Telescope.

The Messenger is published in electronic form twice per year. ESO produces and distributes a wide variety of media connected to its activities. For further information, contact the ESO Department of Communication at:

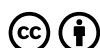
ESO Headquarters
Karl-Schwarzschild-Straße 2
85748 Garching bei München, Germany
Phone +498932006-0
information@eso.org

The Messenger
Editor: Mariya Lyubenova
Editorial assistant: Isolde Kreutle
Copy-editing: Peter Grimley
Graphics, Layout, Typesetting:
Lorenzo Benassi
Design, Production: Jutta Boxheimer
messenger.eso.org

Unless otherwise indicated, all images in The Messenger are courtesy of ESO, except authored contributions which are courtesy of the respective authors.

© ESO 2023
ISSN 0722-6691

The Messenger and all articles are published open access under a Creative Commons Attribution 4.0 International License.



Contents

Astronomical Science

Mainieri, V. et al. – The 4MOST Community Surveys	3
Toloza, O. et al. – The White Dwarf Binary Survey (WDB)	4
Sacco, G. G. et al. – The 4MOST Survey of Young Stars (4SYS)	7
Ibata, R. et al. – 4MOST Gaia RR Lyrae Survey (4GRounds)	10
Lucatello, S. et al. – Stellar Clusters in 4MOST	13
Pawlak, M. et al. – Spectroscopic Discovery of Binaries with Dormant Black Holes	17
Skúladóttir, Á. et al. – The 4MOST Survey of Dwarf Galaxies and their Stellar Streams (4DWARFS)	19
Iovino, A. et al. – Stellar Population Survey Using 4MOST (4MOST-StePS)	22
Duncan, K. et al. – Optical, Radio Continuum and HI Deep Spectroscopic Survey (ORCHIDSS)	25
Gruen, D. et al. – 4MOST Complete Calibration of the Colour-Redshift Relation (4C3R2)	28
Haines, C. et al. – CHANCES: A CHILEAN Cluster galaxy Evolution Survey	31
Bauer, F. E. et al. – Chilean AGN/Galaxy Extragalactic Survey (ChANGES)	34
Krogager, J.-K. et al. – The 4MOST–Gaia Purely Astrometric Quasar Survey (4G-PAQS)	38
Peroux, C. et al. – Transform our Understanding of the Baryon Cycle with High-Resolution Quasar Spectroscopy (ByCycle)	42
Taylor, E. N. et al. – The 4MOST Hemisphere Survey of the Nearby Universe (4HS)	46
Collett, E. T. et al. – The 4MOST Strong Lensing Spectroscopic Legacy Survey (4SLSLS)	49

Telescopes and Instrumentation

Martinez, P. et al. – SPEED — Get Ready for the (PCS) Rush Hour	55
De Rosa, R. J. et al. – Effects of the Hunga Tonga–Hunga Ha'apai Volcanic Eruption on Observations at Paranal Observatory	58

Astronomical News

Jerabkova, T. et al. – The First Results of Distributed Peer Review at ESO Show Promising Outcomes	63
Paladini, C. et al. – Report on the IAU Hands-on Workshop	67
Rivera G. C., Ginolfi M., Seidel J. V., Abdul-Masih M. – Fellows at ESO	70

Front Cover: Chile has hosted ESO's telescopes since the 1960s, in observatories based at La Silla, Paranal, and Chajnantor Plateau. Shown here is the Visible and Infrared Survey Telescope for Astronomy (VISTA), situated at Paranal Observatory. Perched atop a mountain adjacent to Cerro Paranal, the home of the flagship Very Large Telescope (VLT), VISTA is the largest telescope in the world designed to survey the sky in near-infrared light. Credit: ESO/B. Tafreshi (twanight.org)



The 4MOST Community Surveys

Vincenzo Mainieri¹
 Bruno Leibundgut¹
 Roelof S. de Jong²
 J. Miguel Mas-Hesse³
 Jochen Liske⁴
 Karin Lind⁵
 Jon Loveday⁶

¹ ESO

² Leibniz Institute for Astrophysics,
 Potsdam, Germany

³ Department of Astrophysics, Centre for
 Astrobiology (CSIC-INTA), Torrejón de
 Ardoz, Spain

⁴ Hamburg Observatory, University of
 Hamburg, Germany

⁵ Department of Physics and Astronomy,
 Uppsala University, Sweden

⁶ University of Sussex, Brighton, UK

The 4-metre Multi-Object Spectroscopic Telescope (4MOST) is a new high-multiplex, wide-field spectroscopic survey facility under construction for the four-metre-class Visible and Infrared Survey Telescope for Astronomy (VISTA) at Paranal. Its key specifications are: a large field of view of 4.2 square degrees and a

high multiplex capability, with 1624 fibres feeding two low-resolution spectrographs ($R = \lambda/\Delta\lambda \sim 6500$), and 812 fibres transferring light to the high-resolution spectrograph ($R \sim 20\,000$). It was decided from the start to use the instrument in a survey mode only. The 4MOST consortium prepared ten survey proposals (see the papers in issue 175 of *The Messenger*) spanning the whole sky accessible from Paranal and addressing many science goals. The surveys were presented at a dedicated workshop entitled *Preparing for 4MOST: A community workshop introducing ESO's next generation spectroscopy survey facility*, held in May 2019¹.

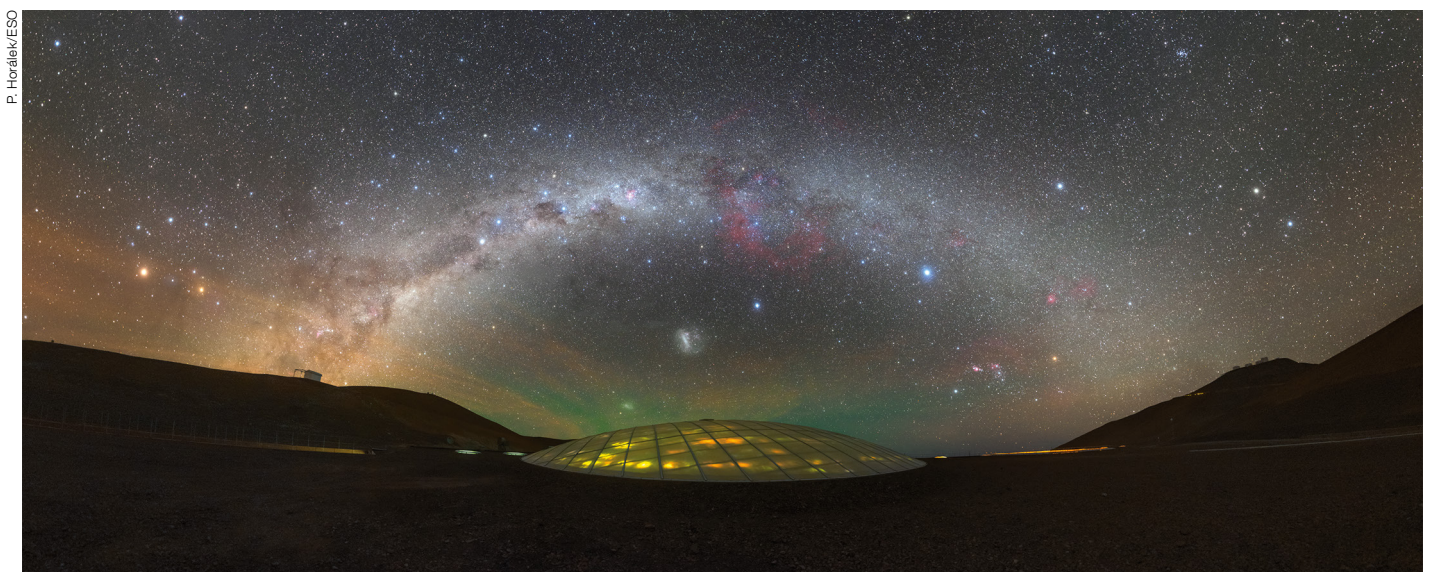
The 4MOST consortium will receive 70% of the available fibre-hours in the first five years of operation in return for building the facility and supporting ESO with its operation. The remaining 30% of the observing time in the first five years is available to conduct surveys led by the ESO Community. The selection of these Community Surveys went through the two-step process for ESO Public Surveys. A Call for Letters of Intent was issued in 2019. The submitted science cases were reviewed by the Public Survey Panel

(PSP) composed of scientific experts from the ESO Community. A subset of the proposing teams was invited to submit full proposals by December 2020, which were again evaluated by the PSP. Finally, considering the scientific merit of the proposals and the technical boundary conditions of 4MOST, the PSP recommended the implementation of 15 Community Surveys. The selection was endorsed by the Observing Programmes Committee at its meeting in November 2021.

The selected Community Surveys have now joined the ten Consortium Surveys to form the final 4MOST survey programme for the first five years of operation. This joint set of surveys covers a very wide range of Galactic and extragalactic science cases. This issue of the *Messenger* contains a detailed description of the selected Community Surveys, which complements the description of the Consortium Surveys in *Messenger* 175.

Links

¹ Preparing for 4MOST workshop:
<https://www.eso.org/sci/meetings/2019/4MOST.html>



Since construction of the ESO Residencia was completed in 2002, it has been a home from home for the astronomers, engineers and technicians working at ESO's Paranal Observatory in Chile. The sleek building sits 2400 metres above sea level in the

Mars-like Atacama Desert, just a few kilometres from Cerro Paranal — the mountain that hosts ESO's Very Large Telescope (VLT) and Visible and Infrared Survey Telescope for Astronomy (VISTA).

The White Dwarf Binary Survey (WDB)

Odette Toloza¹
 Alberto Rebassa-Mansergas²
 Roberto Raddi²
 Nicole Reindl³
 Boris Gaensicke⁴
 Nicola Gentile Fusillo⁵
 Simone Scaringi⁶
 Diogo Belloni¹
 Elme Breedt⁷
 Maria Camisassa²
 Tim Cunningham⁴
 Domitila de Martino⁸
 Alessandro Ederoclitte⁹
 Stephan Geier³
 Matthew Green¹⁰
 Keith Inight⁴
 Thomas Kupfer¹¹
 Jesús Maldonado¹²
 Tom Marsh⁴
 Anna Francesca Pala⁵
 Steven Parsons¹³
 Ingrid Pelisoli⁴
 Juanjuan Ren¹⁴
 Pablo Rodriguez-Gil¹⁵
 Snehalata Sahu⁴
 Linda Schmitdobreick¹⁶
 Matthias Schreiber¹
 Axel Schwöpe¹⁷
 Danny Steeghs⁴
 Paula Szkody¹⁸
 Silvia Toonen¹⁹
 Pier-Emmanuel Tremblay⁴
 Monica Zorotovic²⁰

¹⁷ Leibniz Institute for Astrophysics,
 Potsdam, Germany
¹⁸ University of Washington, USA
¹⁹ University of Amsterdam, the
 Netherlands
²⁰ University of Valparaíso, Chile

Binary systems containing one or two white dwarfs are important for studying stellar evolution and interactions under a wide range of astrophysical conditions. Thanks to the Gaia mission we have identified the first statistically significant and unbiased sample of ~ 170 000 white dwarf binary candidates. It comprises both systems that never interacted that are part of common proper motion pairs and systems that evolved through mass transfer episodes resulting in close white dwarf binaries. White dwarf binaries hold the potential to observationally constrain a wide variety of key ingredients that currently limit the validity of theoretical models.

Scientific context

Over 90 per cent of stars are born with masses $< 8\text{--}10 M_{\odot}$, with the certain fate of ending up as white dwarfs (WDs). Moreover, about half of the main sequence (MS) stars in the Milky way are found in binary systems. The binary separation determines the evolution of these systems. If the binary components are separated enough to avoid mass transfer episodes (≥ 10 au), they can evolve as single stars. In these binaries, the more massive star evolves first through the typical nuclear burning phases and ends its life as a WD (García-Berro, Ritossa & Iben, 1997). The orbital separations of the resulting detached WD+MS binaries widen with time as a result of modest velocity kicks caused by asymmetric mass loss of the WD progenitors (El-Badry & Rix, 2018). In these cases, the WDs can be used as reliable cosmo-chronometers to measure stellar ages, a difficult endeavour that is otherwise subject to substantial uncertainties (Soderblom, 2010). These wide WD+MS binaries are excellent probes of the evolution of age-related changes in activity, rotation, and metallicity of the MS companions. Conversely, for smaller initial separations (< 10 au), mass-transfer interactions ensue, which

lead to a common-envelope phase and to a dramatic shrinkage of the orbit (Ivanova et al., 2013). These close WD+MS binaries have orbital periods ranging from a few hours to several days and the companions sample a wide range of spectral types (A, F, G, K, M). Hence, they hold the potential to give rise to a wide range of important outcomes, for example type Ia supernovae (SN Ia), gravitational wave sources, and WD pulsars, or themselves being outcomes of fascinating phenomena, such as planetary nebulae. Indeed, binaries are overrepresented in the central star planetary nebula population (Jones & Boffin, 2017). In particular, the bipolar structures in planetary nebulae cannot be explained by single-star evolution. The WD binary survey aims to resolve a wide variety of important open problems which will ultimately help to understand the evolution of close and wide WD binaries.

Specific scientific goals

The 4MOST WD binary survey is divided into three sub-surveys, as outlined below, each aiming for different goals.

The compact white dwarf binary (CWDB) sub-survey. Within this sub-survey we aim to address important aspects of close WD evolution such as the mechanisms of angular momentum loss, the energy sources during the common-envelope phase, understanding the formation of magnetic WDs in close binaries, identifying the progenitors of AM CVn stars, and determining the dominant fate of close WD binaries. With 4MOST, the current samples of the distinct types of binaries will be significantly enlarged, without bias. The 4MOST spectra will provide the effective temperatures, surface gravities, radii, and masses that will allow the characterisation of the stellar components, while the orbital periods will be measured from the photometric data from Vera C. Rubin Observatory. These parameters will ultimately provide observational constraints to the evolutionary models.

The common proper motion pairs (CPMP) sub-survey. This sub-survey aims at using WDs as ‘clocks’ to provide additional observational input for improving our understanding of the chemical evolution of the Milky Way and

¹ Federico Santa Maria Technical University, Valparaíso, Chile
² Catalunya Polytechnic University, Barcelona, Spain
³ Potsdam University, Germany
⁴ University of Warwick, Coventry, UK
⁵ ESA
⁶ Durham University, UK
⁷ University of Cambridge, UK
⁸ INAF–Capodimonte Astronomical Observatory, Naples, Italy
⁹ University of Sao Paulo Institute of Astronomy, Brazil
¹⁰ Tel Aviv University, Israel
¹¹ University of California at Santa Barbara, USA
¹² INAF–Palermo Astronomical Observatory, Italy
¹³ University of Sheffield, UK
¹⁴ National Astronomical Observatories – Chaoyang Beijing, China
¹⁵ Canary Islands Institute of Astrophysics, Tenerife, Spain
¹⁶ ESO

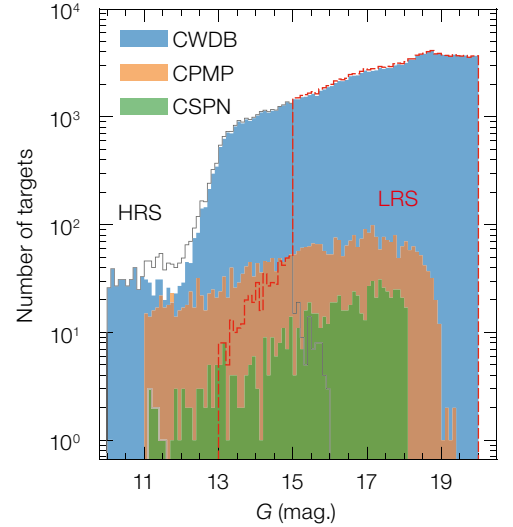
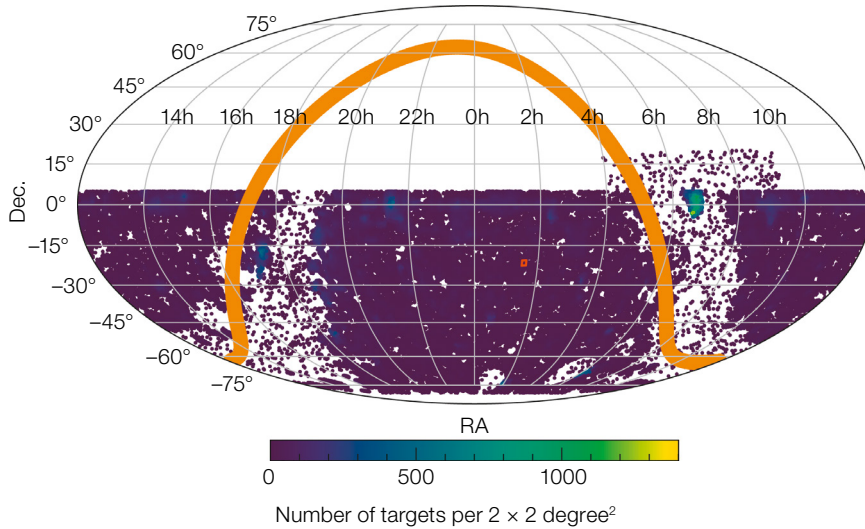


Figure 1. Left: Density map of the target catalogue in equatorial coordinates; the orange line represents the galactic plane which lacks GALEX data. We aim to follow up at least 41% and 95% of our catalogues that will be observed with the low-resolution and high-resolution spectrographs, respectively.

Right: Distribution of the white dwarf binary targets for each sub-survey as a function of Gaia G magnitude (0.1 mag. bin). Black and red lines show the total number of targets requested to be observed with the high-resolution (HRS) and low-resolution (LRS) spectrograph, respectively.

number of targets per sub-survey for each spectral resolution is shown in Table 1.

Target selection and survey area

The compact WD binary catalogue uses the WD ultraviolet excess as a selection tool (Parsons et al., 2016). Therefore, GALEX DR6/7 is crossmatched with Gaia DR3 (Gentile-Fusillo et al. in preparation), where a simple linear cut in the GALEX/FUV-Gaia/ G colour-magnitude diagram selects most binaries below the main sequence. QSOs are the major source of contaminants, and most of them can be identified by their lack of proper motion. Moreover, we performed a quality filter based on an astrometric excess noise cut and finally we excluded the Magellanic Clouds because of bad astrometry in crowded regions. A sample of CPMPs containing WDs is identified by cross-matching the Gentile-Fusillo et al. (2021)

the mechanisms that govern its dynamical heating. Moreover, by using the WD ages we will analyse the dependency between age, magnetic activity, and rotation in MS stars. Finally, these wide binaries will allow the mass-radius relation for WDs to be tested. To achieve these goals, we will use the 4MOST spectra of the MS companions of these WDs to measure their composition, effective temperatures, surface gravities and radial velocities and to detect signs of magnetic activity.

The central star of planetary nebulae (CSPN) sub-survey. This sub-survey aims to unravel the nature of the central star by searching for signs of binarity (for

example, emission lines from an irradiated companion, double-lined He II lines, and central stars with F/G/K companions displaying emission of H α and Ca H&K lines). The 4MOST spectra will also allow us to check the spectral type of each central star and to perform a spectral analysis to derive their effective temperatures, surface gravities, masses, radii, and luminosities. The same analysis can be applied to the binary component if spectral lines are visible, for example for double-lined and double-degenerate systems.

Each sub-survey contains targets that will be observed with the low-resolution and high-resolution spectrographs. The total

	SSC: S/N for LRS	SSC: S/N for HRS	Number of targets for LRS	Number of targets for HRS	FoM for LRS	FoM for HRS
CWDB	CaT or H α or BLUE > 13 (up to 100 for $G = 15$)	H α > 150 (up to 500 for $G = 10$)	142 000	22 000	40%	95%
CPMP	H α_{wing} > 30	BLUE $_{narrow}$ > 30	2800	900	70%	90%
CSPN	H α_{wing} > 50	H α_{wing} > 250	670	70	71%	95%

Table 1. Relevant parameters for the three sub-surveys, compact white dwarf binary (CWDB), common proper motion pairs (CPMP), and central star planetary nebulae (CSPN), for the low-resolution spectra (LRS) and high-resolution spectra (HRS). The spectral success criteria (SSC) correspond to the

median of the S/N per Ångstrom calculated assuming grey conditions. The S/N is calculated within a wavelength range as follows: BLUE = MEDIAN(S/N 4000–4500 Å); BLUE $_{narrow}$ = MEDIAN(S/N 4000–4300 Å); H α = MEDIAN(S/N 6512–6612 Å); H α_{wing} = MEDIAN(S/N 6400–6500 Å);

CaT = MEDIAN(S/N 8350–8850 Å). The low-resolution spectra of the CWDB sub-survey utilise the combination of three wavelength ranges. The fraction of observed targets is calculated for a figure of merit (FoM) of 0.5 for each sub-survey.

catalogue with non-degenerate stars in the Gaia DR3, by adopting the selection and quality cuts defined by El Badry et al. (2021), Rebassa-Mansergas et al. (2021), and Raddi et al. (2022). The contaminants from open clusters (Cantat-Gaudin et al., 2018) are removed. Finally, the targets for the central star of planetary nebulae catalogue were selected from the catalogues of González-Santamaría et al. (2021) and Chornay & Walton (2021). In general, the combined catalogue comprises approximately 170 000 targets with brightnesses within $G = 10$ and $G = 20$ mag. (see right panel of Figure 1). Most of the targets of all the sub-surveys cover the 4MOST footprint, i.e., sky declinations $-80 < \text{dec} < +5$ (see left panel in Figure 1).

Spectral success criterion and figure of merit

In general, we utilise the signal to noise ratio (S/N) per Ångström as the spectral success criterion. The spectral energy distribution of close WD binaries results in a composite spectrum, which is either dominated by the WD or by the non-degenerate companion, depending on the temperature and radius of either of them. In the case of interacting binaries, line

emission and continuous emission from an accretion disc can also be observed. The minimum requirement is an optical spectrum with sufficient S/N to recognise key features for classification of the type of binary (for example, cataclysmic variables, AM CVn stars, double WDs, post-common-envelope binaries or symbiotic binaries). The spectra with higher S/N will be fitted with templates to determine stellar parameters. In the common proper motion sub-survey, we aim to determine precise abundances, radial velocities, and stellar parameters, as well as an estimate of stellar activity by measuring the flux of chromospheric emission lines such as H α and Ca H&K or the IR triplet. Thus, we will acquire high-resolution and low-resolution spectroscopy for the F/G/K stars and M-type companions, respectively. Finally, for the central star planetary nebula sub-survey it is important to avoid any (strong) nebular or photospheric lines when calculating the S/N such that spectral analysis can be performed. Our S/N requirements for each sub-survey are listed in Table 1.

The figure of merit (FoM) measures the scientific success of each sub-survey. Table 1 shows the fraction of targets that need to be observed for each of the

sub-surveys such that the success rate is 0.5, which is the minimum requirement such that the scientific goals can be achieved. However, the overall success of the WDB survey is dictated by a combined FoM, which is defined as the weighted average of all the individual FoMs.

Acknowledgements

ARM acknowledges support from the Spanish MINECO grant PID2020-117252GB-I00 and from the AGAUR grant SGR-386/2021. OT was supported by FONDECYT project 321038.

References

- Cantat-Gaudin, T. et al. 2018, *A&A*, 618, A93
 Chornay, N. & Walton, N. A. 2021, *A&A*, 656, A110
 El-Badry, K. & Rix, H.-W. 2018, *MNRAS*, 480, 4884
 El-Badry, K., Rix, H.-W. & Heintz, T. M. 2021, *MNRAS*, 506, 2269
 García-Berro, E., Ritossa, C. & Iben, I. 1997, *ApJ*, 485, 765
 Gentile-Fusillo, N. P. et al. 2021, *MNRAS*, 508, 3877
 González-Santamaría, I. et al. 2021, *A&A*, 656, A51
 Ivanova, N. et al. 2013, *A&ARv*, 21, 59
 Jones, D. & Boffin, H. M. J. 2017, *Nature Astronomy*, 1, 0117
 Parsons, S. G. et al. 2016, *MNRAS*, 463, 2125
 Raddi, R. et al. 2022, *A&A*, 658, A22
 Rebassa-Mansergas, A. et al. 2021, *MNRAS*, 506, 5201
 Soderblom, D. R. 2010, *ARA&A*, 48, 581

Y. Beletsky (LCO)/ESO



Located deep in the Chilean Atacama Desert, far from the light pollution associated with human activity, ESO's Paranal Observatory enjoys some of the darkest skies on Earth. Paradoxically, it is this extreme darkness that allows the sky to light up in

technicolour in this image. The striking radiant light visible in the sky here is a phenomenon called airglow, which is created as atoms and molecules in the atmosphere combine and emit radiation.

The 4MOST Survey of Young Stars (4SYS)

G. Germano Sacco¹
 Rob Jeffries²
 Alex Binks³
 Laura Magrini¹
 Francesco Damiani⁴
 Nicholas Wright²
 Loredana Prisinzano⁴
 Eleonora Zari⁵
 Christian Schneider⁶
 Giacomo Beccari⁷
 George Weaver²
 Valentina D'Orazi^{8,9}
 Katia Biazzo¹⁰
 Brunella Nisini¹⁰
 Simone Antonucci¹⁰
 Elena Franciosini¹
 Jan Røhrade⁶
 Beate Stelzer¹¹
 Emilio J. Alfaro¹²
 João Alves¹³
 Amelia Bayo^{7,14}
 Henri Boffin⁷
 Rosaria Bonito⁴
 Hervé Bouy¹⁵
 Anthony Brown¹⁶
 Edvige Corbelli¹
 Scilla Degl'Innocenti¹⁷
 Davide Fedele¹
 Jonathan Gagné^{18,19}
 Philip Galli²⁰
 Josefa Großschedl¹³
 Tereza Jerabkova⁷
 Joel Kastner²¹
 Daisuke Kawata²²
 Stefan Meingast¹³
 Núria Miret-Roig¹³
 Estelle Moraux²³
 Javier Olivares²⁴
 Richard J. Parker²⁵
 Pier Giorgio Prada Moroni¹⁷
 Timo Prusti²⁶
 Sofia Randich¹
 Veronica Roccatagliata¹
 Lorenzo Spina⁹

¹ INAF–Arcetri Astronomical Observatory, Florence, Italy

² Astrophysics Group, Keele University, UK

³ MIT Kavli Institute for Astrophysics and Space Research, Massachusetts Institute of Technology, Cambridge, MA, USA

⁴ INAF–Palermo Astronomical Observatory, Italy

⁵ Max Planck Institute for Astronomy, Heidelberg, Germany

⁶ Hamburg Observatory, University of Hamburg, Germany

⁷ ESO

⁸ Department of Physics, Tor Vergata University of Rome, Italy

⁹ Department of Physics and Astronomy, University of Padua, Italy

¹⁰ INAF–Rome Astronomical Observatory, Italy

¹¹ Institute for Astronomy & Astrophysics, Eberhard Karls University, Tübingen, Germany

¹² Andalucía Institute of Astrophysics (CSIC), Granada, Spain

¹³ Department of Astrophysics, University of Vienna, Austria

¹⁴ Institute of Physics and Astronomy, Faculty of Science, University of Valparaíso, Chile

¹⁵ Bordeaux Astrophysics Laboratory, University of Bordeaux, CNRS, Pessac, France

¹⁶ Leiden Observatory, Leiden University, the Netherlands

¹⁷ Enrico Fermi Department of Physics, University of Pisa, Italy

¹⁸ Rio Tinto Alcan Planetarium, Space For Life, Montreal, Canada

¹⁹ Institute for Research on Exoplanets, Department of Physics, University of Montreal, Canada

²⁰ Centre for Theoretical Astrophysics, São Paulo City University, Brazil

²¹ School of Physics and Astronomy, Rochester Institute of Technology, NY, USA

²² Mullard Space Science Laboratory, University College London, UK

²³ University of Grenoble Alpes, CNRS, IPAG, France

²⁴ National University for Distance Learning, Spain

²⁵ Department of Physics and Astronomy, University of Sheffield, UK

²⁶ European Space Agency, European Space Research and Technology Centre (ESTEC), the Netherlands

Most nearby young stars (with ages < 100 Myr) in the Galactic disc no longer reside in their dense, clustered birth-places; they are found all around us. The 4MOST Survey of Young Stars will identify a representative sample of about 10⁵ young, low-mass stars within 500 pc of the Sun and will measure their chemistry, 3D kinematics and ages in order to: trace the spatial and dynamical evolution of star-forming structures; quantify the star formation rate and chemical

inhomogeneity in the local disc; vastly expand the number of identified young stars for exoplanetary studies; and provide huge coeval samples to improve young stellar evolutionary models.

Scientific context

The distribution of young stars in space, kinematics, chemistry and age is of key importance in understanding the processes that drive star formation, the origins of the Galactic field population, and the early evolution of stars, their discs and planetary systems. Most stars (including the Sun; Adams, 2010) are born in clusters of various sizes in the Galactic disc, but most of these clusters disperse into the field on timescales of 10–100 Myr (Lada & Lada, 2003; Krumholz, McKee & Bland-Hawthorn, 2019). Most young stars (with ages < 100 Myr) in the Galactic disc, including the nearest ones, are not located in compact clusters and star-forming regions (for example, Zari et al., 2018); they are instead part of the field population. Decades of work have revealed a population of about 1500 young stars within 100 pc of the Sun, a volume that contains no significant clusters (for example, Gagné & Faherty, 2018). Many, but not all, are part of kinematically coherent, roughly coeval ‘moving groups’ of large spatial extent (for example, Torres et al., 2006). Members of this widespread population trace the recent star formation history in the Milky Way disc on a variety of scales and, because of their proximity, have become exemplars for studying early stellar evolution and planet formation; yet their origins and birth environments remain obscure. While the census of young stars within 100 pc is substantially complete, much less is known about their chemistry or the spatial and kinematic properties of young stars outside this radius, beyond the biased perspective offered by high-density compact clusters and star-forming regions. The Gaia astrometry satellite¹ is revolutionising this field (for example, Kounkel & Covey, 2019; Cantat-Gaudin, 2022; Alfaro et al., 2022; Prisinzano et al., 2022). Precise astrometry and homogeneous photometry can place stars in Hertzsprung–Russell diagrams and provide 2D tangential motions. Early studies are providing tantalising glimpses of rich

complexity in the young stellar population — mapping the extended populations of dissolving clusters and associations (Meingast, Alves & Rottensteiner, 2021; Gagné et al., 2021) and finding evidence for kinematically coherent streams arranged in grand filamentary structures on scales > 100 pc (for example, Beccari, Boffin & Jerabkova, 2020).

These studies will continue to be limited in several important ways, however, until they are supplemented by spectroscopy of large and representative samples: (1) samples selected by astrometry and photometry alone are heavily contaminated with older stars; (2) astrometry yields only 2D kinematics, but 3D velocities are important for determining the history and subsequent evolution of star-forming structures; and (3) information about detailed chemistry and chemical (in) homogeneity is absent, but such information is a key diagnostic of the star formation history, of mixing in the interstellar medium and of the co-spatial or coeval nature of star forming events.

Specific scientific goals

Age, chemistry and kinematics are stellar properties that cannot easily be determined. Spectroscopy is essential to identify young stars, eliminate contamination, improve age estimates, and obtain precise chemical abundances and radial velocities (RVs). The 4MOST Survey of Young Stars (4SYS) is aimed at observing a representative sample of $\sim 100\,000$ candidate young low-mass stars within 500 pc of the Sun, increasing the volume probed and numbers of identified young field stars by two orders of magnitude. 4SYS will cover the spatial scales of grand structures recently found in the disc (Zari et al., 2018), and closely match the sensitivity of the TESS satellites and the eROSITA instrument on board the SRG satellite (Ricker et al., 2015; Predehl et al., 2021). The 4SYS targets are split between two samples. The first, mostly observed at low resolution, is selected from absolute colour–magnitude diagrams based on Gaia data² and targets pre-main-sequence stars cooler than spectral type K7 with ages < 40 Myr, with a focus on accurate demographics and kinematics, and using stars at the peak of the stellar

initial mass function ($0.2\text{--}0.5 M_{\odot}$). The second, observed at high resolution with a focus on precise kinematics and chemistry, selects brighter G7–K7 stars on or above the zero-age main sequence (ZAMS), and filters them using TESS rotation periods and X-ray activity from eROSITA, in order to remove binaries and giants and to include stars younger than 100 Myr. The overarching objective of 4SYS is to construct a catalogue of 3D positions (to 1 pc precision), 3D space motions (to $< 1 \text{ km s}^{-1}$ precision), stellar parameters (effective temperature, surface gravity and global metallicity), stellar properties (mass and age), diagnostics of magnetic activity and accretion from the disc for the majority of objects, detailed chemistry and projected rotation rates for the high-resolution sample. These will be combined with data from TESS, eROSITA and the WISE satellite. Uniquely, 4SYS is not biased towards dense, clustered young populations; instead, it will capture the dominant dispersed young population that can be used to address key science areas: (1) to understand the origins of the

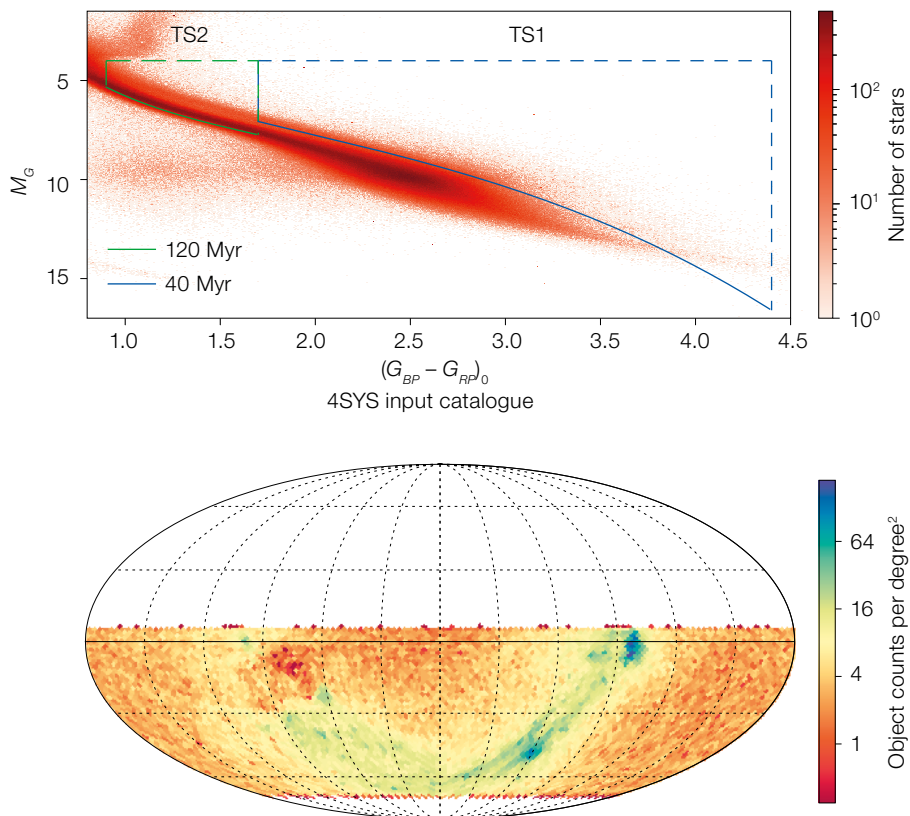


Figure 1. Top panel: two-dimensional histogram representing the absolute G magnitude M_G vs. dereddened $(Bp-Rp)_0$ colour of all the stars in the Gaia DR3 catalogue with parallax > 2 milliarcseconds, $-70 < \text{Declination} < 5$ deg, which meet the standard quality criteria for photometry discussed in Riello et al. (2021). The blue and green continuous lines represent the empirical isochrones used to identify stars younger than 40 and 120 Myr, respectively. The areas included within the isochrones and the dashed blue and green lines are used to select stars for the target sample 1 and to pre-select stars for the target sample 2, respectively. Bottom panel: sky distribution of the targets in the 4SYS input catalogue.

young field population and initial conditions for star formation by mapping the spatial and kinematic evolution of star-forming structures on scales of 1–500 pc over the last 100 Myr and determining the extent of chemical homogeneity in the local young population; (2) to expand the number, and determine the properties and origins, of nearby young stars, which serve as the prime targets for studies of protoplanetary discs and young exoplanetary systems with current and next generation facilities (for example JWST and ESO’s Extremely Large Telescope);

and (3) to identify the missing ingredients in current models of early stellar evolution, provide the large samples necessary to improve the next generation of evolutionary models, and empirically determine how stars and their discs, accretion, rotation and magnetic activity, change during the epoch of planet formation.

Target selection and survey area

4SYS aims to select a large sample of young stars, with excellent astrometry and photometry, that has a well understood selection function and which is as complete as possible, but with low contamination by older objects. We include stars with ages from 1 to 100 Myr, covering the main epochs over which star-forming clusters evolve dynamically and disperse, planetary systems form, discs disperse, and PMS stars with $0.5 < M/M_{\odot} < 1.0$ reach the ZAMS. To obtain the necessary resolution in time and space, the volume needs to be sampled by many stars. We therefore choose low-mass targets with spectral types G7–M6 that are at or near the peak of the initial mass function. These targets have the added benefit that their youth can initially be guessed from their position in absolute colour-magnitude diagrams (CMDs) and then unambiguously confirmed with spectroscopy using the lithium absorption feature at 670.8 nm and/or gravity- and activity-sensitive diagnostics. We started from a parent catalogue including all the stars in the Gaia DR3 catalogue (Gaia Collaboration, 2022) with parallax > 2 milliarcseconds ($d < 500$ pc) and $-70 < \text{Declination} < 5$ deg, which meet standard quality criteria for photometry discussed in Riello et al. (2021). Stars later than K7 and younger than 40 Myr are well separated from the main sequence, in particular they are high enough above the ZAMS to avoid heavy contamination by unresolved binaries. Older/hotter stars are closer to the ZAMS and we cannot rely on CMDs alone to select these targets. We therefore defined two main samples.

Target sample 1 comprises stars in the magnitude range $10 < G < 18.5$ mag that lie in two CMDs (M_G vs. $(G-Rp)_0$ and M_G vs. $(Bp-Rp)_0$) above a 40 Myr isochrone, derived empirically using data from star

clusters, with absolute G magnitude $M_G > 4$, and in a colour range that corresponds to the spectral types K7–M6 (see blue dashed lines in the upper panel of Figure 1). It includes a total of about 100 000 stars. Closer stars in the magnitude range $10 < G < 15.5$ will be observed at high resolution, while fainter stars with $15.5 < G < 18.5$ will be observed with the low-resolution mode. Contaminants will include some unresolved binaries/triples with high mass ratios, subgiants, and unusually reddened old field stars. 4MOST spectroscopic measurements of gravity, Li and chromospheric activity are needed to exclude these.

Target sample 2 comprises stars in the magnitude range $10 < G < 15.5$ mag, that in the same CMDs used for target sample 1 lie above the 120 Myr isochrone (and are hence likely to be aged 100 Myr or younger), with absolute G magnitude $M_G > 4$ (to exclude turn-off stars and subgiants) and within a colour range that corresponds to spectral types G7–K7 (see green box in the upper panel of Figure 1). Since young stars are fast rotators and strong X-ray emitters, we are using rotation periods derived from the TESS light curves and X-ray fluxes from eROSITA to complement the CMD-based selection, which otherwise will be affected by severe contamination. To home in on young stars, we select those stars that have either rotation periods smaller than the upper envelope of the rotation-colour relation defined by members of the 120 Myr Pleiades cluster and/or a ratio between the flux in X-rays and in the G band higher than a threshold defined using stars in young clusters that have been detected with eROSITA. In total, target sample 2 is composed of about 40 000 stars that will be observed at high resolution.

The bottom panel of Figure 1 shows the distribution on the sky of the stars in the input catalogue of 4SYS. As expected, the stars are located mostly in the galactic disc with lower densities in the area of high extinction. The areas with the highest densities correspond to well-known star-forming complexes or young associations like Orion (RA = 83.8 deg, Dec. = -5.44 deg) and Vela OB2 (RA = 122.4 deg, Dec. = -47.34 deg). When the survey is completed, more than 66% of the input catalogue will have been

observed. The level of completeness will be approximately homogeneous across the observed area and as a function of the stellar distance.

Acknowledgements

Funding for the TESS mission is provided by NASA's Science Mission directorate. This work presents results from the European Space Agency (ESA) space mission Gaia. Gaia data are being processed by the Gaia Data Processing and Analysis Consortium (DPAC). Funding for the DPAC is provided by national institutions, in particular the institutions participating in the Gaia MultiLateral Agreement (MLA).

References

- Adams, F. C. 2010, *ARA&A*, 48, 47
- Alfaro, E. J. et al. 2022, *ApJ*, 937, 114
- Beccari, G., Boffin H. & Jerabkova, T. 2020, *MNRAS*, 491, 2205
- Cantat-Gaudin, T. 2022, *Universe*, 8, 111
- Gagné, J. & Faherty, J. K. 2018, *ApJ*, 862, 138
- Gagné, J. et al. 2021, *ApJL*, 915, L29
- Gaia Collaboration et al. 2022, arXiv:2208.00211
- Kounkel, M. & Covey, K. 2019, *AJ*, 158, 122
- Krumholz, M. R., McKee, C. F. & Bland-Hawthorn, J. 2019, *ARA&A*, 57, 227
- Lada, C. J. & Lada, E. A. 2003, *ARA&A*, 41, 57
- Meingast, S., Alves, J. & Rottensteiner, A. 2021, *A&A*, 645, A84
- Predehl, P. et al. 2021, *A&A*, 647, A1
- Prisinzano L. et al. 2022, *A&A*, 664, A175
- Ricker, G. R. et al. 2015, *JATIS*, 1, 014003
- Riello, M. et al. 2021, *A&A*, 649, A3
- Torres, C. A. O. et al. 2006, *A&A*, 460, 695
- Zari, E. et al. 2018, *A&A*, 620, A172

Links

- ¹ Gaia mission website: <https://www.cosmos.esa.int/web/gaia>
- ² Gaia data archive: <https://gea.esac.esa.int/archive/>

4MOST Gaia RR Lyrae Survey (4GRoundS)

Rodrigo Ibata¹
 Giuseppina Battaglia²
 Michele Bellazzini³
 Gisella Clementini³
 Raphael Errani¹
 Benoit Famaey¹
 Alessia Garofalo³
 Vanessa Hill⁴
 Nicolas Martin¹
 Alessio Mucciarelli³
 Giacomo Monari¹
 Lorenzo Posti¹
 Ása Skúladóttir⁵
 Antonio Sollima³
 Arnaud Siebert¹
 Guillaume Thomas²
 Khyati Malhan⁶
 Jonathan Freundlich¹
 Anke Arentsen⁷
 Zhen Yuan¹

¹ Strasbourg Astronomical Observatory, CNRS, University of Strasbourg, France

² Canary Islands Institute of Astrophysics, Tenerife, Spain

³ INAF–Bologna Astrophysics and Space Science Observatory, Italy

⁴ Lagrange Laboratory, Côte d’Azur Observatory, Côte d’Azur University, Nice, France

⁵ Department of Physics and Astronomy, University of Florence, Italy

⁶ Max Planck Institute for Astronomy, Heidelberg, Germany

⁷ Institute of Astronomy, University of Cambridge, UK

The 4GRoundS survey will measure the radial velocities and metallicities of southern RR Lyrae stars in Gaia Data Release 3. These stars have excellent photometric distances, allowing the exquisite Gaia proper motions to be converted into physically useful transverse velocities. Armed with the missing radial velocity, 4GRoundS will provide the community with a dataset that will enable studies of the orbital structure of the halo and outer disc, and allow realistic modelling of these components. It will also enable the identification of coherent dynamically cold streams. Together these analyses will map the mass of the Milky Way out to 100 kpc and test models of the dark sector.

Scientific context

One of the main motivations for building the 4MOST spectrograph was to be able to undertake ground-breaking studies in Galactic archaeology, by using the kinematics and chemistry of the sub-populations of the Milky Way and its satellites as a means to test cosmology. The flurry of results emerging from analyses of Gaia data testifies to the great promise of this subject. Although Gaia has surveyed the astrometric sky to $G = 21$ mag, it is nevertheless highly limited in its ability to measure radial velocities (which will probably not probe beyond $G = 16$ – 16.5 mag even in the end-of-mission catalogue). Hence there is enormous scientific potential in complementing Gaia with radial velocities and spectroscopy from dedicated ground-based instruments. The 4MOST and WEAVE¹ instruments are in part a response to this clear need expressed by the astronomical community. The scientific goal of this endeavour is to flesh out the origins story of our Milky Way, explaining how it attained its present structure, and to attempt to verify whether its present phase-space configuration is consistent with the Lambda Cold Dark Matter (Λ CDM) cosmological framework that has been developed from the study of large-scale structure. But how can these goals be achieved observationally?

The required key observables are distance and velocity. It is natural to consider employing intrinsically bright stars that have stable atmospheres and narrow absorption lines, such as cool giants. Such stars will be among the most distant tracers that one can use to probe the Galaxy and its environment, and the resulting radial velocity measurements will be the most accurate. This consideration is almost certainly valid out to distances of approximately 10 kpc, where Gaia will provide good-accuracy ($\sim 10\%$) parallaxes to individual stars. For such stars the excellent Gaia proper motions can be converted to physically meaningful transverse velocities given the Gaia parallaxes. However, the Milky Way extends over a much larger volume, and indeed the region that is most dominated by dark matter (and is hence probably the most interesting for cosmology) lies in the outer halo, well beyond Gaia’s ~ 10 kpc parallax horizon. The solution to this

conundrum is for 4MOST to target stars for which alternative distance measurements are possible. The obvious options for tracer populations are Red Giant Branch (RGB) stars, Blue Horizontal Branch (BHB) stars and RR Lyrae stars.

RGB stars

As mentioned above, these yield excellent radial velocities, and their metallicities can be measured easily from spectra with low signal-to-noise (S/N). By assuming an age, the measured spectroscopic [Fe/H] allows one to place the star on a model isochrone and so estimate the star’s distance given a measured photometric colour. However, the resulting distance uncertainties are large ($\sim 26\%$; Thomas et al., 2019), especially for metal-poor stars for which the RGB is nearly vertical in the colour-magnitude diagram. Furthermore, nearby dwarfs will contaminate the sample, which may be problematic at the faint end (which is a particularly interesting regime, since it probes RGBs at large distances) where Gaia parallaxes are uncertain and 4MOST spectra will have low S/N.

BHB stars

These Galactic tracers are also bright and have the desirable property of possessing a high contrast over other sources in the colour range that they cover. They can therefore be selected from photometry alone. Their hot atmospheres make it harder to measure accurate radial velocities, as absorption lines are much broader than in RGB stars. However, the main drawback of these tracers is that they cannot be easily differentiated from the intrinsically fainter blue straggler stars without good spectra. Furthermore, there is considerable spread in the absolute magnitude of BHB stars (Deason, Belokurov & Evans, 2011).

RR Lyrae stars

These variable stars possess several properties that make them essential tracers of the outer halo. First, they are easily identifiable from their photometric variability, including in the third Gaia data release (DR3) which has yielded an

extremely clean all-sky sample (Clementini et al., 2022). Second, they are the best standard candles for old stellar populations, and are very well calibrated. Third, the RR Lyrae population exhibits a wide range of $[\text{Fe}/\text{H}]$ (from above solar to at least as metal poor as -2.9 dex; Hansen et al., 2011), so they are a relatively unbiased tracer of ancient accretions. The main disadvantage of these stars is that their pulsations lead them to vary considerably in magnitude and in radial velocity, with amplitudes in the range from about $20\text{--}30\text{ km s}^{-1}$ up to about 80 km s^{-1} (depending on the pulsation mode). Part of this effect can, however, be corrected by modelling the velocity modulation with template velocity curves (Sesar, 2012) if the pulsation phase is known.

Specific scientific goals

The above considerations are the motivation for the 4MOST Gaia RR Lyrae Survey (4GRRS), a community survey designed to measure the radial velocities and metallicities of as many RR Lyrae variables as possible over the southern sky. The input target list is the full Gaia DR3 sample (avoiding the Magellanic Clouds) which has state-of-the-art astrometric solutions, photometry and full variability characterisation. Subsequent photometry and astrometry from the Legacy Survey of Space and Time (LSST) will complement the Gaia DR3 RR Lyrae sample, providing identification and type classification, distances, completeness and contamination information to the RR Lyrae population down to about 25.7 mag. We believe that the purity of this Gaia DR3 RR Lyrae sample, together with the excellent distance measurements, will enable several legacy studies of the dynamical properties of the stellar populations in the outer halo and distant disc using 4MOST. Given that the typical absolute magnitude of RR Lyrae is $M_G = 0.64$ mag. at $[\text{Fe}/\text{H}] = -1.5$ dex (Muraveva et al., 2018), the limiting magnitude of the Gaia RR Lyrae catalogue of $G = 20.7$ means that we reach a distance horizon of 100 kpc. The scientific applications of this dataset are extremely rich, as the sample will provide a unique six-dimensional view of the outer regions of the Milky Way. While we foresee numerous studies that will be undertaken with the survey data, here we

briefly outline some particularly exciting sub-projects.

Dynamical mass modelling of the outer Galaxy

Supplied with radial velocities and distances, it will be possible to constrain the mass profile of the outer Galaxy, correcting for the measured orbital anisotropy as a function of radius, extending the analysis of Wegg, Gerhard & Bieth (2019). Such approaches based on the Jeans equation or relying on distribution function models (for example, Posti & Helmi, 2019), make the basic assumption that the Galaxy is an equilibrium structure. It will be fascinating to explore how the flattening of the dark matter distribution continues at large distance, and in particular whether the spherical halo shape deduced to ~ 20 kpc persists further out. Such behaviour is expected in some theories of gravity where the baryons source gravity (for example, MOND).

Stellar streams in the outer Galaxy

Gaia has identified many stellar streams in the inner Galaxy (Ibata et al., 2021). These structures are also very promising as probes of the acceleration field, and have the added advantage that they do not require the halo to be in equilibrium. By identifying even as few as three RR Lyrae with 4MOST that form a coherent grouping in action space, it will be possible to search around such candidate structures for other stars observed by 4MOST (for example as part of Consortium Survey 1) or for Gaia stars with similar stellar populations (or in deeper surveys such as LSST) to confirm the detection. The 4MOST and Gaia kinematics would yield the orbital properties of the streams. The comparison of the acceleration field measured with streams and that measured with the halo field population promises to reveal the extent to which the halo is out of equilibrium.

Search for low-mass satellites

In similar fashion, very small groupings of as few as two RR Lyrae stars with the same 4MOST radial velocity (and Gaia

astrometry) may reveal the locations of the least luminous satellite galaxies (confirmable with LSST), probing the lowest mass limits of galaxy formation (for example, Sesar et al., 2014; Stringer et al., 2021; Petersen & Penarrubia, 2021). According to LCDM, these dwarf galaxies are the building blocks of the Milky Way and are expected to host an old and metal-poor stellar population. Although the intrinsic frequency of RR Lyrae is relatively small for an old and metal-poor stellar population, the contamination from any hypothetical smooth component sharply decreases with Galactocentric distance, so that overdensities of a few ($\sim 10\text{ degree}^{-2}$) RR Lyrae are statistically significant. Also in this case, candidate dwarf galaxies can be verified with LSST or with dedicated photometric follow up.

Global halo kinematic asymmetry due to the arrival of the Large Magellanic Cloud

Recent models of the evolution of the Local Group suggest that the Large Magellanic Cloud (LMC) formed within an extremely massive halo, which is now just arriving into the Milky Way for the first time. The LMC's mass is large enough to produce a substantial asymmetry in the Milky Way's stellar halo (Garavito-Camargo et al., 2019), which should be detectable given tracers with good distance estimates. This study requires a differential measurement between the northern and southern hemispheres, which is possible as WEAVE will also target Gaia-selected RR Lyrae.

Distant disc

With their low contamination and excellent distances, the RR Lyrae will be wonderful probes of the dynamics of the far side of the (thick) disc, allowing us to study the global response of the disc to the arrival of the LMC and the repeated collisions with the Sagittarius dwarf (Laporte et al., 2018). Iorio & Belokurov (2021) have shown that there appear to be RR Lyrae with dynamical properties consistent with being thin-disc stars. These will be very useful for tracing the early build-up of the thin disc, in particular with the additional metallicity information.

Bulge/inner halo

The RR Lyrae in the inner few kpc of the Milky Way are an extremely old stellar population (13.41 ± 0.54 Gyr; Savino et al., 2020). They form a bulge spheroid, the nature of which is still unclear — it might be a small classical bulge, the result of a puffed up disc, or it could be the inner region of the halo (or a combination of these). Using the largest sample of RR Lyrae with radial velocities in the inner Galaxy to date (2768 stars), Kunder et al. (2020) find some evidence for different spatial and kinematic populations of RR Lyrae in the inner Galaxy. With a sample of inner-Galaxy RR Lyrae that is more than an order of magnitude larger than currently available ($\sim 50\,000$ in the bulge region), 4GRoundS will be able to accurately disentangle the halo and spheroidal bulge for the oldest populations in the inner galaxy, constraining the early formation of the Milky Way. This will provide a complementary perspective to that of 4MOST Consortium Survey 3.

Spatial variations in kinematic coherence through the halo

Λ CDM posits that all galaxies are constituted of a myriad of dark sub-halos. There is the hope of detecting these invisible sub-halos via their heating effect on star streams. Here we propose an alternative means to detect these dark matter substructures. Our simulations

show that dark sub-halos with masses of $10^9 M_{\odot}$ cause large convergent velocity flows of $\sim 15 \text{ km s}^{-1}$ in the stellar halo on scales out to ~ 2 kpc. To detect this signal, it is necessary to have good distance measurements, in order to pick out the populations at the distance of interest (and so suppress contamination from stars at different distances). Again, the excellent RR Lyrae distances are essential, and their 4MOST radial velocities, together with Gaia proper motions, will provide the velocity signal of interest. With this, we aim to construct a three-dimensional map of the velocity coherence (its local convergence and divergence) throughout the halo, and compare this result to numerical simulations in Λ CDM and with other prescriptions for gravity/dark matter. This will allow 4GRoundS to quantify the degree of lumpiness of the halo in the full 6D phase space. We will make use of robust estimators like, for example, the two-point correlation function calculated in this extended space and compare them with the same quantities measured in cosmological simulations and in smooth models of the halo to probe the validity of the currently favoured cosmological paradigm.

Target selection and survey area

The 4GRoundS input catalogue is simply the full Gaia DR3 sample of 271 779 RR Lyrae (Clementini et al., 2022), without any apparent magnitude

cut, from which we aim to select targets as uniformly as possible over the full sky accessible to 4MOST. Assuming approximately 50% completeness in targeting, up to 100 000 RR Lyrae stars may be observed.

Acknowledgements

R. E., B. F., R. I., N. M., G. M., L. P. and A. S. acknowledge funding from the European Research Council (ERC) under the European Unions Horizon 2020 research and innovation programme (grant agreement No. 834148).

References

- Clementini, G. et al. 2022, arXiv:2206.06278
 Deason, A., Belokurov, V. & Evans, N. W. 2011, MNRAS, 416, 2903
 Garavito-Camargo, N. et al. 2019, ApJ, 884, 51
 Hansen, C. J. et al. 2011, A&A, 527, A65
 Ibata, R. et al. 2021, ApJ, 914, 123
 Iorio, G. & Belokurov, V. 2021, MNRAS, 502, 5686
 Kunder, A. et al. 2020, AJ, 159, 270
 Laporte, C. F. P. et al. 2018, MNRAS, 481, 286
 Muraveva, T. et al. 2018, MNRAS, 481, 1195
 Petersen, M. S. & Peñarrubia, J. 2021, Nature Astronomy, 5, 251
 Posti, L. & Helmi, A. 2019, A&A, 621, A56
 Savino, A. et al. 2020, A&A, 641, 96
 Sesar, B. 2012, AJ, 144, 114
 Sesar, B. et al. 2014, ApJ, 793, 135
 Stringer, K. M. et al. 2021, ApJ, 911, 109
 Thomas, G. F. et al. 2019, ApJ, 886, 10
 Wegg, C., Gerhard, O. & Bieth, M. 2019, MNRAS, 485, 3296

Links

- ¹ WEAVE instrument overview: <https://www.ing.iac.es/astronomy/instruments/weave/weaveinst.html>



This picture shows a new view of NGC 3603 (left) and NGC 3576 (right), two stunning nebulae imaged with ESO's Visible and Infrared Survey Telescope for Astronomy (VISTA). This infrared image peers through the dust in these nebulae, revealing details hidden in optical images.

Stellar Clusters in 4MOST

Sara Lucatello^{1,2}
 Angela Bragaglia³
 Antonella Vallenari¹
 Tristan Cantat-Gaudin⁴
 Pete Kuzma⁵
 Mario G. Guarcello⁶
 Lorenzo Spina⁷
 David Aguado⁸
 Ricardo Carrera¹
 Alfred Castro-Ginard⁹
 Francesco Damiani⁶
 Valentina D'Orazi^{1,10}
 Loredana Prisinzano⁶
 Elena Valenti¹¹
 Emilio Alfaro¹²
 Lola Balaguer-Nuñez^{13,14,15}
 Eduardo Balbinot^{9,16}
 David Barrado¹⁷
 Holger Baumgardt¹⁸
 Michele Bellazzini³
 Rosaria Bonito⁶
 Diego Bossini¹⁹
 Giovanni Carraro⁷
 Eugenio Carretta³
 Giovanni Catanzaro²⁰
 Laia Casamiquela²¹
 Santi Cassisi²²
 Emanuele Dalessandro³
 Gayandhi M. De Silva²³
 Annette Ferguson⁵
 Francesco R. Ferraro^{24,3}
 Antonio Frasca²⁰
 Phillip Galli²⁵
 Mark Gieles^{13,26}
 Felipe Gran²⁷
 Raffaele Gratton¹
 Michael Hilker¹¹
 Rob Jeffries²⁸
 Carme Jordi^{13,14,15}
 Anreas J. Korn²⁹
 Barbara Lanzoni^{24,3}
 Søren Larsen³⁰
 John Lattanzio³¹
 Maria Lugaro³²
 Michela Mapelli^{7,1}
 Davide Massari³
 Andrea Miglio^{24,3}
 Nuria Miret-Roig³³
 Yazan Momany¹
 Alessio Mucciarelli^{24,3}
 Javier Olivares³⁴
 Mario Pasquato^{7,35}
 Veronica Roccatagliata³⁶
 Maurizio Salaris³⁷
 Ricardo Schiavon³⁷
 Rodolfo Smiljanic³⁸
 Antonio Sollima³
 Gražina Tautvaišienė³⁹

Anna Lisa Varri⁵
 Nicholas Wright²⁸

- 1 INAF–Padua Astronomical Observatory, Italy
- 2 Institute for Advanced Studies, Technical University of Munich, Germany
- 3 INAF–Bologna Astrophysics and Space Science Observatory, Italy
- 4 Max Planck Institute for Astronomy, Heidelberg, Germany
- 5 University of Edinburgh, UK
- 6 INAF–Palermo Astronomical Observatory, Italy
- 7 Department of Physics and Astronomy, University of Padua, Italy
- 8 Canary Islands Institute of Astrophysics, Tenerife, Spain
- 9 Leiden Observatory, Leiden University, the Netherlands
- 10 Tor Vergata University of Rome, Italy
- 11 ESO
- 12 Spanish National Research Council, Granada, Spain
- 13 Institute of Cosmos Sciences, University of Barcelona, Spain
- 14 Department of Quantum Physics and Astronomy, University of Barcelona, Spain
- 15 Catalunya Institute of Space Studies, Barcelona, Spain
- 16 University of Groningen, the Netherlands
- 17 Centre for Astrobiology (CSIC-INTA), Torrejón de Ardoz, Spain
- 18 University of Queensland, Australia
- 19 Institute of Astrophysics and Space Science – Porto and Lisbon, Portugal
- 20 INAF–Catania Astronomical Observatory, Italy
- 21 GEPI – Paris Observatory, France
- 22 INAF–Abruzzo Astronomical Observatory, Italy
- 23 Macquarie University, Australia
- 24 Department of Physics and Astronomy, University of Bologna, Italy
- 25 São Paulo City University, Brazil
- 26 Catalan Institution for Research and Advanced Studies, Barcelona, Spain
- 27 Lagrange Laboratory, Côte d'Azur University, Nice, France
- 28 Keele University, UK
- 29 Uppsala University, Sweden
- 30 Radboud University, Nijmegen, the Netherlands

- 31 Monash University, Australia
- 32 Konkoly Observatory, CSFK ELKH, Budapest, Hungary
- 33 University of Vienna, Austria
- 34 National University for Distance Learning, Spain
- 35 University of Montreal, Canada
- 36 University of Pisa, Italy
- 37 Liverpool John Moores University, UK
- 38 Nicolaus Copernicus Astronomical Center, Warsaw, Poland
- 39 Vilnius University, Lithuania

The 4MOST Stellar Clusters Survey will target essentially all the Galactic globular and open clusters and star-forming regions accessible to 4MOST (about 120 globulars, 1800 open clusters and 80 star-forming regions). This will: shed light on how clusters form, evolve, dissolve, and populate the Milky Way; calibrate complex physics that affects stellar evolution, on which our ability to measure accurate ages ultimately rests; and evaluate the contribution of star clusters to the formation and evolution of the individual Galactic components with unparalleled statistics.

Scientific context

Traditionally, in the Milky Way (MW) stellar clusters are classified as open clusters (OCs) — low-mass (tens to thousands of stars) objects spanning the whole age range of the disc — and globular clusters (GCs, tens to hundreds of thousands of stars), which are massive, old, and associated with all major Galactic components. Younger GCs are present in the Local Group; for example, the Magellanic Clouds (MCs) host a population of GCs spanning all age ranges.

Clusters are expected to play an important role in the buildup of the Galactic components (see, for example, the cosmological E-MOSAIC simulations; Pfeffer et al., 2018 — and the association of clusters with the different merger events; for example, Massari, Koppelman & Helmi, 2019). The study of the formation, evolution and properties of clusters and their stellar populations is a fundamental ingredient to further our understanding of key issues related to the formation and

evolution of the MW and galaxies in general. These issues are set out below.

Cluster formation and disruption. Stars are thought to form in associations and clusters, the vast majority of which disperse because of dynamical and stellar evolutionary effects, such as supernova feedback. Studying clusters is therefore a key ingredient in the understanding of both star formation and how they populate the Galactic components through disruptive processes. It is currently still unclear whether OCs are the dominant source of stars in the disc, what the role of GCs in building up the Galactic bulge and halo is, and how the multiple populations, a phenomenon observed in virtually all Galactic GCs, form. Chemical information and radial velocities (RVs) for a large sample of clusters, along with Gaia astrometry and precise and independent ages from asteroseismology, will be necessary to make headways on these matters.

Stellar evolution. Our understanding of stellar populations ultimately relies on stellar models: stellar age dating is necessary to investigate galactic formation and evolution and processes such as mass loss and feedback are crucial ingredients in probing the chemical evolution of galaxies. However, the physics of many processes (accretion, convection, rotation, magnetic field, atomic diffusion, mixing, activity, stellar winds, mass loss) is uncertain and is treated in different, simplified ways in stellar models. The large, homogeneously selected and analysed samples of clusters at different ages and chemical compositions we will collect will contribute to considerable advancements in detailed stellar modeling, providing empirical isochrones and calibration of the associated physics.

MW formation. Clusters can be accurately dated and hence their study allows us to place further constraints on Galactic formation, evolution, and structure, complementing the study of the field population. The study of the chemo-dynamical properties of stellar clusters provides important information on the merger events involved in the assembly history of our galaxy. The age-metallicity relation of the MW disc, its radial, azimuthal and vertical metallicity distributions, and their evolution with time can be studied through OCs. The chemo-dynamic study of GCs can answer several major open questions about the Galactic halo and bulge, such as how they came into place, and can help probe the evolution of the MCs and the role of interactions with the MW.

Specific scientific goals

The 4MOST Stellar Clusters Survey aims to obtain spectra of the largest^a uniformly selected and analysed sample of Galactic clusters (and a few MC GCs) and very young clusters (VYCs) in star-forming regions (SFRs), covering metallicities from the $[\text{Fe}/\text{H}] = -2.5$ dex of GCs to super-solar OCs and ages from a few Myr to 13.5 Gyr. We will derive chemical characterisation, probe cluster internal kinematics up to the outskirts, examine dissolving (and dissolved) clusters, and probe the presence and nature of halos and tidal tails. Considering the expected performance of 4MOST, in the time allocated to our survey we expect to reach the following goals:

- Derive homogeneous, full chemo-dynamical characterisation (at 0.05 to 0.1 dex precision) for an unprecedented sample of ~ 120 GCs in the MW and

MCs, including a few newly identified bulge GCs. Elemental abundances probing all nucleosynthetic channels (Fe-peak, light, α , p- and n-capture) will be obtained from high-resolution (HR) spectra for a few tens of stars per cluster (the actual number depending on distance, reddening and concentration) for $\sim 5\,000$ stars with $G < 16.5$. As concerns the study of multiple populations, we will obtain precise abundances of O, Na, Mg and Al, i.e., of the elements defining the classical (anti-)correlations between light elements; this cannot be done using photometry, which traces essentially just N variations (Gratton et al., 2019). RVs, atmospheric parameters, and a few key elements (for example α 's) will be determined from low-resolution (LR) spectra for $\sim 35\,000$ stars with $16.5 < G < 20$ (several tens per cluster) in 140 GCs. This will be by far the largest sample of homogeneously derived detailed compositions and RVs for GC stars.

- Derive chemical abundances (at 0.05 to 0.1 dex precision) in all the nucleosynthetic channels for the vast majority of known OCs accessible to 4MOST. We expect to study $\sim 30\,000$ stars at HR ($G < 14.5$ for most clusters, with $G < 15.5$ in a few tens of clusters, selected to study details of the composition down to the main sequence) and $\sim 75\,000$ at LR ($14.5 < G < 19$). Again, this will be by far the largest sample of homogeneously derived chemical abundances and RVs for OCs.
- Derive the dynamics, study activity indicators and probe the composition of ~ 80 VYCs in nearby SFRs, where stars are still in the pre-main-sequence phase (PMS), and study low-mass PMS stars from already dissolved VYCs.

Subsurvey	Targets	Resolution	G Magnitude range	N expected successfully observed targets
GC HR	MW and MCs GCs	HRS	10–16.5	$\sim 5\,000$
GC LR	MW and MCs GCs	LRS	16.5–20	$\sim 35\,000$
OC HR	MW OCs	HRS	10–14.5 10–15.5 (in selected OCs)	$\sim 30\,000$
OC LR	MW OCs	LRS	14.5–19 15.5–19 (in selected OCs)	$\sim 75\,000$
VYC HR	MW VYCs	HRS	10–15	$\sim 4\,000$
VYC LR	MW VYCs	LRS	15–18	$\sim 10\,000$

Table 1. Magnitude ranges and expected successful target numbers for the six sub-surveys.

This unprecedented suite of homogeneous and precise elemental abundances and RVs, in combination with the datasets and results obtained by the 4MOST Galactic Consortium Surveys, Gaia data, stellar and dynamical models, will allow us to:

- determine key properties (such as composition, kinematics and, in GCs, the incidence of the multiple population phenomenon) across a wide range of cluster properties;
- characterise cluster velocity fields in three dimensions, investigate their dispersions and rotation as a function of radius, probing the outskirts of a large sample of clusters for the first time; quantify processes such as evaporation, tidal stripping, dynamical ejection, and possibly GC black hole retention;
- build a homogeneous database to be compared with the predictions of stellar evolutionary models. This, together with asteroseismology, will impact on a number of fundamental issues, such as the initial mass function slope and its universality, the timescale of star formation and star formation histories, improving field-star age determination. The calibration of the stellar models, when coupled with multi-band photometry, will also provide stellar fiducials (for the different sub-populations, in the case of GCs) for population synthesis models that will be used to interpret the properties of unresolved stellar populations in distant galaxies;
- derive constraints on PMS models, which currently have factors of two uncertainties in predictions of mass and age, thanks to key information (rotational velocity, atmospheric parameters, RVs, activity indicators) for representative samples of PMS stars (either still inside their native VYC or already lost). This will help establish the empirical timescales for star and planet formation, disc dispersion and the dynamical timescales for cluster dissolution;
- investigate the early evolution of clusters and their interplay with their environment; identify the stars lost from clusters (or belonging to dissolving/dissolved clusters) through chemodynamical tagging, thus constraining their role in the buildup of the Galactic components;

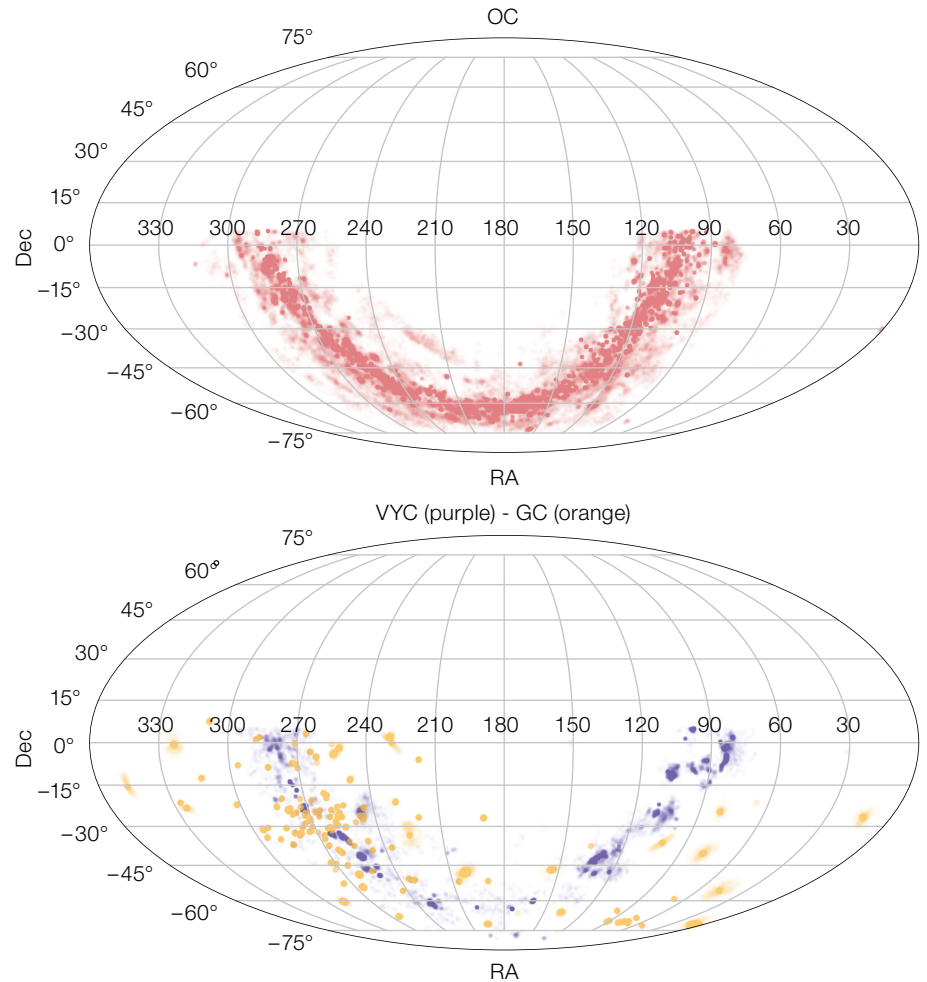


Figure 1. Spatial distribution of the targets in the input catalogue for our survey. OCs are shown in the upper panel, while GCs and VYCs are shown in the lower panel, in orange and purple respectively.

- precisely and homogeneously trace the chemical abundance distributions and gradients in the disc, along with their evolution, including the so far poorly quantified effect of radial mixing, which spreads chemical signatures associated with a star/cluster birthplace across a range of Galactocentric distances;
- define a uniform metallicity scale from $[Fe/H] = -2.5$ to $+0.5$ dex, for dwarfs and giants, for stars of a large range of age (i.e., mass), providing an ideal sample for both internal calibration of the Galactic 4MOST surveys and for cross-calibration with other large surveys.

Target selection

Each class of objects — GCs, OCs, and VYCs — has two dedicated sub-surveys, one in HR and one in LR, making a total of six sub-surveys.

Most of our targets are located in fields with considerable contamination (for example OCs and VYCs in the disc, GCs in the bulge and the MCs) and are characterised by high spatial densities (especially GCs). Careful attribution of membership is crucial, as it is to exclude stars with bright neighbours which can act as contaminants in the collected spectra.

The grand total of selected targets for the input catalog in HR is $\sim 100\,000$, while in LR it is close to $300\,000$, a number considerably larger than the number of stars we aim to observe. This strategy has been adopted to allow flexibility for the tiling and allocation algorithms, which operate on the combined catalogue for all the 4MOST

surveys, while ensuring the maximisation of the number of successfully observed targets. Estimates of the number of stars we will successfully observe, based on simulations performed within the 4MOST collaboration, are listed in Table 1, along with a few key facts about targets for the six sub-surveys. More details of the criteria for the different classes of objects in our sample are given below along with a visual representation of the input catalogue target distribution in Figure 1.

GCs. Our aim is to target all visible GCs, from centre to outskirts (comprising halos and tails). Targets are selected on Gaia DR3 astrometry (for example, Vasiliev & Baumgardt, 2021) and colour–magnitude diagrams. To allow for an easier allocation, LR targets were selected to be outside a few core radii from the centre of the clusters, where the bulk of HR stars are located. Magnitude ranges for LR and HR targets are reported in Table 1. All selected targets are of FGK spectral type; (almost) all HR targets are giants, while both giants and dwarfs are observed in LR mode.

OCs. We plan to observe all OCs accessible to 4MOST, sampling from the centre to the outskirts. The original selection based on Gaia DR2 membership (based, for example, on Cantat-Gaudin et al., 2020) was refined with Gaia DR3. Targets were selected to be of spectral type FGK (both giants and dwarfs), with $A_V < 2$. HR targets

were selected to have $10 < G < 14.5$, with the exception of a few tens of OCs, chosen to study the detailed chemistry down to the main sequence, where we selected targets with $10 < G < 15.5$. LR targets span from the faint end of the HR to $G = 19$. Stars bright enough for HR, but with Gaia DR3 broadening parameter $v_{\text{broad}} > 30 \text{ km s}^{-1}$, have been included in the LR rather than HR sample, as for objects of such rotational velocity HR does not allow to derive additional information over LR. The HR sample includes red-clump stars out to distances of ~ 10 kpc, and the LR sample includes faint K stars within 6 kpc.

VYCs. We selected targets from the catalogues of Dias et al. (2002, and revised online in 2015¹) and Cantat-Gaudin et al. (2020), including all VYCs in the 4MOST footprint for which a signal-to-noise ratio of about 40 \AA^{-1} could be reached in 1 hour of exposure time in HR. This includes objects within 2.5 kpc of the Sun, with reddening $E(B-V) < 2.5$, and ages 2–20 Myr. Magnitude ranges for LR and HR targets are reported in Table 1. Stars brighter than $G = 15$, but with Gaia DR3 broadening parameter $v_{\text{broad}} > 30 \text{ km s}^{-1}$, have been included in the LR rather than the HR sample.

Acknowledgements

This work was partially funded by the PRIN INAF 2019 grant ObFu 1.05.01.85.14 (Building up the halo:

chemo-dynamical tagging in the age of large surveys; PI S. Lucatello). This research has been partly funded by the Spanish MICIN/AEI/10.13039/501100011033 and by ERDF A way of making Europe by the European Union through grant RTI2018-095076-B-C21 and PID2021-122842OB-C21, and the Institute of Cosmos Sciences University of Barcelona (ICCUB, Unidad de Excelencia ‘Maria de Maeztu’) through grant CEX2019-000918-M.

References

- Cantat-Gaudin, T. et al. 2020, *A&A*, 640, A1
 Dias, W. S. et al. 2002, *A&A*, 389, 871
 Gaia Collaboration et al. 2023, *A&A*, in press, arXiv:2206.05534
 Gratton, R. et al. 2019, *A&A*Rev., 27, 8
 Massari, D., Koppelman, H. H. & Helmi, A. 2019, *A&A*, 630, L4
 Pfeffer, J. et al. 2018, *MNRAS*, 475, 4309
 Vasiliev, E. & Baumgardt, H. 2021, *MNRAS*, 505, 5978

Links

- ¹ Revised catalogue of optically visible open clusters (after Dias et al., 2002): <http://cdsarc.u-strasbg.fr/viz-bin/qcat?J/A+A/389/871>

Notes

- ^a Actually, the Gaia RVS instrument is producing the largest database of intermediate resolution spectra, providing RVs, metallicity and a set of chemical abundances for ten of millions stars; some of those belong to stellar clusters (see Gaia Collaboration et al., 2023, where the metallicity of about 600 open clusters has been derived from an average of three member stars). However, the magnitude limit for Gaia spectroscopy is bright (implying that GC stars are rarely observed), only a limited set of abundances is measured, and there is no controlled selection of cluster stars to be observed.



This infrared image shows the star-forming region 30 Doradus, also known as the Tarantula Nebula, highlighting its bright stars and light, pinkish clouds of hot gas. The image is a composite: it was captured by the HAWK-I instrument on ESO’s Very Large Telescope (VLT) and the Visible and Infrared Survey Telescope for Astronomy (VISTA).

Spectroscopic Discovery of Binaries with Dormant Black Holes

Michał Pawlak¹
Tsevi Mazeh²
Simchon Faigler²
Tomer Shenar³
Hugues Sana⁴
Dolev Bashi²

¹ Astronomical Observatory, Jagiellonian University, Kraków, Poland

² School of Physics and Astronomy, Tel Aviv University, Israel

³ Anton Pannekoek Institute for Astronomy, Amsterdam, the Netherlands

⁴ Institute of Astronomy, KU Leuven, Belgium

The goal of the Spectroscopic Discovery of Binaries with Dormant Black Holes survey is to spectroscopically follow up stars that might have dormant compact companions, either black holes or neutron stars. These stars have been identified as ellipsoidal binaries in the Magellanic Clouds by the Optical Gravitational Lensing Experiment (OGLE). A sample of more than 700 ellipsoids with periods shorter than 10 days will be observed to obtain multi-epoch radial-velocity measurements. 4MOST radial velocities in conjunction with OGLE photometry will allow the determination of the secondary component mass and hence the identification of systems with compact companions.

Scientific context

Stellar black holes (BH) and neutron stars (NS) are the end products of massive stars that collapse after they have consumed their energy reservoirs. In NS, gravitational contraction breaks the protons of all atoms and creates one big nucleus of 10^{57} neutrons. BH are even more exotic objects — their entire mass is collapsed into one singular point, such that nothing, including electromagnetic waves, has enough energy to escape its event horizon. Because dormant BH do not emit any electromagnetic radiation, they are very difficult to discover. Only about 20 dynamically confirmed stellar BH are known to reside in X-ray binary systems with low-mass stellar companions. These are, along with Cyg X-1 and several other

high-mass binary candidates, the only confirmed stellar-mass BH in the Galaxy (see, for example, BlackCAT; Corral-Santana et al., 2016). Most of the stellar-mass BH known so far have been discovered by their X-ray emission, which is due to either mass transfer from the low-mass (mostly F–K-type) companion overflowing its Roche lobe (BH low-mass X-ray binaries, BH-LMXBs), or accretion from the stellar wind coming from the high-mass (OB star) companion (BH high-mass X-ray binaries BH-HMXBs). The known masses of stellar X-ray BH as a function of their orbital periods (Tetarenko et al., 2016) are plotted in Figure 1. As can be seen, most of the known BH binaries have relatively short periods, with a median at about 0.5 days. The X-ray emission of the BH-LMXBs is characterised by luminous ($L_x \sim 10^{37}$ erg s^{-1}) outbursts, lasting for about a month, followed by decades-long periods of quiescence ($L_x \sim 10^{31-33}$ erg s^{-1}) (see Remillard and McClintock, 2006 for a review).

According to the commonly accepted model, outbursts from BH-LMXB systems are due to accretion disc instabilities that modulate the accretion rates onto the BH. Between eruptions, these systems are barely detectable, because a substantial part of the energy generated by the small mass flow is not radiated but stored as thermal energy in the accretion discs. Thus, many BH-LMXB remain undetected, because they have been in their quiescent state since X-ray surveys began.

A much larger fraction of BH with low-mass stellar companions are not yet detected because their optical counterparts are within their Roche lobes. In these systems, mass is not transferred, and X-rays are not generated, making these systems dormant BH. For example, Breivik, Chatterjee & Larson (2017) estimated that there should be 106 Galactic BH binary systems, most of which are still waiting to be discovered. One such system, Gaia-BH1, was discovered recently using astrometry (El-Badry et al., 2023).

All of the 19 confirmed short-period BH-LMXBs show periodic optical brightness modulations on the order of a few percent on the timescale of the orbital period (for example, XTE J1118+48 and A0620-00). This is mostly due to the

ellipsoidal effect, induced by tidal forces exerted by the BH on its optical companion. For a general discussion of the ellipsoidal effect see, for example, Mazeh (2008).

The goal of the survey is to discover tens of those unknown dormant BH. The new discoveries will allow us to study the characteristics of the dormant objects in detail. We will be able to understand how frequent compact objects are, as well as the range and distribution of their masses. This will lead to a much better understanding of the astrophysics behind the formation of dormant compact systems.

Specific scientific goals

We plan to use ellipsoidal modulation (Faigler & Mazeh, 2011; Faigler et al., 2012) to discover tens of new unknown dormant BH binaries. Since BH binaries are rare, we have to search for these systems in large samples, on the order of 10^6 or more stars. Astronomy is now at a unique point in its history, where enough stellar light curves with adequate precision to measure ellipsoidal modulation are available for the first time.

The key step is identifying stars with photometric periodic ellipsoidal modulations that indicate the existence of companions more massive than the optical components. If the optical star is on the main sequence (MS), then the more massive unseen companion must be a compact object. To confirm our detection of a compact companion and identify false alarm cases, we will measure the radial velocity (RV) of the candidates and find the systems displaying ellipsoidal modulations with large amplitudes. The mass of the companion will be derived from the combination of the RVs and the ellipsoidal modulation. The companion can be either a white dwarf (very rare), or a NS, with a mass at around $1.4 M_{\odot}$ or a BH (with a larger mass). We can discover only binaries for which the orbital separation is not too large, otherwise the ellipsoidal effect will be too small to detect. From the OGLE light curves available, we were able to detect tens of binaries with an ellipsoidal modulation of 1% or larger, corresponding to binaries with separations which are larger than the radius of the visible companion by up to a factor of 10.

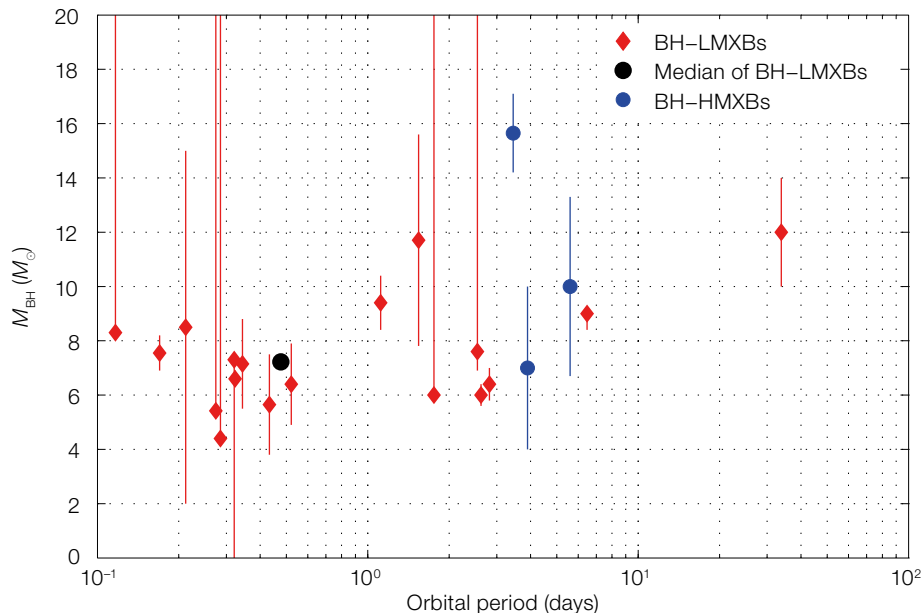


Figure 1. Known masses of stellar BH of the X-ray binaries as a function of their orbital periods. Blue circles represent BH-HMXBs and red diamonds BH-LMXBs. The black point represents the median mass and period of the known BH-LMXBs.

To measure our candidates' mass ratios, we will obtain six RV measurements per system and fit the RV points using the period and ephemeris known from the photometric data. For such short periods, we can safely assume that most of our candidates have a circular orbit. In such cases, the only two unknown parameters of the RV model are the center-of-mass velocity and the RV amplitude. We expect the RV modulation to be on the order of hundreds of km s^{-1} , so the expected accuracy of a few km s^{-1} per RV point will allow us to obtain an accurate solution for each system. This will allow us to identify the systems with a high mass ratio where the secondary component remains unseen, such as BH or NS-binaries.

As a by-product of our search, we will obtain the companion mass for all observed ellipsoidal variables, many of which have stellar companions. This will enable us to derive the mass-ratio distribution of the short-period MS binary population in the Magellanic Clouds.

Target selection and survey area

We use the OGLE-IV photometry (Udalski, Szymański & Szymański, 2015) of the LMC and SMC (80×10^6 stars) as our basis data. An extensive search for binary stars, including ellipsoidal binaries, has been carried out during both the OGLE-III

and OGLE-IV projects and resulted in catalogues of 6581 binaries in the Magellanic Clouds (Pawlak et al., 2016). The sample spans the magnitude range from 13 to 18 mag. in the *G* band. The orbital periods for the ellipsoidal binaries with a MS primary are typically 0.2–10 days, while those with giants as primaries range from tens to hundreds of days.

Out of the entire sample of OGLE binaries, we selected more than 700 MS ellipsoidal binaries in the Magellanic Clouds with $P < 10$ days. This cutoff period allows us to separate the MS systems from the systems with giants. We decided to focus only on the MS stars as these are the only systems where we can unambiguously identify the compact companions based on the mass ratios. If we derive a mass ratio larger than one in a system with a MS primary, then there is a less luminous (likely invisible) but more massive secondary in the system, which means that the secondary is probably a compact object.

Apart from the ellipsoidal binary candidates, we will also monitor over 100 known Wolf–Rayet (WR) stars in the Large Magellanic Cloud. A non-negligible fraction ($\sim 3\%$) of O-type stars are expected to orbit black holes (Langer et al., 2020) with periods of the order of months to years. It can be shown from lifetime arguments that this fraction

becomes even larger for the evolved descendants of O-type stars, the WR stars, reaching up to $\sim 25\%$ (Xu et al., in preparation). Hence, WR populations offer an attractive sample with which to uncover a population of dormant black holes. Previous low-resolution RV monitoring campaigns of the bulk of the WR populations in the Magellanic Clouds (for example, Foellmi, Moffat & Guerrero, 2003; Schnurr et al., 2008) did not attain the needed accuracy to probe the predicted period ranges of WR+BH binaries (~ 1 yr; Langer et al., 2020). In contrast, 4MOST monitoring of this population will enable us to probe binaries with periods up to a few years.

Furthermore, we plan to observe a small sample of known X-ray binaries, which will be used as science validation targets. We will also observe a number of faint X-ray sources in the field of the Magellanic Clouds to search for quiet X-ray binaries like VFTS 243 (Shenar et al., 2022).

Acknowledgements

We thank Maria-Rosa Cioni, Karin Lind, and Michael Hayden for revision of the manuscript. MP is supported by the SONATINA grant 2020/36/C/ST9/00103 from the Polish National Science Center.

References

- Breivik, K., Chatterjee, S. & Larson, S. L. 2017, *ApJL*, 850, L13
- Corral-Santana, J. M. et al. 2016, *A&A*, 587, A61
- El-Badry, K. et al. 2023, *MNRAS*, 518, 1057
- Faigler, S. & Mazeh, T. 2011, *MNRAS*, 415, 3921
- Faigler, S. et al. 2012, *ApJ*, 746, 185
- Foellmi, C., Moffat, A. F. J. & Guerrero, M. A. 2003, *MNRAS*, 338, 1025
- Langer, N. et al. 2020, *A&A*, 638, A39
- Mazeh, T. 2008, *EAS*, 29, 1
- Pawlak, M. et al. 2016, *AcA*, 66, 421
- Remillard, R. A. & McClintock, J. E. 2006, *ARA&A*, 44, 49
- Tetarenko, B. E. et al. 2016, *ApJS*, 222, 15
- Shenar, T. et al. 2022, *Nature Astronomy*, 6, 1085
- Schnurr, O. et al. 2008, *MNRAS*, 389, 806
- Udalski, A., Szymański, M. K. & Szymański, G. 2015, *AcA*, 65, 1

The 4MOST Survey of Dwarf Galaxies and their Stellar Streams (4DWARFS)

Ása Skúladóttir^{1,2}
 Arthur Alencastro Puls³
 Anish M. Amarsi⁴
 Giuseppina Battaglia^{5,6}
 Sven Buder^{7,8}
 Simon Campbell^{8,9}
 Salvador Cardona-Barrero^{5,6}
 Norbert Christlieb¹⁰
 Diane K. Feuillet¹¹
 Viola Gelli^{1,2}
 Camilla J. Hansen^{3,12}
 Vanessa Hill¹³
 Rodrigo Ibata¹⁴
 Pascale Jablonka¹⁵
 Nikolay Kacharov¹⁶
 Amanda Karakas^{8,9}
 Andreas J. Koch-Hansen¹⁷
 Karin Lind¹⁸
 Linda Lombardo¹⁹
 Romain E. R. Lucchesi¹
 Maria Lugaro^{20,21,22,9}
 Nicolas Martin^{14,12}
 Davide Massari²³
 Thomas Nordlander^{7,8}
 Moritz Reichert²⁴
 Martina Rossi^{1,2}
 Ashley J. Ruiter²⁵
 Stefania Salvadori^{1,2}
 Ivo R. Seitenzahl²⁵
 Eline Tolstoy²⁶
 Theodora Xylakis-Dornbusch^{10,27}
 Kristopher C. Youakim¹⁸

- 1 Department of Physics and Astronomy, University of Florence, Italy
- 2 INAF–Arcetri Astronomical Observatory, Florence, Italy
- 3 Institute of Applied Physics, Goethe University Frankfurt, Germany
- 4 Theoretical Astrophysics, Department of Physics and Astronomy, Uppsala University, Sweden
- 5 Canary Islands Institute of Astrophysics, Tenerife, Spain
- 6 University of La Laguna, Tenerife, Spain
- 7 Research School of Astronomy and Astrophysics, Australian National University, Canberra, Australia
- 8 ARC Centre of Excellence for All Sky Astrophysics in 3 Dimensions, Australia
- 9 School of Physics and Astronomy, Monash University, Australia
- 10 Astronomy Centre, Heidelberg University, Germany.
- 11 Department of Astronomy and Theoretical Physics, Lund Observatory, Sweden
- 12 Max Planck Institute for Astronomy, Heidelberg, Germany

- 13 Lagrange Laboratory, Côte d’Azur Observatory, Côte d’Azur University, Nice, France
- 14 Strasbourg Astronomical Observatory, CNRS, University of Strasbourg, France
- 15 Astrophysics Laboratory, Physics Institute, École Polytechnique Fédérale, Lausanne, Switzerland
- 16 Leibniz Institute for Astrophysics, Potsdam, Germany
- 17 Computational Astronomy Institute, Centre for Astronomy, Heidelberg University, Germany
- 18 Department of Astronomy, Stockholm University, Sweden
- 19 GEPI, Paris Observatory, France
- 20 Konkoly Observatory, Research Centre for Astronomy and Earth Sciences, Eötvös Loránd Research Network, Budapest, Hungary
- 21 CSFK, MTA Centre of Excellence, Budapest, Hungary
- 22 Institute of Physics, ELTE Eötvös Loránd University, Budapest, Hungary
- 23 INAF–Bologna Astrophysics and Space Science Observatory, Italy
- 24 Department of Astronomy and Astrophysics, University of València, Spain
- 25 School of Science, University of New South Wales, Sydney, Australia
- 26 Kapteyn Astronomical Institute, University of Groningen, the Netherlands
- 27 International Max Planck Research School for Astronomy & Cosmic Physics at the University of Heidelberg, Germany

The present-day Milky Way is the result of a long history of mergers and interactions with smaller galaxies. The 4DWARFS survey will target the dwarf galaxies and stellar streams in the 4MOST footprint, and unveil their chrono-chemo-kinematical properties. The survey will provide radial velocities, chemical abundances and stellar ages for 140 000 stars, and thus increase the number of stars with detailed information in such systems by several orders of magnitude. 4DWARFS will provide a new, deeper view of the Milky Way environment, shedding light on the first stars, chemical evolution, dark matter halos, and hierarchical galaxy formation down to the smallest scales.

Scientific context

The Milky Way environment is rich in satellite galaxies, stellar streams and accreted systems, that trace galaxy evolution and chemical enrichment throughout cosmic time. Because they are close by, these relics of early galaxy formation can be studied in extraordinary detail, star by star, giving invaluable insight into stellar evolution and nucleosynthesis, as well as the Milky Way’s hierarchical growth. This provides a clear motivation for the 4MOST survey of dwarf galaxies and their stellar streams (4DWARFS) which aims to study and map these individual structures. 4DWARFS will target all ~ 50 of the known Milky Way satellite dwarf galaxies in the southern hemisphere, covering over three orders of magnitude in galaxy mass. Additionally, 4DWARFS will observe dozens of already identified stellar streams in the Galactic halo which are the remnants of currently interacting or previously dissolved systems (Figure 1).

The dwarf galaxy satellites of the Milky Way are intrinsically metal-poor, with a dominant old stellar population, making them ideal fossils with which to study the imprints of the first stars in the Universe. Their star formation was inefficient, making the effects of delayed nucleosynthetic channels (type Ia supernovae [SN Ia], asymptotic giant branch [AGB] stars, neutron star mergers) especially prominent and straightforward to study, at various metallicities and star formation histories (for example, Tolstoy, Hill & Tosi, 2009), providing unique insights into chemical evolution and nucleosynthesis.

These small systems are relics of hierarchical structure formation, opening up the possibility of tracing mass assembly, and both *ex-situ* and *in-situ* star formation in the Milky Way environment. Dwarf galaxies are dominated by dark matter, and can be used as probes of cosmology and galaxy formation. Those that halted star formation long ago are likely the best examples of pristine dark-matter halos in the Universe, and they are the ideal probes to understand the nature of dark matter through the study of their stellar 3D kinematics (for example, Massari et al., 2018). Furthermore, the stellar streams observed in the Galactic halo

represent clear evidence of systems currently being accreted, allowing us to study their tidal disruption in incomparable detail. In particular, the Sagittarius dwarf spheroidal (dSph) is the prime example of a tidally disrupted Milky Way satellite galaxy, and it leaves a trail of stars that wraps more than a full orbit around the Galaxy (Figure 1). This makes it a major contributor to the Milky Way stellar halo along with other past mergers. Sagittarius and its stream therefore provide one of the best opportunities to study a galaxy that is currently undergoing disruption.

A careful study of dwarf galaxies and their stellar streams is thus of fundamental importance to obtaining a complete picture of the evolution of our Galaxy. Furthermore, this will enable us to understand in detail the properties of the dwarf galaxies themselves, which are the earliest and most common type of galaxy in the Universe.

Specific scientific goals

The main goal of 4DWARFS is to characterise dwarf galaxies and stellar streams by mapping their chrono-chemo-kinematical properties. We will derive radial velocities, chemical abundances and stellar ages (for example, Feuillet et al., 2016) for stars in all known dwarf galaxies (smaller than the Small Magellanic Cloud) and stellar streams in the 4MOST footprint of the Milky Way halo. Using both high-resolution (HR) and low-resolution (LR) spectra, our survey will provide 10–25 elemental abundances for 100 000 stars in dwarf galaxies, and 30 000 stars in stellar streams (Figure 1). In addition, we will push down to the fainter dwarf galaxies and smaller stellar streams, retrieving abundances of around five elements for a further 10 000 stars. The homogeneity of this sample will be unprecedented in comparison to the present literature.

The 4DWARFS dataset is therefore incredibly rich, and will impact several fields, ranging from cosmology to stellar physics. The key scientific questions that 4DWARFS will attack are listed below.

What are the properties of the first stars?

The chemical yields of the first stars (Pop III) are thought to be preserved on the surfaces of low-metallicity, low-mass, long-lived stars (for example, Hansen et al., 2020). 4DWARFS will identify the most metal-poor stars of dwarf galaxies, increasing their numbers by more than an order of magnitude. Furthermore, we will quantify the properties of metal-poor stars across different galaxies, for example the fraction of carbon-enhanced metal-poor stars which are thought to be the descendants of faint Pop III supernovae (for example, Iwamoto et al., 2005). We will search for and identify rare fossils and descendants of the first stars (Rossi, Salvadori & Skúladóttir, 2021), such as those formed in the ejecta of zero-metallicity pair-instability supernovae, and high-energy Pop III supernovae. This will allow us to put constraints on the intrinsic properties of the first stellar population, such as their mass distribution and the energy distribution of their supernovae.

How are the chemical elements created and distributed?

Even after decades of study, the fundamental physical conditions of major nucleosynthetic sites remain obscure. Investigating different galaxies with a variety of star formation and chemical enrichment histories is key to breaking degeneracies in chemical evolution (for example, Skúladóttir & Salvadori, 2020). Dwarf galaxies have intrinsically low star formation rates compared to larger galaxies, and all long-timescale nucleosynthetic channels, such as SN Ia, AGB stars and neutron star mergers are thus more prominent relative to core-collapse SN (short timescales). Compared to the Milky Way, dwarf galaxies have much simpler star formation histories, which makes them easier to model, providing a more detailed understanding. 4DWARFS will constrain the fundamental physics of nucleosynthetic sites: their rates, yields, metallicity dependence and time-delay distribution functions. In this way, 4DWARFS will provide key insights into the elusive progenitors of SN Ia (for example, Maoz, Mannucci & Nelemans, 2014), as well as the various production sites of neutron-capture elements, such as AGB

stars (s- and i-processes) and the kilonovae of neutron star mergers (r-process).

What are the dynamical properties of dwarf galaxies?

By providing an unprecedented sample of precise radial velocities and coupling those with Gaia proper motion measurements, 4DWARFS will determine the dark matter profile of almost 50 galaxies, thereby shedding light on the nature of dark matter itself. We will drastically increase observations in the outskirts of these galaxies, which will allow us to test whether dwarf galaxies are in equilibrium, as commonly assumed, or if they exhibit more complex kinematics (for example, Martin et al., 2016). These dynamical studies will benefit hugely from the fact that 4DWARFS will constrain the binary fraction and period distribution of stars in dwarf galaxies, which are currently essentially unknown. Understanding their binary properties will also provide fresh insights into star formation and stellar evolution at low metallicities.

What are the small-scale limits of hierarchical galaxy formation?

In recent years the complexity in the Milky Way environment has been revealed, with dozens of identified structures. The progenitors of these systems are still being investigated, but they are likely a mixed bag of objects: a variety of dwarf galaxies and disrupted globular clusters with different ages and metallicities. 4DWARFS will characterise the accreted systems of the Galactic halo both kinematically and chemically, uncovering their metallicity distribution, chemical evolution and star formation history. This will allow us to understand the progenitors of these streams and the systems that build up the Milky Way halo (for example, Ibata et al., 2021). In particular, we will map and characterise the currently ongoing disruption of the Sagittarius dSph in extraordinary detail. Finally, we will move to even smaller scales of accretion, and for the first time identify in a systematic way mergers that have happened within the dwarf galaxies themselves (for example, Cicuendez & Battaglia, 2018), thus quantifying hierarchical galaxy formation down to the smallest scales.

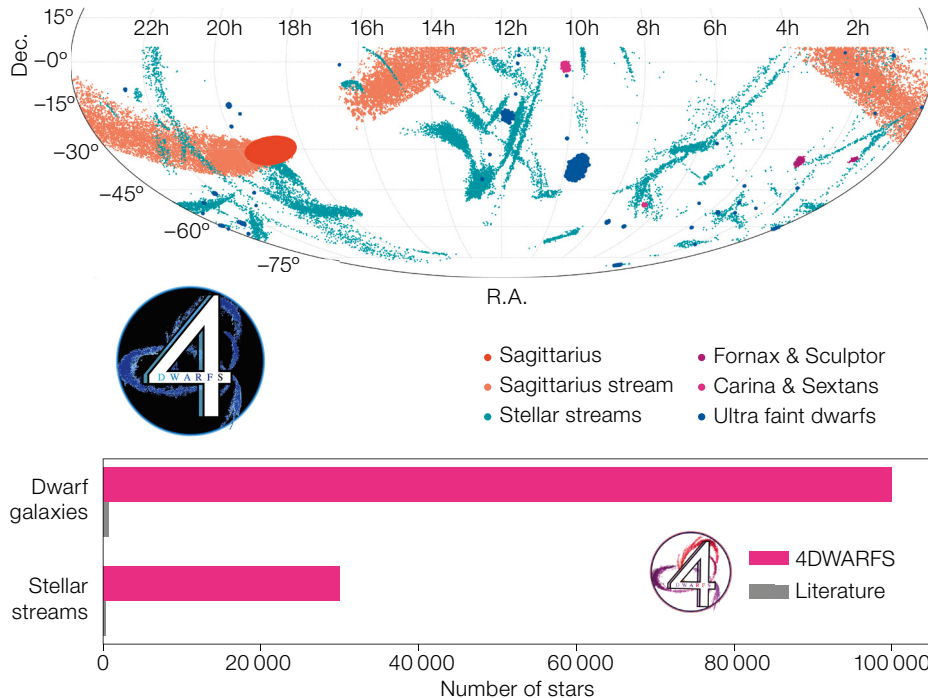


Figure 1. The scope of 4DWARFS. Top: the distribution of 4DWARFS targets on the sky. Bottom: the number of stars in 4DWARFS with ≥ 10 elemental abundances, compared to what is currently available in the literature. The 4DWARFS logo was designed by M. Rossi.

combination of 4DWARFS and other Galactic surveys within 4MOST will therefore allow us to paint a comprehensive picture of the formation and evolution of the Milky Way environment, from cosmic dawn until the present day.

Acknowledgements

This project has received funding from the European Research Council under the European Union’s Horizon 2020 research and innovation programme (grant agreement No 804240). A.M.A. acknowledges support from the Swedish Research Council (VR 2020-03940). M. Reichert acknowledges support from the grants FJC2021-046688-I and PID2021-127495NB-I00, funded by MCIN/AEI/10.13039/501100011033 and by the European Union “NextGenerationEU”, as well as “ESF Investing in your future”. Additionally, he acknowledges support from the Astrophysics and High Energy Physics programme of the Generalitat Valenciana ASFAE/2022/026 funded by MCIN and the European Union Next-GenerationEU (PRTR-C17.11). A.J.K.H. gratefully acknowledges funding by the Deutsche Forschungsgemeinschaft (DFG, German Research Foundation), Project-ID 138713538, SFB 881 The Milky Way System, subprojects A03, A05, A11. G.B. acknowledges support from the Agencia Estatal de Investigación del Ministerio de Ciencia en Innovación (AEI-MICIN) and the European Regional Development Fund (ERDF) under grant number PID2020-118778GB-I00/10.13039/501100011033 and the AEI under grant number CEX2019-000920-S. We would like to thank H. W. Rix and R. Andrae, as well as the Pristine collaboration for sharing their catalogue of metal-poor stars in the Galactic halo, and A. Arentsen for sharing a Pristine catalogue of the Sagittarius dSph.

References

- Battaglia, G. et al. 2022, *A&A*, 657, A54
 Cicuendez, L. & Battaglia, G. 2018, *MNRAS*, 480, 251
 Feuillet, D. K. et al 2016, *ApJ*, 817, 40
 Gaia collaboration et al. 2018, *A&A*, 616, A12
 Hansen, C. J. et al. 2020, *A&A*, 643, A49
 Ibata, R. et al. 2021, *ApJ*, 914, 123
 Iwamoto, N. et al. 2005, *Science*, 309, 451
 Maoz, D., Mannucci, F. & Nelemans, G. 2014, *ARA&A*, 52, 107
 Martin, N. F. et al. 2016, *ApJ*, 818, 40
 Massari, D. et al. 2018, *Nature Astronomy*, 2, 156
 Rossi, M., Salvadori, S. & Skúladóttir, Á. 2021, *MNRAS*, 503, 6026
 Skúladóttir, Á. & Salvadori, S. 2020, *A&A*, 634, L2
 Tolstoy, E., Hill, V. & Tosi, M. 2009, *ARA&A*, 47, 371
 Xylakis-Dornbusch, T. et al. 2022, *A&A*, 666, A58

The 4DWARFS survey will therefore provide the most complete overview available of the evolution of dwarf galaxies, reconstructing their histories from formation to disruption.

Target selection and survey area

The 4DWARFS survey will target all known dwarf galaxies and stellar streams in the Milky Way halo observable from the Southern hemisphere, $-80^\circ < \text{Dec.} < +5^\circ$ (Figure 1), at $|b| \geq 20$. The density of our target catalogue varies drastically, from fewer than five targets per square degree in the more diffuse stellar streams, to more than 1000 in the central fields of larger dwarf galaxies.

The largest dSph galaxies, Sagittarius, Fornax, and Sculptor, will be targeted with both LR and HR fibres, and their central fields will be covered by longer exposure times (≥ 6 hours) compared to the fiducial 2-hour 4MOST footprint. The smaller dwarf galaxies, Carina, Sextans and the more than 40 ultra-faint dwarf galaxies, will be observed in LR, following the 4MOST footprint. Furthermore, 4DWARFS will target the prominent Sagittarius stream, along with all southern stellar streams

that have been identified in the Milky Way halo through Gaia DR3. The streams will be observed with both HR and LR within the fiducial 4MOST footprint, taking advantage of existing deep fields. We emphasise that both HR and LR spectra will be used for chemical analysis, as well as radial velocities.

The 4DWARFS target catalogue is based on Gaia DR3. The member stars of the Sagittarius dSph main body are selected following the approach of the Gaia collaboration et al. (2018), taking into account photometry, proper motions, and parallaxes from Gaia. The target catalogues of all other dwarf galaxies are adopted from Battaglia et al. (2022), which is based on Gaia early DR3 photometry and astrometry. The target selection of the stream stars is done with the STREAMFINDER algorithm, as described in Ibata et al. (2021). Furthermore, special emphasis will be placed on observing metal-poor stars in dwarf galaxies and stellar streams, following an approach similar to that presented in Xylakis-Dornbusch et al. (2022).

The selection of our targets is highly complementary to other 4MOST surveys, in particular the Milky Way halo surveys, and the Magellanic Clouds survey. The

Stellar Population Survey Using 4MOST (4MOST-StePS)

Angela Iovino¹
 Amata Mercurio²
 Anna Rita Gallazzi³
 Francesco La Barbera²
 Marcella Longhetti¹
 Crescenzo Tortora²
 Stefano Zibetti³
 Francesco Belfiore³
 Matteo Bianconi⁴
 Giovanni Busarello²
 Enrico M. Corsini⁵
 Luca Costantin⁶
 Gabriella De Lucia⁷
 Roberto De Propris⁸
 Francesco D'Eugenio⁹
 Fabio Fontanot⁷
 Rubén García-Benito¹⁰
 Michaela Hirschmann⁷
 Christopher Haines¹¹
 Filippo Mannucci³
 Sean McGee⁴
 Paola Merluzzi²
 Lorenzo Morelli¹¹
 Alessia Moretti¹²
 Anna Pasquali¹³
 Bianca Poggianti¹²
 Lucia Pozzetti¹⁴
 Giulia Rodighiero⁵
 Patricia Sánchez-Blázquez¹⁵
 Arjen van der Wel¹⁶
 Alexandre Vazdekis¹⁷
 Benedetta Vulcani¹²
 Anita Zanella¹²
 Marianna Annunziatella⁶
 Alice Concas¹⁸
 Letizia P. Cassarà¹⁹
 Giovanni Cresci³
 Mirko Curti⁹
 Adriana de Lorenzo-Cáceres¹⁷
 Anna Ferre Mateu¹⁷
 Rosa M. González Delgado¹⁰
 Chiara Mancini⁵
 Camilla Pacifici²⁰
 Enrique Perez-Montero¹⁰
 Alessandro Pizzella⁵
 Pablo G. Perez-Gonzalez⁶
 Scott C. Trager²¹
 Daniela Vergani¹⁴

⁶ Centre for Astrobiology (CSIC-INTA),
 Torrejón de Ardoz, Spain
⁷ INAF–Trieste Astronomical Observatory,
 Italy
⁸ Turku University, Finland
⁹ Kavli Institute for Cosmology,
 Cambridge, UK
¹⁰ Andalucía Institute of Astrophysics,
 Granada, Spain
¹¹ University of Atacama, Copiapó, Chile
¹² INAF–Padua Astronomical Observatory,
 Italy
¹³ Heidelberg University, Germany
¹⁴ INAF–Bologna Astrophysics and Space
 Science Observatory, Italy
¹⁵ Madrid Complutense University, Spain
¹⁶ Ghent University, Belgium
¹⁷ Canary Islands Institute of Astrophysics,
 Tenerife, Spain
¹⁸ ESO
¹⁹ INAF–Institute of Space Astrophysics
 and Cosmic Physics, Milan, Italy
²⁰ Space Telescope Science Institute,
 Baltimore, USA
²¹ University of Groningen,
 the Netherlands

Galaxy spectra encode in their continuum and absorption/emission features a wealth of information on galaxy physics, mass assembly and chemical enrichment history. The 4MOST-StePS survey will collect high-quality spectra (with a median signal-to-noise ratio of about 30 \AA^{-1} , and resolution $R \sim 5000$) for a sample of about 3300 galaxies brighter than $I_{AB} = 20.5$ within the RA-Dec-z footprint of the WAVES-Deep survey. These spectra will provide a precise empirical description of the evolutionary path of massive galaxies in the intermediate redshift range ($0.3 < z < 0.7$) between the LEGA-C and SDSS surveys. The locations of the galaxies within the cosmic web, unveiled by WAVES-Deep, will disclose the connection between galaxy properties and environment, down to the scales of galaxy pairs.

Scientific context

The complex physical processes that cause the formation and evolution of luminous structures to deviate from the assembly history of dark matter (DM) halos are yet to be fully understood. On galactic scales (below ~ 1 Mpc), highly

non-linear processes are at play (for example, energetic feedback, both from active galactic nuclei [AGN] and star formation, and mergers). A detailed comparison between observational data, simulations and advanced theoretical models can shed light on the mechanisms that regulate the connection between galaxies and their DM halos.

Good quality (both in resolution and signal-to-noise ratio [SNR]) spectra provide information about the current physical conditions of the multiple components in a galaxy (stars, gas and, indirectly, DM), while simultaneously unveiling the archaeological treasure that is encoded in its stellar populations. The whole past star formation and chemical-enrichment history of a galaxy are reflected in its present stellar population properties. The chemical abundance of gas and stars in a galaxy holds the memory of the baryonic cycle that regulates its star formation, by balancing the inflow of pristine gas, the outflow of metal-loaded gas blown out by stellar/AGN winds, and the re-accretion of this metal-enriched gas (Hunt et al., 2020).

The study of galaxies in the local Universe has greatly enriched our understanding of galaxy evolution. The spectra from the Sloan Digital Sky Survey (SDSS; York et al., 2000) have provided a robust $z \sim 0$ anchor to both theoretical and empirical approaches, proving to be an immensely valuable tool to understand the physics of galaxies. Unfortunately, the so-called archaeological reconstruction from $z \sim 0$ galaxies is limited by inherent physical degeneracies between different parameters (for example age and metallicity) and by the similarity of stellar population spectra with ages greater than 5 Gyr; together these prevent an accurate reconstruction of a galaxy's ancient star formation history. To circumvent this problem a direct look-back approach is needed, i.e., observing galaxies at high redshifts to make a direct census of different populations at different remote cosmic epochs. High-quality galaxy spectra, observed in different environments and across a continuous range of cosmic times, provide precise measurements of a variety of physical parameters of galaxies, enabling the star formation and chemical enrichment histories at early times to be unveiled. This strategy in

¹ INAF–Brera Astronomical Observatory,
 Italy

² INAF–Capodimonte Astronomical
 Observatory, Naples, Italy

³ INAF–Arcetri Astronomical Observatory,
 Florence, Italy

⁴ University of Birmingham, UK

⁵ University of Padua, Italy

turn opens up the possibility of connecting lower-redshift galaxies to their statistically plausible progenitors. So far, the only notable survey designed to obtain high-quality spectra in the relatively distant Universe is LEGA-C (van der Wel et al., 2021), covering the redshift window $0.6 \leq z \leq 1.0$ for a sample of ~ 3200 galaxies within the COSMOS field. LEGA-C spectra (median SNR $\sim 20 \text{ \AA}^{-1}$, resolution $R \sim 2500$) have shown the power of high-quality continuum spectroscopy as a fundamental tool with which to study galaxies, but many questions remain open. Analysis of LEGA-C spectra has shown that, contrary to what was previously thought, even the most massive galaxies today may experience new star formation episodes between $z \sim 0.8$ and $z \sim 0$ (Chaume et al., 2018; Wu et al., 2021). Identifying the mechanisms that give rise to a rekindling of star formation activity will provide crucial information needed to reconstruct the evolutionary paths of galaxies.

However, the intermediate window remains unexplored, as even at these modest redshifts it is challenging to produce a large sample of high-quality spectra.

A first step towards filling this gap is provided by the WEAVE-Stellar Population Survey, using the WEAVE multi-object spectrograph at the William Herschel Telescope (WEAVE-StePS; Iovino et al., 2022). WEAVE is a spectrograph similar in overall performance to 4MOST, and over the next 5 years WEAVE-StePS will observe $\sim 25\,000$ galaxies over $\sim 25 \text{ deg}^2$, selected to be brighter than $I_{\text{AB}} \sim 20.5 \text{ mag}$ and at redshift $z > 0.3$. WEAVE-StePS spectra, observed at resolution $R \sim 5000$, will access important physical properties of galaxies, such as a basic characterisation of the star formation history, as well as stellar and nebular metallicities and dynamical properties. However, this large sample will be at a typical SNR of $\sim 10 \text{ \AA}^{-1}$ in the I band, and the uncertainties in the parameters will rapidly grow, on average, for fainter/less massive galaxies.

Specific scientific goals

The 4MOST Stellar Population Survey (4MOST-StePS) seizes the opportunity to

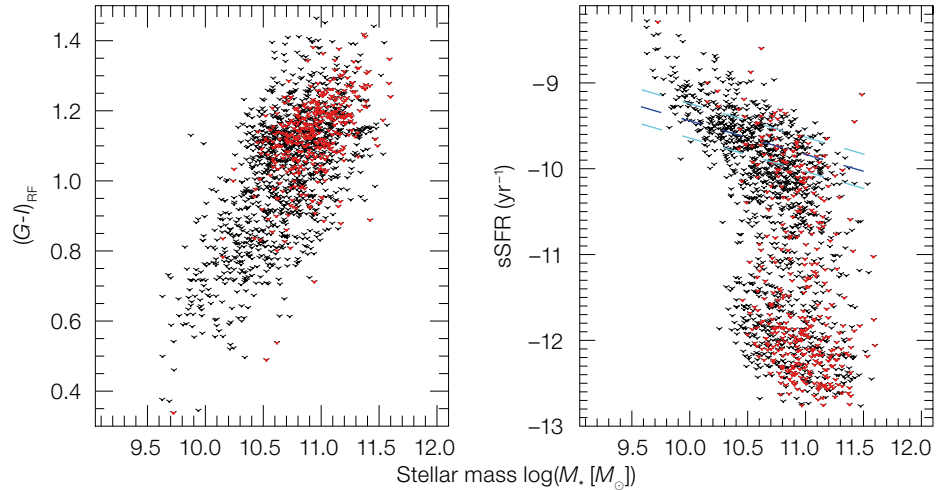


Figure 1. Overview of the target galaxy sample in terms of stellar mass (based on Bruzual & Charlot (2003) models and assuming Chabrier (2003) initial mass function), optical colours and specific star formation rate (sSFR). Left panel: rest-frame $(G-I)$ colour vs. stellar mass. Right panel: sSFR vs. stellar mass plots for galaxies selected at $I_{\text{AB}} \leq 20.5$ and $0.3 < z < 0.7$. Values of rest-frame colours, stellar

masses and sSFR are obtained from a compilation of spectroscopic data in the COSMOS field. Black points indicate the total sample selected using 4MOST-StePS constraints in magnitude and redshift, and red points indicate the highest quartile SNR sub-sample. The blue and cyan lines on the right panel display the main sequence location and its scatter (Speagle et al., 2014).

piggyback on the WAVES-Deep areas (Driver et al., 2019), to obtain deep low-resolution-mode observations ($T_{\text{exp}} \sim 30$ hours) for a sample of ~ 3300 bright galaxies ($I_{\text{AB}} \leq 20.5$) embedded within the RA-Dec- z footprint of WAVES-Deep (i.e., at $0.3 < z < 0.7$). The design of 4MOST-StePS mimics that of WEAVE-StePS, targeting the massive tail ($\log(M/M_{\odot}) \geq 10.5$) of the galaxy population, but the focus is on a smaller yet representative sample of galaxies, similar in size to LEGA-C, trading the sample size for a much higher SNR (see Figure 1).

The goal is to capture the richness (including the inherently stochastic nature) of the various processes involved in galaxy evolution, and to pin down the different mechanisms (both internal and external) capable of modulating/shutting down star formation activity in galaxies. The superb high-quality individual spectra of 4MOST-StePS will yield the fundamental physical properties needed to address a range of questions accessible only for a tiny ($< 5\%$) and biased minority of the galaxies observed by WEAVE-StePS at the William Herschel Telescope.

4MOST-StePS galaxies will amount to a statistically robust, intermediate-redshift

sample, complementing both the LEGA-C higher-redshift sample and the SDSS local sample.

The main physical quantities we will obtain for our sample are:

- The mean age of the stellar component, and the timescale of the star formation activity. The rest-frame ultraviolet and its absorption indices — sensitive tracers of young stars — will be used to identify recent minor episodes of star formation on top of an old stellar population, providing a census of the so-called ‘rejuvenation’ phenomenon, whereby passive galaxies go back (temporarily) to an actively star-forming state. This observable will constrain the evolutionary patterns of galaxies in the mass–star-formation-rate space, and clarify to what extent the passive evolution scenario can apply to present-day passive and massive galaxies in different environments;
- The metal abundances in stars and gas. A SNR of $\geq 20 \text{ \AA}^{-1}$ is needed to obtain accurate measurements of metal-sensitive absorption features, limiting stellar metallicity uncertainty to < 0.1 dex for the most evolved galaxies and to $< 0.2\text{--}0.25$ dex for younger, star-forming

systems (Gallazzi et al., 2005, 2014). This allows the evolution of different scaling relations and their intrinsic scatter to be tracked. Unbiased values of metallicity can be obtained with detailed analysis of single element abundance ratios (for example, $[Mg/Fe]$, $[Ca/Fe]$, $[C/Fe]$), measured with an accuracy of 0.1 to 0.25 dex (depending on the element) for intermediate-age populations based on an $SNR > 30 \text{ \AA}^{-1}$. Gas-phase metallicity can also be accurately measured using the faint auroral lines (for example, Maiolino & Mannucci, 2019) that can be detected in these high-SNR spectra, after stacking. These quantities can constrain the physical processes of chemical enrichment in galaxies, as well as the timescale of quenching processes and of the main star formation event (Sánchez-Blázquez et al., 2003; Carretero et al., 2004);

- Characterisation of the kinematics of the stellar and gaseous components (velocity distribution, inflows/outflows). An accurate estimate of dynamical masses can be obtained with a formal accuracy of $\sim 25\%$ (40%) using spectra with $SNR \sim 30$ (20 \AA^{-1}), by using Jeans modelling of the 4MOST aperture velocity dispersion of individual galaxies. Its comparison with stellar masses is crucial to linking the evolution of galaxies to their DM halos (Tortora et al., 2018) and to providing dynamical constraints on one of the most disputed ingredients in stellar populations, i.e., the shape of the stellar initial mass function (IMF; for example, Tortora, Romanowsky & Napolitano, 2013). The excellent spectral quality will reveal the demographic of gas outflows/inflows traced by interstellar absorption and broad high-velocity nebular emission as done at $z \sim 0$ with the SDSS galaxy spectra (Concas et al., 2017, 2019).

All these quantities will be complemented by the environment information provided by WAVES-Deep and compared with state-of-the-art large-scale cosmological simulations (Fontanot et al., 2017, 2021). The 4MOST-StePS sample will be the ideal observational counterpart to synthetic spectral energy distributions obtained from galaxy formation simulations in a cosmological context — including the stellar continuum and the nebular emission lines of various origins (Hirschmann et al., 2017).

The interplay between theoretical rendition and 4MOST-StePS observed spectra will enable a uniquely accurate two-way comparison of theoretical predictions with observational data. This kind of approach is needed for a quantitative understanding of the processes driving the evolution of massive galaxies.

4MOST-StePS data will lift the degeneracies of the interpretation that WEAVE-StePS will not be able to do, given its lack of detail.

Finally, our observational strategy will provide a tail of galaxies with excellent $SNR (> 40 \text{ \AA}^{-1})$ in the I band; red points in Figure 1), enabling innovative science. For this higher-SNR sample, we will derive precise individual abundance ratios, constrain the stellar IMF from key sensitive features, detect even tiny fractions (at the 1% level) of residual young stars, detect faint auroral lines for direct gas metallicity estimates in star-forming galaxies and identify gas flows probed by absorption and emission lines. The higher moments of the line-of-sight velocity dispersion will also be retrievable, improving dynamical mass estimates. The high-SNR sample will be used to test for systematics in our estimates (for example the accurate reconstruction of star formation histories at lower SNR values).

Target selection and survey area

We will pool our targets with those of Consortium Surveys in the $\sim 66\text{-deg}^2$ footprint of the WAVES-Deep survey (four so-called Deep Drilling Fields and the GAMA23 Deep field). The choice of these sky regions is driven by observational strategy advantages and significant scientific benefits. All the WAVES-Deep areas possess a variety of ancillary photometric data that can be used to complement the 4MOST high-quality spectroscopic information on a wider wavelength range. In these fields, we can take advantage of the repeated passes needed to achieve the sampling rate requested by WAVES-Deep and successfully pursue our 30-hour exposure time strategy, while using a minimal fraction of fibre hours: less than 0.5% of the total amount available to Community surveys in low-resolution mode.

Our sample is positioned within the Large-Scale Structure web, revealed in fine detail by WAVES-Deep (see Driver et al., 2019). This accurate environmental information will enable us to explore the connection between the different galaxy properties and the environment where galaxies reside in an evident and advantageous synergy with WAVES-Deep.

4MOST-StePS will push the 4MOST spectrograph to the limit of its performance, well beyond its redshift machine capabilities. Our survey will obtain high-quality data, bridging the gap in our knowledge in the intermediate redshift range, which still lacks such high-quality data, and will put to full use the environment characterisation provided by WAVES-Deep. The synergy with the science case of WAVES-Deep is a win-win opportunity that our project fully exploits, making 4MOST-StePS a low-cost survey with the potential for a very high scientific return.

References

- Bruzual, G. & Charlot, S. 2003, MNRAS, 344, 1000
 Carretero, C. et al. 2004, ApJ, 609, L45
 Chabrier, G. 2003, PASP, 115, 763
 Chauke, P. et al. 2018, ApJ, 861, 13
 Concas, A. et al. 2017, MNRAS, 468, 1747
 Concas, A. et al. 2019, A&A, 622, A188
 Driver, S. P. et al. 2019, The Messenger, 175, 46
 Fontanot, F. et al. 2017, MNRAS, 464, 3812
 Fontanot, F. et al. 2021, MNRAS, 504, 4481
 Gallazzi, A. et al. 2005, MNRAS, 362, 41
 Gallazzi, A. et al. 2014, ApJ, 788, 72
 Hirschmann, M. et al. 2017, MNRAS, 472, 2468
 Hunt, L. et al. 2020, A&A, 643, A180
 Iovino, A. et al. 2022, submitted to A&A
 Maiolino, R. & Mannucci, F. 2019, A&ARv, 27, 3
 Sánchez-Blázquez, P. et al. 2003, ApJ, 590, L91
 Speagle, J. S. et al. 2014, ApJS, 214, 15
 Tortora, C., Romanowsky, A. J. & Napolitano, N. R. 2013, ApJ, 765, 8
 Tortora, C. et al. 2018, MNRAS, 473, 969
 van der Wel, A. et al. 2021, ApJS, 256, 44
 Wu, P.-F. et al. 2021, AJ, 162, 201
 York, D. G. et al. 2000, AJ, 120, 1579

Optical, Radio Continuum and HI Deep Spectroscopic Survey (ORCHIDSS)

Kenneth Duncan¹
 Andrew Baker²
 Philip Best¹
 Sarah Blyth³
 Nina Hatch⁴
 Benne Holwerda⁵
 Matt Jarvis⁶
 Natasha Maddox⁷
 Daniel J. B. Smith⁸
 Marina Arnaudova⁸
 Laurent Chemin⁹
 Romeel Dave¹
 James Dunlop¹
 Bradley Frank¹⁰
 Eric Gawiser²
 Anniëk Gloude-mans¹¹
 Catherine Hale¹
 Ian Heywood⁶
 Sheila Kannappan¹²
 Rohit Kondapally¹
 Ross McLure¹
 Leah Morabito¹³
 Nicole Nesvadba¹⁴
 Hengxing Pan¹⁰
 Anastasia Ponomareva⁶
 Matt Prescott¹⁵
 Hayley Roberts¹⁶
 Huub Röttgering¹¹
 Rachel Somerville¹⁷
 Madalina Tudorache⁶
 Mattia Vaccari³
 Imogen Whittam⁶
 John Wu¹⁸
 Martin Zwaan¹⁹

¹ University of Edinburgh, UK

² Rutgers University, USA

³ University of Cape Town, South Africa

⁴ University of Nottingham, UK

⁵ University of Louisville, USA

⁶ University of Oxford, UK

⁷ University of Bristol, UK

⁸ University of Hertfordshire, UK

⁹ Andres Bello University, Santiago, Chile

¹⁰ South African Radio Astronomy Observatory, South Africa

¹¹ Leiden University, the Netherlands

¹² University of North Carolina at Chapel Hill, USA

¹³ Durham University, UK

¹⁴ Lagrange Laboratory, Côte d'Azur Observatory, Côte d'Azur University, Nice, France

¹⁵ University of the Western Cape, South Africa

¹⁶ University of Colorado at Boulder, USA

¹⁷ Flatiron Institute, New York, USA

¹⁸ Space Telescope Science Institute, USA

¹⁹ ESO

Galaxy evolution is regulated by the continuous cycle of gas accretion, consumption and feedback. Crucial in this cycle is the availability of neutral atomic (HI) and molecular hydrogen. Our current inventory of HI, however, is very limited beyond the local Universe ($z > 0.25$), resulting in an incomplete picture. ORCHIDSS is designed to address this critical challenge, using the powerful combination of 4MOST spectroscopy and sensitive radio observations from the MeerKAT deep extragalactic surveys to trace the evolution of neutral gas and its lifecycle within galaxies across the bulk of cosmic history.

Scientific context

On galactic scales, star formation is regulated by the complex cycling of gas in and out of the interstellar medium (ISM; Kereš et al., 2005). This cycle starts with primordial gas accretion, which fuels star formation and accretion onto black holes. Feedback in the form of stellar winds, supernovae and active galactic nuclei (AGN) jets shock heats the gas and drives outflows. The last stage of the cycle is the cooling of the recycled gas from the hot halo, some of which then accretes into the ISM and restarts the cycle. Large investments have been made in studying the coolest, dense molecular gas and the hottest, most rarefied gas halos of galaxies (with, for example, ALMA, XMM and Chandra). However, the cycling of cold atomic gas, the cleanest probe of the ISM, is poorly understood. This gas can be traced by the 21-cm transition line of neutral hydrogen (HI), but sensitivity limits have restricted such studies to the local Universe (Catinella & Cortese, 2015).

In the local Universe, the instantaneous star formation rate (SFR) in galaxies is much more tightly connected to molecular gas than to the neutral atomic gas from which molecular clouds condense (for example, Bigiel et al., 2011). Galaxy evolution models that incorporate this connection have been able to account for the sharp increases with redshift of the

cosmic SFR density and the cosmic molecular gas mass fraction (for example, Davé et al., 2020). However, these models' predictions of more modest redshift evolution in the cosmic HI density can presently be compared only to absorption-line studies, where the exact relationships between galaxies and absorbers remain uncertain, and where possible relationships between HI content and star formation averaged over Gyr timescales cannot be explored at all. Testing these models and fully understanding the buildup of stellar mass over cosmic time requires directly observing all components of the gas reservoirs in galaxies, out to significant cosmological redshifts that have not been accessible until now.

Thanks to the ongoing revolution in radio astronomy, it is now possible to probe these regimes and begin to tackle a number of key challenges in our understanding of galaxy formation: what is the cosmic history of neutral hydrogen? what is the lifecycle of gas within galaxies? and how does feedback impact the gas reservoirs of galaxies?

At the forefront of this revolution is the MeerKAT telescope, its radio continuum surveys now simultaneously providing one of the most reliable, obscuration-free, probes of star formation and a means of tracing black hole accretion in AGN. Furthermore, its surveys of the 21-cm HI emission line provide a powerful new probe of the ISM of galaxies up to $z = 1.4$.

MeerKAT's flagship deep extragalactic surveys, MeerKAT International GHz Tiered Extragalactic Exploration (MIGHTEE; Heywood et al., 2022) and Looking at the Distant Universe with the MeerKAT Array (LADUMA; Blyth et al., 2016), are breaking new ground in the study of neutral atomic gas in galaxies. MIGHTEE will directly detect HI in several hundred galaxies at $z < 0.2$, and a few of the rarest, most HI-massive galaxies out to $z = 0.5$ thanks to the large volume probed over its multiple fields ($> 10^7$ Mpc³ at $0.45 < z < 0.55$). Reaching ~ 4.5 times deeper in HI sensitivity at $z < 0.5$ and extending frequency coverage of HI to $z = 1.4$ in a single field, LADUMA will detect larger samples of lower-mass galaxies and enable detection of the most HI-massive galaxies out to $z = 1$. Despite

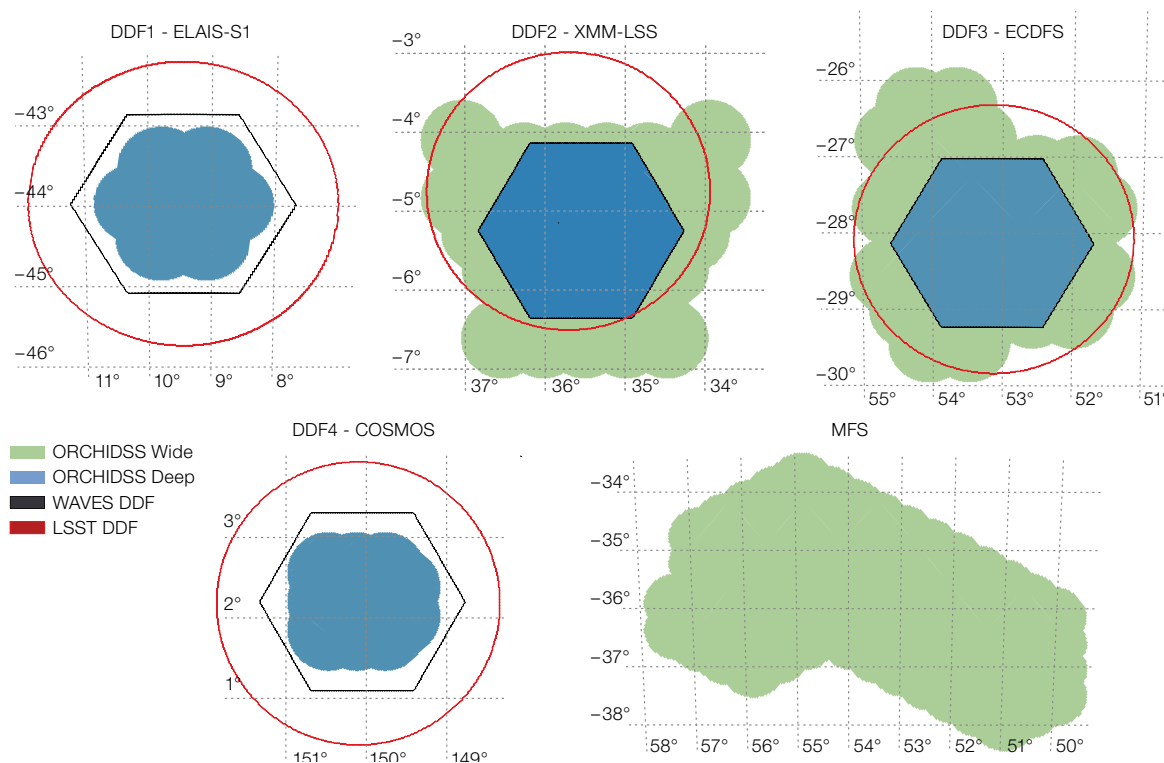


Figure 1. Planned survey fields and maximum potential footprint for the ORCHIDSS Survey. The ORCHIDSS Deep fields (blue shading) align with the WAVES Deep Drilling Fields, targeting MIGHTEE radio-detected sources out to $z_{\text{phot}} < 1.4$. ORCHIDSS Wide targets will be drawn from the MIGHTEE and MFS coverage to probe a wider range of cosmic environments out to $z_{\text{phot}} < 0.57$.

these substantial advances, however, the 21 cm flux-limited nature of these surveys means that, by themselves, they will preferentially detect only the most HI-rich galaxies.

The full potential of MeerKAT's surveys will only be realised if they are matched with extensive optical spectroscopy. By building a large, representative sample of galaxies with accurate spectroscopic redshifts, we can spectrally align and stack the radio data to extract HI measurements below the MIGHTEE and LADUMA noise thresholds (Chowdhury, Kanekar & Chengalur, 2022; Pan et al., 2022), revealing the neutral gas properties of representative samples of the full galaxy population over much of cosmic history.

Specific scientific goals

Combining the deep radio observations offered by MeerKAT and the high-multiplex optical spectroscopy offered by 4MOST, the Optical, Radio Continuum and HI Deep Spectroscopic Survey (ORCHIDSS) will address the key scientific challenges outlined below.

The cosmic history of neutral hydrogen

Galaxy evolution is driven by the availability of atomic and molecular hydrogen in the ISM of galaxies. The large, homogeneously selected and highly complete spectroscopic samples provided by ORCHIDSS will allow us to trace the HI content in normal galaxies out to $z = 1.4$. ORCHIDSS will provide the most reliable measurement of the evolution of the cosmic HI density and HI mass function out to the epoch where galaxy formation peaked.

The lifecycle of gas in galaxies

The stellar growth of galaxies is regulated by the continuous cycle of gas accretion, consumption and feedback. The parameters governing the flow of this gas cycle, such as the primordial gas accretion rate and efficiency of stellar feedback, are highly uncertain and yet vital to obtain for any successful model of galaxy evolution (Somerville & Davé, 2015). For the first time, ORCHIDSS will measure these parameters via the fundamental relations between the neutral gas content of galax-

ies and key physical properties (SFR/stellar mass/metallicity; Davé et al., 2020), measured by 4MOST and the wealth of available photometric data, over 9 Gyr of cosmic history.

The role of feedback in regulating the gas reservoir of galaxies

MeerKAT will identify star formation and AGN activity across the bulk of cosmic history with a single, unified dataset, unbiased by obscuration. ORCHIDSS will enable us to relate that accretion and SFR to gas properties. With kinematic constraints on both the ionised gas (via optical emission/absorption lines) and neutral gas components providing direct evidence of outflows, we will explore the complex interplay between star formation/AGN fuelling, activity and feedback for the multi-phase warm gas in galaxies.

Legacy value

ORCHIDSS will enable a huge range of additional science. For example, the combination of large optical spectro-

scopic samples and MeerKAT’s spectral sensitivity will also enable unique measurements of the baryonic Tully-Fisher relation (McGaugh et al., 2000). Moreover, we will probe extreme star formation and galaxy mergers using OH megamasers (Glowacki et al., 2022), with the ORCHIDSS spectra providing both robust disambiguation of HI and OH spectral detections and enabling OH stacking measurements. More broadly, our survey has also been planned with significant legacy value in mind, including but not limited to:

- A complete census of AGN and star formation activity in the Legacy Survey of Space and Time Deep Drilling Fields (DDF). The large and complete samples of AGN observed over the four DDF will allow us to study whether and how key properties of the AGN correlate with host properties like stellar mass and star formation history, as well as with environment and redshift. By enabling robust source classification down to the faintest limits of the radio continuum luminosity function, ORCHIDSS and MeerKAT combined will provide a highly complete, obscuration-free picture of the cosmic accretion and star formation histories since the epoch of peak galaxy formation.
- A platform for the Square Kilometre Array Observatory (SKAO). The spectroscopic samples provided by ORCHIDSS are designed to facilitate HI science beyond the nominal detection limits of MeerKAT. However, as the full 4MOST surveys are completing, the SKAO will be coming into the first stages of operation. The results obtained by ORCHIDSS and MeerKAT will be essential in defining the scope for future SKA HI surveys. Furthermore, as the fields with the best ancillary multiwavelength data in the southern hemisphere, the ORCHIDSS fields will be the natural targets for future SKA deep continuum and HI surveys. Pre-existing spectroscopy will therefore offer huge legacy value for many years to come, as we move from the broad statistical constraints possible with MeerKAT and ORCHIDSS to the resolved 21 cm and radio continuum studies of individual galaxies with the SKA.

Target selection and survey area

Given the strong correlation between SFR and gas mass (Catinella et al., 2018), and that radio continuum provides an obscuration-free tracer of the ongoing SFR, radio continuum surveys offer an extremely efficient means of selecting an HI-rich population. ORCHIDSS will obtain spectra of a highly complete sample of galaxies selected on the basis of their MeerKAT radio continuum fluxes, with additional photometric redshift cuts limiting the sample to redshifts where the 21 cm emission line falls within the available frequency coverage.

The extent and locations of the ORCHIDSS survey fields (illustrated in Figure 1) are defined by the footprint of the deep MeerKAT extragalactic surveys, including MIGHTEE (which overlaps and extend beyond the four DDF) and the very deep LADUMA field (CDFS) outlined above, supplemented with the MeerKAT Fornax Survey (MFS). The survey is split into two tiers:

- ORCHIDSS Deep will extend the spectroscopic coverage of the four WAVES Deep Drilling fields to higher redshifts and fainter optical magnitudes, targeting $\sim 120\,000$ radio continuum detections down to the flux limit of the MIGHTEE survey ($S_{1.3\text{ GHz}} \geq 15\ \mu\text{Jy}$) that have photometric redshifts $z_{\text{phot}} < 1.4$.
- ORCHIDSS Wide will target a further $\sim 75\,000$ radio-detected sources at $z_{\text{phot}} < 0.57$ within the remaining area of the full MIGHTEE and MFS footprints (green shaded areas in Figure 1), doubling the cosmological volume in which sensitive HI constraints can be made at $z < 0.57$ and enabling critical measurements of the dependence of HI content across the full range of cosmic environments.

Across both tiers, our sample will be complete down to the typical SFR of Milky Way-like galaxies across their respective redshift ranges and complete for all powerful AGN, regardless of obscuration. Our sample selection and scientific goals are carefully chosen to complement existing and planned spectroscopic surveys and to maximise the synergy with current and future radio facilities in the southern hemisphere.

Spectral success criteria and survey figure of merit

The primary requirement for individual ORCHIDSS spectra is the measurement of a high-confidence spectroscopic redshift. Given that, our spectral success criteria will match those of the WAVES 4MOST Consortium survey (Driver et al., 2019), with a requirement that a redshift be measured by the 4MOST Extragalactic Analysis pipeline with $> 90\%$ confidence. We note that while our planned sample selection does not include an explicit optical magnitude cut, the selection based on activity ensures that redshift confirmation remains efficient, with over 90% of targets meeting the success criteria within the maximum exposure times of three and seven hours (Wide and Deep respectively).

Finally, since ORCHIDSS science is driven by maximising the spectroscopic completeness within a limited target sample, our figure of merit (FoM) is defined such that $\text{FoM} = 0.5$ at 90% completeness.

Acknowledgements

The authors acknowledge funding from the European Union’s Horizon 2020 programme, the UK STFC (via grants ST/W003120/1 and ST/V000624/1) and the Leverhulme Trust.

References

- Bigiel, F. et al. 2011, *ApJL*, 730, L13
 Blyth, S. et al. 2016, *Proc. of Science*, 277 (MeerKAT2016), 4
 Catinella, B. & Cortese, L. 2015, *MNRAS*, 446, 3526
 Catinella, B. et al. 2018, *MNRAS*, 476, 875
 Chowdhury, A., Kanekar, N. & Chengalur, J. N. 2022, *ApJ*, 937, 103
 Davé, R. et al. 2020, *MNRAS*, 497, 146
 Driver, S. P. et al. 2019, *The Messenger*, 175, 46
 Glowacki, M. et al. 2022, *ApJL*, 931, L7
 Heywood, I. et al. 2022, *MNRAS*, 509, 2150
 Kereš, D. et al. 2005, *MNRAS*, 363, 2
 McGaugh, S. S. et al. 2000, *ApJL*, 533, L99
 Pan, H. et al. 2020, *MNRAS*, 491, 1227
 Somerville, R. S. & Davé, R. 2015, *ARA&A*, 53, 51

4MOST Complete Calibration of the Colour-Redshift Relation (4C3R2)

Daniel Gruen¹
 Jamie McCullough^{2,3,1}
 Alexandra Amon^{4,5}
 Gary Bernstein⁶
 Jan Luca van den Busch⁷
 Rebecca Canning⁸
 Francisco Castander^{9,10}
 Joseph DeRose¹¹
 William Hartley¹²
 Hendrik Hildebrandt⁷
 Konrad Kuijken¹³
 Jochen Liske¹⁴
 Daniel Masters¹⁵
 Ramon Miquel^{16,17}
 Andrea Pocino Yuste^{9,10}
 Aaron Roodman^{2,3}
 Stella Seitz¹
 Roberto Saglia¹
 Daniel Stern¹⁸
 Luca Tortorelli¹
 Angus H. Wright⁷

¹ University Observatory, Faculty of Physics, Ludwig Maximilians University, Munich, Germany

² Kavli Institute for Particle Astrophysics and Cosmology, Stanford University, USA

³ SLAC National Accelerator Laboratory, USA

⁴ Institute of Astronomy, University of Cambridge, UK

⁵ Kavli Institute for Cosmology, University of Cambridge, UK

⁶ Department of Physics & Astronomy, University of Pennsylvania, USA

⁷ German Centre for Cosmological Lensing, Astronomical Institute, Faculty of Physics and Astronomy, Ruhr University Bochum, Germany

⁸ Institute of Cosmology and Gravitation, University of Portsmouth, UK

⁹ Catalunya Institute of Space Studies, Barcelona, Spain

¹⁰ Institute of Space Sciences (ICE, CSIC), Barcelona, Spain

¹¹ Lawrence Berkeley National Laboratory, Berkeley, USA

¹² Department of Astronomy, University of Geneva, Switzerland

¹³ Leiden Observatory, Leiden University, the Netherlands

¹⁴ Hamburg Observatory, University of Hamburg, Germany

¹⁵ IPAC, California Institute of Technology, USA

¹⁶ Institute of High-Energy Physics, Barcelona Institute of Science of Technology, Spain

¹⁷ Catalan Institution for Research and Advanced Studies, Barcelona, Spain

¹⁸ Jet Propulsion Laboratory, California Institute of Technology, USA

Accurate knowledge of the redshift distributions of faint samples of galaxies selected by broad-band photometry is a prerequisite for future weak lensing experiments to deliver precision tests of our cosmological model. The most direct way to measure these redshift distributions is spectroscopic follow-up of representative galaxies. For this to be efficient and accurate, targets have to be selected such that they systematically cover a space defined by apparent colours in which there is little variation in redshift at any point. 4C3R2 will follow this strategy to observe over 100 000 galaxies selected by their KiDS-VIKING *ugriZYJK_s* photometry over a footprint identical to that of the WAVES survey, to constrain the colour-redshift relation with high multiplicity across two-thirds of the colour space of future Euclid and Rubin samples.

Scientific context: the colour-redshift relation for weak lensing surveys

Our cosmological model predicts the growth of large-scale structure to be highly sensitive to the densities and fundamental physical laws of the different constituents of cosmic energy density, among them the elusive dark matter, dark energy, and massive neutrinos. Photometric surveys can directly probe the large-scale matter density distribution via the apparent distortion of the shapes of galaxy images. These distortions are caused by tidal gravitational forces that act on the distant galaxy's light along its path to us, the so-called weak gravitational lensing effect. The strength of the distortion depends not only on the matter distribution these experiments intend to measure, but also on the distances to the lensed galaxies. This has motivated the development of a range of techniques to not just estimate photometric redshifts but also accurately calibrate the redshift distributions of photometrically selected

samples of galaxies (see, for example, Newman & Gruen, 2022 for a review). The direct determination of the redshift distribution with spectroscopy is advantageous in multiple ways. However, present samples of spectroscopic redshifts allow for a calibration of galaxy distances that is only scarcely sufficient for the ongoing lensing experiments (Hildebrandt et al., 2021; Myles et al., 2021; Rau et al., 2022). The currently required calibration uncertainties on the mean redshift are of order $|\Delta z| \sim 0.01$. But the next generation of surveys by Euclid, Vera C. Rubin Observatory, and the Nancy Grace Roman Space Telescope are predicted to need an order of magnitude improvement, with the calibrated mean redshift accurate to a few parts in a thousand and stringent requirements as well on the calibration of the width of redshift distributions. We will thus be severely limited in testing cosmological models unless large, systematically selected and highly complete spectroscopic samples can be obtained.

Complete calibration of the colour-redshift relation

Direct calibration of redshift distributions (for example, Hildebrandt et al., 2017) effectively consists of making a histogram of spectroscopic redshifts. For this estimate of the redshift distribution to be unbiased, the spectroscopic sample has to be representative of the set of galaxies in question that results from some photometric selection. For the estimate to be of sufficiently small statistical uncertainty, the spectroscopic sample has to be collected over a large enough volume and with high multiplicity. With current instruments this is prohibitively demanding of exposure time for weak lensing source galaxy samples. This is not just because the galaxies in these samples are faint and thus their spectroscopic redshifts difficult to acquire. In addition, the large variation in the redshifts of galaxies selected from noisy, few-broadband photometry means (i) that incompleteness can strongly bias the sample if the success of a spectroscopic observation depends on the redshift of a targeted galaxy (for example, Gruen & Brimiouille, 2017), and (ii) that a very large number of randomly sampled spectroscopic redshifts is required to achieve a sufficiently small

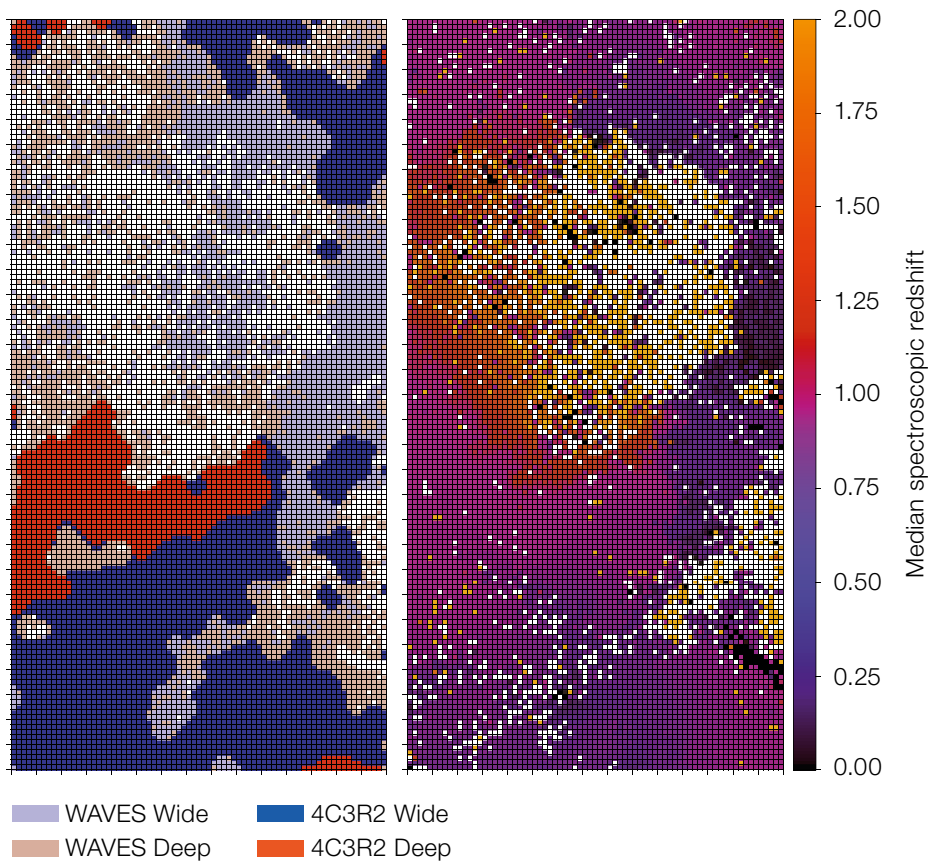


Figure 1. The $ugriZYJHK_s$ colour space of galaxies is discretised by the self-organising map (SOM) of Masters et al. (2015) that is shown in two ways here. The left panel illustrates which cells of the SOM constitute the colour selections for 4C3R2-Wide/Deep and parts of colour space covered by the preliminary WAVES-Wide/Deep selections, which are not always

cell-complete. The right panel shows the median redshift of existing archival samples across the same SOM. Of importance for our selections are the $z = 0.2$ and $z = 0.8$ transitions where WAVES-Wide/Deep become incomplete by design, and above which 4C3R2 selects representative subsets of galaxies for targeting.

statistical error (for example, Newman & Gruen, 2022, their section 3.3).

A much more efficient strategy is to bin galaxies by colour in a set of bands such that in each bin there is as little scatter in redshift and as little evolution of redshift with apparent magnitude as possible. A technique that has been used for this extensively in the literature involves so-called self-organising maps (SOMs). These are few-dimensional grids of colour values contiguously embedded into the high-dimensional space of observed galaxy colours. The embedding is optimised in such a way that each galaxy can be assigned to a grid cell with small colour separation. Figure 1 shows the SOM of Masters et al. (2015). By appropriately sampling each bin, i.e., each cell of the

map, relatively few spectroscopic observations of relatively bright galaxies constrain the statistical relation between colour and redshift. For surveys observing in a smaller or slightly different set of photometric bands, or observing at higher noise levels, any selection of galaxies can still be approximately expressed as a linear combination of the original SOM cells, and thus its redshift calibration can be related to the SOM's colour-redshift relation (Buchs et al., 2019; Myles et al., 2021). This has motivated a set of optical and near-infrared spectroscopic surveys to sparsely cover the cells of this particular SOM (Masters et al., 2017, 2019; Euclid Collaboration et al., 2020), in addition to survey data from the Dark Energy Spectroscopic Instrument (McCullough et al., in preparation). The right panel of

Figure 1 shows the state of spectroscopically calibrating the median redshift across this SOM. The achievable effective resolution of this map is limited by photometric noise in the observing survey, as galaxies can scatter (also asymmetrically) between neighbouring cells.

Specific scientific goals: densely probe galaxy colour space with 4MOST spectra

The observing programmes outlined above have the common goal of a complete calibration of the colour-redshift relation (C3R2) and this survey adds a 4MOST component to that effort. Approximately two thirds of the colour bins defined by C3R2 (Masters et al., 2015) contain galaxies bright enough to achieve high redshift completeness with 4MOST spectroscopy in a feasible exposure time. Unlike many of the deep, sparse surveys performed so far, 4MOST offers the unique possibility of achieving high multiplicity in each of these cells, i.e., to probe the full distribution of redshift given colour. This will allow us to address pressing questions about redshift calibration with the colour-SOM method, such as whether the presence of rare redshift outliers at a given observed colour is a relevant effect. It also allows the dependence of redshift on magnitude at fixed colour to be accurately tested and calibrated. The latter is critical for utilising the relatively bright subset of galaxies observed spectroscopically for calibrating the redshift distributions of faint, photometric samples of equal colour. The resulting sample will form the broad basis for a wedding-cake C3R2 strategy that continues to require 8-metre-class and/or infrared spectroscopy for the parts of colour and magnitude space inaccessible to 4MOST.

Target selection and survey area: synergies with KiDS-VIKING and WAVES

Photometry in the $ugriZYJHK_s$ bands from the Kilo-Degree Survey and the VISTA Kilo degree Infrared Galaxy survey (KiDS-VIKING) provides the basis for selecting targets across a highly informative colour space and over an unprecedented volume for a photometric redshift calibration survey. 4C3R2 does this from

the same photometric catalogue and over the same area as the Wide Area Vista Extragalactic Survey (WAVES), spanning more than 1170 square degrees (Driver et al., 2019). Unlike the high completeness strategy of WAVES, 4C3R2 requests only a small subset of the potential targets. This allows for flexible fibre assignment and a high degree of synergy. The two surveys are currently optimising their joint selection through simulations, including an exploration of whether entirely disjoint target selections or partial overlap between the two surveys' samples is the most efficient option. The preliminary choice of the limiting magnitude of $z = 21.6$ in 4C3R2-Wide is slightly deeper than WAVES, with a $z = 22$ selection in 4C3R2-Deep that matches WAVES-Deep. The left panel of Figure 1 depicts the colour selection of 4C3R2 targets for both the wide and deep surveys. Cells that contain WAVES targets, estimated according to existing photometric redshifts, are indicated by light colours. 4C3R2 intentionally does not select from areas in the map that are dominated by low-redshift

galaxies, for example the low-redshift ($z < 0.2$) filament that runs across the right half of the left panel of Figure 1. This results in a complementary proposal of acquiring redshifts that are representative (4C3R2) by colour and magnitude where they cannot be complete (as for the WAVES selection) for as much of the physical manifold of colour and redshift as possible. Specifically, 4C3R2 aims to sample targets from cells whose redshifts have a high probability of being within the range of $0.2 < z < 1.55$ in wide, and similarly $0.8 < z < 1.55$ in deep. The lower limit is motivated by the WAVES selection, while the upper limit is constrained by spectroscopic features redshifting out of 4MOST's sensitivity wavelength range. While colour-redshift calibration is the primary purpose of 4C3R2, the survey data will thus also optimally complement WAVES. 4C3R2 empirically determines the targeting incompleteness of WAVES over the redshift ranges the latter intends to cover. In addition, the 4C3R2 sample extends the subset of galaxy evolution science cases that can be studied with

representative but incomplete sampling over a wider redshift range and to somewhat fainter objects.

Acknowledgements

This work was funded by the Deutsche Forschungsgemeinschaft (DFG, German Research Foundation) under Germany's Excellence Strategy – EXC-2094 – 390783311. DG (daniel.gruen@lmu.de) and JM (jmccull@stanford.edu) as corresponding authors acknowledge support by the Bavaria California Technology Center (BaCaTeC).

References

- Buchs, R. et al. 2019, MNRAS, 489, 820
 Driver, S. P. et al. 2019, The Messenger, 175, 46
 Euclid Collaboration et al. 2020, A&A, 642, A192
 Gruen, D. & Brimiouille, F. 2017, MNRAS, 468, 1, 769
 Hildebrandt, H. et al. 2017, MNRAS, 465, 1454
 Hildebrandt, H. et al. 2021, A&A, 647, A124
 Masters, D. et al. 2015, ApJ, 813, 53
 Masters, D. C. et al. 2017, ApJ, 841, 111
 Masters, D. C. et al. 2019, ApJ, 877, 81
 Myles, J. et al. 2021, MNRAS, 505, 4249
 Newman, J. A. & Gruen, D. 2022, ARAA, 60, 363
 Rau, M. M. et al. 2022, arXiv:2211.16516

Zdeněk Berdon (berdon.cz)/ESO



In this picture, Venus is shining brightly over ESO's La Silla Observatory in Chile. The picture was taken just before dawn, towards the East, and also features the diffuse zodiacal light — sunlight scattered by dust particles in the Solar System. The three domes to the left of the road are the BlackGEM

telescopes, built by Radboud University, the Netherlands Research School for Astronomy (NOVA), and KU Leuven in Belgium. BlackGEM will search for the afterglow of some of the most dramatic events in the Universe, such as the collision of black holes and neutron stars.

CHANCES: A CHileAN Cluster galaxy Evolution Survey

Christopher Haines¹
 Yara Jaffé²
 Nicolás Tejos³
 Antonela Monachesi⁴
 Emanuela Pompei⁵
 Alexis Finoguenov⁶
 Cristóbal Sifón³
 Sebastian Lopez⁷
 Amrutha Belwadi Manjunatha¹
 Lawrence Bilton^{2,3}
 Johan Comparat⁸
 Rodrigo Cuellar⁷
 Giuseppe D'Ago⁹
 Ricardo Demarco¹⁰
 Ciria Lima-Dias⁴
 Elismar Lösch¹¹
 Paola Merluzzi¹²
 Analía Smith Castelli^{13,14}
 Laerte Sodre¹¹
 Erik Vinicius¹¹
 and the CHANCES team

¹ University of Atacama, Copiapó, Chile

² University of Valparaíso, Chile

³ Pontificia Universidad Católica de Valparaíso

⁴ University of La Serena, Chile

⁵ ESO

⁶ University of Helsinki, Finland

⁷ University of Chile, Santiago, Chile

⁸ Max Planck Institute for Extraterrestrial Physics, Germany

⁹ Pontificia Universidad Católica de Chile

¹⁰ University of Concepción, Chile

¹¹ University of São Paulo, Brazil

¹² INAF–Capodimonte Astronomical Observatory, Naples, Italy

¹³ La Plata Institute of Astrophysics (CONICET–UNLP), Argentina

¹⁴ National University of La Plata, Argentina

CHANCES, the CHileAN Cluster galaxy Evolution Survey, will study the evolution of galaxies in and around ~ 150 massive galaxy clusters, from the local Universe out to $z \sim 0.45$. It will target $\sim 300\,000$ $r_{\text{AB}} < 20.5$ galaxies with 4MOST, providing comprehensive spectroscopic coverage of each cluster out to $5r_{200}$ in synergy with eROSITA. Its wide and deep scope will trace massive and dwarf galaxies from the surrounding filaments and groups to the cores of galaxy clusters, enabling the study of galaxy pre-processing and the role of the evolving environment on galaxies. We will also study the effect of clusters

on the cold circumgalactic medium by targeting 50 000 cluster–QSO pairs.

Scientific context

Understanding what drives the evolution of galaxies and determines whether they end up as star-forming spirals or quiescent early-type galaxies by the present day remains a fundamental task within astrophysics. Both internal energetic mechanisms (like active galactic nucleus feedback or stellar winds) and external environmental processes are expected to play major roles in transforming galaxies. While most isolated galaxies remain as gas-rich star-forming spirals to the present day, the bulk of galaxies within massive clusters have lost their gas and have been transformed into quiescent elliptical or lenticular galaxies. A variety of physical mechanisms capable of transforming galaxies as they fall into the clusters have been proposed, including gas stripping by the intracluster medium (ICM; for example ram-pressure stripping and starvation), and gravitational interactions among galaxies or between the galaxies and the cluster (Boselli & Gavazzi, 2006; Cortese, Catinella & Smith, 2021).

Adding to the complexity is the fact that the matter distribution in the Universe evolves dynamically within a web-like large-scale structure in which filaments connect and feed massive galaxy clusters located at their nodes. These structures are composed of dark matter and galaxies, as well as diffuse matter that dominates the baryon budget. In this picture, each galaxy is surrounded by a multi-phase, metal-enriched, and diffuse circumgalactic medium (CGM) shaped by the interplay between accretion from the intergalactic medium and feedback processes occurring within galaxies. Any attempt to comprehend galaxy formation and evolution must therefore measure observational signatures of galaxy and CGM properties against a wide range of environments — both locally and on large scales.

There is a growing appreciation of the need to place massive galaxy clusters in their full cosmological context, not only to explain their own growth and assembly, but also to understand the evolution of their member galaxies. A corollary of the

current concordance Λ CDM cosmology is that galaxy clusters continue to grow with cosmic time, doubling their masses since $z \sim 0.5$. In fact, a large fraction of cluster galaxies were accreted within galaxy groups (McGee et al., 2009) and filaments (Kuchner et al., 2020), which can ‘pre-process’ the galaxies prior to entering the cluster (Zabludoff et al., 1996). Recent observations have confirmed that significant pre-processing of galaxies is indeed required (Haines et al., 2015; Bianconi et al., 2018), but large homogeneous studies that are both deep and wide are still rare. Hydrodynamical simulations of galaxies around massive clusters find a systematic depletion of both hot and cold gas in cluster galaxies caused by ram-pressure stripping, that translates into a lower fraction of star-forming galaxies as far out as $\sim 5r_{200}$ from the host cluster, where r_{200} is the virial radius inside which the average density is 200 times the critical density (Bahé et al., 2013), motivating large-scale environmental studies.

CHANCES¹, the CHileAN Cluster galaxy Evolution Survey, is a 4MOST community survey designed to uncover the relationship between the formation and evolution of galaxies and hierarchical structure formation as it happens, through deep and wide multi-object spectroscopy. It will target cluster galaxies out to $5r_{200}$, the distance at which environmental effects acting on infalling galaxies are expected to be sufficient to start removing their extended hot gas atmospheres, starving them of future gas, and well beyond the maximum distance of $2\text{--}3r_{200}$ to which ‘back-splash’ galaxies can reach. CHANCES will permit the effects of pre-processing of galaxies in infalling X-ray groups and filaments (detectable by eROSITA) to be quantified in unprecedented detail. The survey will also have an important legacy value, by providing detailed spectroscopic information which will complement X-ray observations of clusters and groups by eROSITA, and future radio observations by the Square Kilometre Array and the Australian SKA Pathfinder (ASKAP), as well as current and planned large optical surveys such as the DESI Legacy Survey DR10 (LSDR10), the Southern Photometric Local Universe Survey (S-PLUS) and the Legacy Survey of Space and Time (LSST).

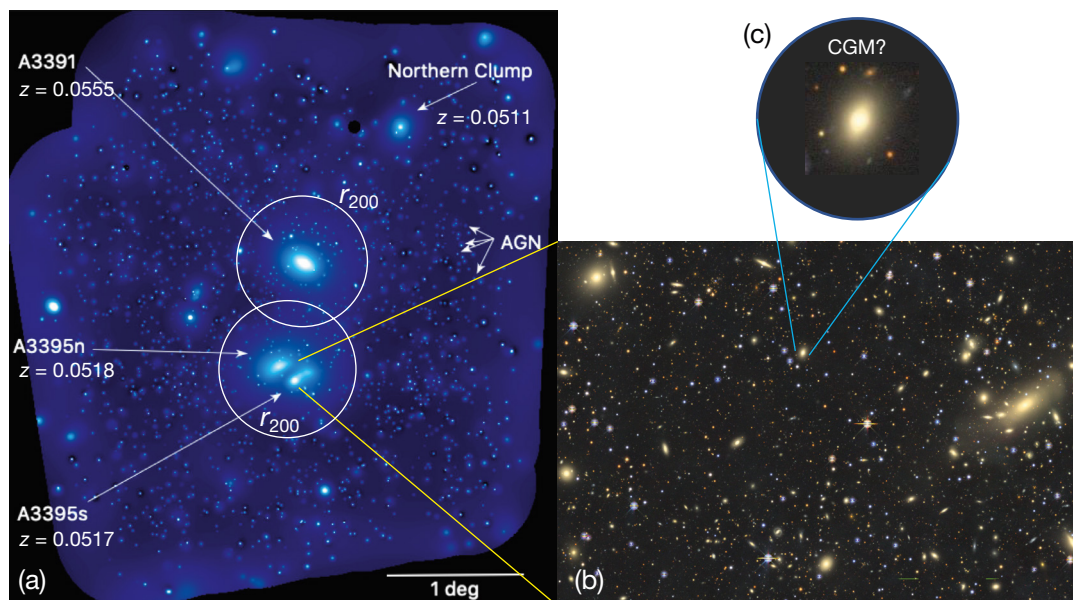


Figure 1. An example of a CHANCES target from the Low- z sub-survey: the A3391/A3395 galaxy cluster system at $z \sim 0.05$ observed by eROSITA (panel a; from Reiprich et al., 2021) and Legacy Survey DR10 (panel b; from *Sky Viewer*). The large-scale structure around the system and the many substructures visible are ideal laboratories in which to study the effect of pre-processing of galaxies. Panel c represents our CHANCES-CGM sub-survey (although at $z > 0.35$), in which we explore the effect of the environment in the circumgalactic medium (CGM) of galaxies, poorly understood to date.

Specific scientific goals

CHANCES comprises three sub-surveys, described below, each with different scientific objectives.

The CHANCES Low- z sub-survey will quantify the impact of environment on galaxies from high masses ($10^{11} M_{\odot}$) down to the dwarf regime ($10^{8-9} M_{\odot}$). Dwarf ellipticals (dE) are the numerically-dominant population in galaxy clusters (Binggeli, Sandage & Tammann, 1988). Their formation via cluster-related processes and evolution remains largely unexplored outside local clusters such as Virgo and Fornax (for example, Eigenthaler et al., 2018; Choque-Challapa et al., 2021), as is their evolution in the infall regions beyond r_{200} .

This sub-survey will provide a large-scale homogenous spectroscopic dataset for galaxies covering more than three orders of magnitude in stellar mass, in and around a representative sample of clusters. It will enable us to constrain many open questions, including: the efficiency of cluster mechanisms transforming galaxies; the timescales for quenching star formation; the long-term survivability of dwarfs in groups and clusters; the role of pre-processing in groups and filaments; and the contribution of galaxy disruption to intracluster light. There is also a natural synergy with ongoing and future HI sur-

veys from ASKAP and MeerKAT, since most HI detections from these surveys will be from dwarf galaxies, owing to their high gas fractions. Their large HI discs are highly susceptible to gas and tidal stripping processes, making HI a sensitive trace of environmental effects.

The CHANCES Evolution sub-survey aims to continuously track the evolution of cluster galaxies over the last four billion years, and measure when, where and how quickly spiral galaxies are being transformed in and around clusters. Cluster galaxies have not always been as inactive as they are at the present epoch. The fraction of blue (star-forming) galaxies among cluster members increases from almost zero in the local Universe to 20% by $z \sim 0.4$ (the Butcher-Oemler effect; Butcher & Oemler, 1984), implying a rapid evolution in the cluster galaxy population. Moreover, since more than half of the galaxy populations of local clusters were only accreted after $z \sim 0.4$, the transformation of star-forming spirals into quiescent early-types as they encounter group or cluster environments is mostly taking place at late epochs. The previous large cluster galaxy evolution surveys (WINGS, LoCuSS) were limited to a single epoch, while attempts to track the evolution of cluster galaxies over $0 < z < 0.5$ have had to resort to aggregating heterogeneous datasets from the literature, and with only a handful of clus-

ters beyond $z = 0.3$. While WINGS and LoCuSS have allowed us to quantify where galaxies are being transformed within clusters and on what timescales at a single epoch, CHANCES will permit us to extend these analyses over four billion years of cosmic time within a single overarching survey.

The CHANCES CGM sub-survey will study the effect of group and cluster environments on the diffuse gaseous content of galaxies traced by MgII absorption towards projected QSOs at redshifts $0.35 < z < 0.7$. Although MgII probes cold (10^4 K) gas, given that the CGM is multi-phase, it provides a good opportunity to test models of gas disruption in clusters as a function of cluster- and absorber-centric distances (for example, Dutta, Sharma & Nelson, 2022). CHANCES CGM is similar to the ‘quasars behind clusters’ survey (Lopez et al., 2008), the difference being that special attention is given to biases and selection effects by positioning fibres not only in cluster-selected sightlines but also on control samples. In addition, and in contrast to what has been previously done, CHANCES CGM will also provide a wealth of information on the projected population of galaxies close to the QSO sightlines over CGM scales. Results from this survey will have implications for the relation between dark matter halos and the properties of galaxies in these dense and

extreme environments, and for the overall population of MgII systems.

Target selection

CHANCES targets are taken from the LSDR10 outside the Galactic plane ($|b| > 20^\circ$).

The CHANCES Low- z survey will target 50 clusters at $z < 0.07$ and with a mass range of 10^{13} – $10^{15} M_\odot$, as well as large regions around known superclusters such as Shapley and Horologium-Reticulum, each containing > 20 clusters within a rich cosmic web.

The cluster sample is X-ray selected, using latest cluster samples that combine a reanalysis of ROSAT all-sky X-ray survey data, detecting X-ray emission for unresolved sources (CODEX; complete down to the flux level of 2×10^{-13} ergs s^{-1} cm^{-2} ; Finoguenov et al., 2020) and extended sources on scales of 6–24 arcminutes (CODEX3; complete down to 6×10^{-13} ergs s^{-1} cm^{-2} ; Finoguenov et al., in preparation) with the redMaPPer cluster red sequence finder applied to LSDR10. We essentially select the most massive clusters applying a redshift-dependent mass threshold, and add lower-mass clusters randomly, preferring clusters with auxiliary data. Our sample includes well-studied clusters such as those from the WINGS survey, and the nearby Fornax and Hydra clusters. An example of a low-redshift target, the galaxy cluster system A3391/A3395 at $z \sim 0.05$, is shown in Figure 1.

For each cluster, 4MOST targets are first selected from the LSDR10 (Figure 1b) as galaxies brighter than $r_{AB} = 20.5$ and within $5r_{200}$ of the cluster centre. To improve the efficiency of observing cluster members rather than background galaxies, we use photometric redshifts from S-PLUS (Mendes de Oliveira et al., 2019) that is imaging ~ 8000 deg 2 of the southern sky in 12 optical bands to $r_{AB} \sim 21$ using the T80-South 0.8-metre telescope at Cerro Tololo Inter-American Observatory in Chile. The S-PLUS photometric system has been shown to deliver much more accurate photometric redshifts than standard broadband surveys and has been shown to be particularly effective at

selecting members of $z \sim 0.05$ clusters with photometric redshift uncertainties of $\sim 0.02(1+z)$ at $r_{AB} \sim 19.7$ (Lima et al., 2022). Additionally, we have been carrying out our own T80 observing programmes to cover those $z \sim 0.05$ clusters outside the S-PLUS main survey footprint, including the entirety of the Shapley supercluster. For brighter cluster galaxies we require spectra with signal-to-noise ratios greater than 20 \AA^{-1} in the continuum to permit velocity dispersions and stellar population parameters to be measured, while the spectral requirement for the faintest low-surface brightness dwarf galaxies will be to measure a redshift.

The CHANCES Evolution sub-survey will target 50 of the most massive galaxy clusters distributed evenly over $0.07 < z < 0.45$. We use the second Planck catalogue of Sunyaev–Zeldovich sources (PSZ2; Planck Collaboration et al., 2016), which provides a homogenous sample of massive clusters over this redshift range, selecting the 50 most massive galaxy clusters in four redshift intervals. At $0.2 < z < 0.45$ this corresponds to $M_{200} > 7 \times 10^{14} M_\odot$, while at lower redshifts the mass limit is progressively reduced to account for the smaller volume available. Most of the CHANCES Evolution cluster sample is covered by the CHEX-MATE XMM Heritage programme (Arnaud et al., 2021), providing high-quality X-ray data suitable for characterising the ICM and mass distribution of each CHANCES cluster.

To select probable cluster members and exclude foreground/background galaxies and stars we use infrared photometry. Specifically, we use the linear relation in the $(J-K)$ vs. K colour–magnitude diagram, which has been demonstrated to be bias-free with respect to star formation activity (Haines et al., 2009). For this purpose, CHANCES Evolution clusters have been observed with VIRCAM on the 4-metre VISTA telescope at Paranal. In addition to the $J-K$ selection, we require targets to have $r_{AB} < 20.5$, to lie within $5r_{200}$ of each cluster, and to have a signal-to-noise ratio greater than 5 \AA^{-1} in the continuum to be sure of obtaining a reliable redshift measurement.

The CHANCES CGM sub-survey is composed of three main selections:

i) targeted MgII in clusters already identified from the SDSS at Dec. $< +5^\circ$ and corresponding control samples; ii) blind MgII searches in clusters targeting QSOs (confirmed and candidates) in the southern sky covered by different 4MOST surveys; and iii) targeting QSOs behind CHANCES Evolution clusters. In all of these we target not only the QSOs but also $r_{AB} < 20.5$ galaxies within ~ 1 arcminute (Figure 1c) around each QSO sightline probing relevant CGM scales. For the QSOs we aim at a signal-to-noise greater than 10 \AA^{-1} in the continuum, allowing us to reach MgII absorption down to 0.3 \AA rest-frame equivalent width, a regime where MgII strongly correlates with the presence of galaxies.

Acknowledgements

YJ, AM, RD, CS, and GD acknowledge funding from ANID BASAL Project No. FB210003. CPH, CS and AM acknowledge funding from FONDECYT Regular projects 1211909, 11191125 and 1212046, respectively. CLD acknowledges support by Joint Committee ESO-Government of Chile 2022. LSJ acknowledges support from CNPq (308994/2021-3) and FAPESP (2011/51680-6). ASC acknowledges funding from Agencia I+D+i (PICT 2019-03299) and CONICET (PIP 1504) and thanks Rodrigo Haack, Amanda Reis Lopes and Luis Angel Gutierrez Soto for their help in selecting Fornax targets.

References

- Arnaud, M. et al. 2021, *A&A*, 650, A104
Bahé, Y. M. et al. 2013, *MNRAS*, 430, 3017
Bianconi, M. et al. 2018, *MNRAS*, 473, L79
Binggelli, B., Sandage, A. & Tammann, G. A. 1988, *ARA&A*, 26, 509
Boselli A. & Gavazzi G. 2006, *PASP*, 118, 517
Butcher H. & Oemler A. 1984, *ApJ*, 285, 426
Choque-Challapa, N. et al. 2021, *MNRAS*, 507, 6045
Cortese, L., Catinella, B. & Smith, R. 2021, *PASA*, 38, 35
Dutta, A., Sharma, P. & Nelson, D. 2022, *MNRAS*, 510, 3561
Eigentaler, P. et al. 2018, *ApJ*, 855, 142
Finoguenov, A. et al. 2020, *A&A*, 638, A114
Haines, C. P. et al. 2009, *ApJ*, 704, 126
Haines, C. P. et al. 2015, *ApJ*, 806, 101
Kuchner, U. et al. 2020, *MNRAS*, 494, 5473
Lima, E. V. R. et al. 2022, *A&C*, 38, 100510
Lopez, S. et al. 2008, *ApJ*, 679, 1144
McGee, S. L. et al. 2009, *MNRAS*, 400, 937
Mendes de Oliveira, C. et al. 2019, *MNRAS*, 489, 241
Planck Collaboration et al. 2016, *A&A*, 594, A27
Reiprich, T. H. et al. 2021, *A&A*, 647, A2
Zabludoff, A. I. et al. 1996, *ApJ*, 466, 104

Links

¹ CHANCES website: <https://chances.uda.cl/>

Chilean AGN/Galaxy Extragalactic Survey (ChANGES)

Franz E. Bauer^{1,2}
 Paulina Lira³
 Timo Anguita^{4,2}
 Patricia Arevalo⁵
 Roberto Assef⁶
 Felipe Barrientos¹
 Trystyn Berg⁷
 Santiago Bernal⁵
 Fuyan Bian⁸
 Médéric Boquien⁹
 Veronique Buat¹⁰
 Igor Chilingarian^{11,12}
 Paolo Coppi¹³
 Demetra De Cicco¹⁴
 Yaherlyn Diaz⁶
 Kirill Grishin^{15,12}
 Lorena Hernandez-Garcia^{2,5}
 Darshan Kakkad¹⁶
 Ivan Katkov^{17,12}
 Jens-Kristian Krogager¹⁸
 Elena López-Navas⁵
 Laura N. Martínez-Ramírez^{1,2}
 Chiara Mazzucchelli⁶
 Veronica Motta⁵
 Federica Ricci¹⁹
 Claudio Ricci⁶
 Alejandra Rojas^{9,6}
 Benedict Rouse¹
 Paula Sánchez-Sáez⁸
 Victoria Toptun¹²
 Ezequiel Treister¹
 Fabio Vito²⁰

¹ Pontificia Universidad Católica de Chile, Santiago, Chile

² Millennium Institute of Astrophysics, Pontificia Universidad Católica de Chile, Santiago, Chile

³ University of Chile, Santiago, Chile

⁴ Universidad Andrés Bello, Santiago, Chile

⁵ Universidad de Valparaíso, Chile

⁶ Diego Portales University, Santiago, Chile

⁷ Milan-Bicocca University, Italy

⁸ ESO

⁹ University of Antofagasta, Chile

¹⁰ Marseille Astrophysics Laboratory, France

¹¹ Center for Astrophysics, Harvard and Smithsonian, USA

¹² Sternberg Astronomical Institute, M.V. Lomonosov Moscow State University, Russia

¹³ Yale University, New Haven, USA

¹⁴ Federico II University of Naples, Italy

¹⁵ APC Laboratory, University of Paris, France

¹⁶ Space Telescope Science Institute, Baltimore, USA

¹⁷ New York University Abu Dhabi, UAE

¹⁸ Lyon Astrophysics Research Centre, France

¹⁹ Roma Tre University, Italy

²⁰ INAF-OAS, Bologna, Italy

4MOST-ChANGES will target a legacy sample of active galactic nuclei (AGN), based on optical continuum variability and spectral energy distribution (SED) selection from several existing surveys, and ultimately complemented by Rubin LSST to: 1) constrain the low- M_{BH} , low- L/L_{Edd} end of the accretion and black hole (BH) density functions to $z \sim 1$, and, by extension, BH seed models; 2) investigate correlations among AGN (M_{BH} , L/L_{Edd} , ultraviolet slope, outflows, variability) and host properties (stellar age, metallicity, kinematics); 3) confirm/characterise rare BH subsamples (extreme variability, tidal disruption events, lensed, intervening absorption line systems) for detailed multi-wavelength follow-up studies.

Scientific context

The last ~ 60 years have seen us go from discovering the first black hole (BH) in Cygnus X-1 to detecting $\geq 10^6$ supermassive BHs (SMBHs, $\geq 10^5 M_{\odot}$) and hundreds of intermediate-mass BH (IMBHs, $\sim 10-10^5 M_{\odot}$) candidates across the Universe (for example, Greene, Strader & Ho, 2020; Flesch, 2021). Nevertheless, critical portions of the active galactic nuclei (AGN) discovery space remain poorly explored. The overwhelming majority of published AGN optical spectra ($\geq 600\,000$; for example, Pâris et al., 2018) stem from the galaxy ($z \leq 0.1$) or quasi-stellar object (QSO, $M_B < -23$; blue-colour-selected) samples of the Sloan Digital Sky Survey (SDSS), and hence have poor overlap with key southern hemisphere observatories (for example, the Very Large Telescope [VLT] and the Atacama Large Millimeter/submillimeter Array). And while SDSS has likely discovered ~ 80% of bright type 1 QSOs with $i_{\text{AB}} < 19$ out to $z \sim 2$ (where the BH accretion density peaks; for example, Aird et al., 2015), fainter and/or redder AGN ($g-r > 0.6$; for example due

to weaker accretion, lower AGN-to-host light ratios, broad absorption lines and modest dust obscuration) have yet to be systematically targeted in large numbers beyond $z \sim 0.1$. More inclusive selection techniques based on variability and/or ultraviolet–mid-infrared (UV–MIR) spectral energy distributions (SEDs) have been shown to be more effective than optical colours alone (for example, Peters et al., 2015; Tie et al., 2017; Sánchez-Sáez et al., 2019) in selecting such ignored AGN populations. Yet the largest spectroscopically confirmed variability-selected samples number $\sim 13\,000$ AGN from SDSS Stripe 82 (~ 14% reddened fraction; Peters et al., 2015) and 1263 AGN from the Dark Energy Survey (DES) supernova fields (6% reddened fraction; Tie et al., 2017), probing a tiny fraction of the parent population. More recent studies with La Silla-QUEST (LSQ) and the Zwicky Transient Facility (ZTF) to $r_{\text{AB}} \sim 20-21$ recover reddened fractions of 10–15% (for example, Sánchez-Sáez et al., 2019), while deeper high-cadence VLT Survey Telescope (VST) imaging in COSMOS and CDF-S to $r_{\text{AB}} \sim 23.5$ (for example, De Cicco et al., 2021) identify ~ 300 variability-selected AGN deg^{-2} , with reddened AGN fractions of ~ 30% (the majority of which notably have X-ray fluxes below the eROSITA all-sky survey limit). The latter studies imply that the SDSS and DES variability samples still suffer strong biases and represent just the tip of the iceberg of a much larger population awaiting confirmation with 4MOST.

Among upcoming surveys, the Vera C. Rubin Observatory (Rubin) Legacy Survey of Space and Time (LSST) is expected to have a truly profound impact on AGN science. With its ~ 18 000- deg^2 footprint, *ugrizy* coverage (0.4–1 μm), ~ 1–3-day temporal sampling, and $r_{\text{AB}} \sim 24.5$ single-epoch 5σ -depth, the LSST will produce a high-purity sample of $> 2 \times 10^7$ AGNs between $z = 0$ and $z = 7$, with $> 50\%$ identified in the first 1–2 years. Such numbers will quickly surpass past/current AGN samples, extending to lower luminosities, higher extinction $E(B-V) \sim 0.3-1$, and higher z , and enlarging rare AGN samples. Each AGN will ultimately have ≥ 800 visits (≥ 130 per filter) over the 10-year survey, enabling unique analyses. Deep LSST *ugrizy* imaging, particularly in concert with Euclid *YJHK* imaging, will

Subsurvey Name	Area (deg ²)	Parent sample (Completeness)	Limiting magnitude	Selection notes
W_VARZ+W_VARG+W_VARL	> 10 ⁴	~ 1.5 × 10 ⁶ (60%)	$r \sim 21$	Variability from ZTF, Gaia, LSQ
W_SED	> 10 ⁴	~ 1.8 × 10 ⁶ (35%)	$r \sim 22.5$	DELVE+VHS+WISE
W_MUL	> 10 ⁴	~ 4 × 10 ⁵ (50%)	$r \sim 20.5$	2+ visits, > 6 months apart
W_HIZ	> 10 ⁴	~ 3 × 10 ⁴ (75%)	$i, z \sim 22.5$	$z > 4$
D_ALL	16	~ 1 × 10 ⁴ (90%)	$r \sim 23$	X-ray, MIR, radio, optical
T_TDE + T_TDEHOST	> 10 ⁴	~ 3 × 10 ⁴ (3%/50%)	$r \sim 21$	TDEs + Hosts
T_LST	> 10 ⁴	~ 2 × 10 ⁵ (25%)	$r \sim 22.5$	EVAGN, LLAGN
T_LEN	> 10 ⁴	~ 3 × 10 ³ (75%)	$r \sim 22.5$	QSO + lens galaxy

Table 1. Properties and selection criteria of the ChANGES subsurveys.

offer relatively accurate photometric redshifts and spatially resolved SEDs for a substantial fraction of its anticipated $\sim 2 \times 10^9$ extragalactic detections. This will ultimately allow statistical comparisons between AGN and inactive galaxies across redshift, environment, luminosity, and some (deblended) host properties. However, in order to extract detailed physical constraints (for example precise stellar properties, BH masses, accretion rates, line kinematics), and to study accretion physics and address fundamental evolutionary questions, spectroscopy is required. To this end, the Chilean AGN/Galaxy Extragalactic Survey (ChANGES) will acquire ≈ 1.79 Mhrs of 4MOST low-resolution spectroscopy for a large, representative sample of AGN within the LSST footprint ($\gtrsim 10\,000$ deg²), selected primarily via variability and optical/NIR/MIR SEDs from existing imaging data within the LSST’s footprint.

Target selection and survey area

Table 1 specifies our current survey design, indicating the survey regions and input catalogues. The selection functions for our two primary samples are driven by variability features and full optical-MIR SED modelling, respectively, allowing us to overcome past optical colour selection biases. Target completeness is further weighted by the relative number of targets across bins of colour, estimated redshift/luminosity, and variability timescale and amplitude. The variability sample is based on ZTF-DR11, Gaia-DR3, and LSQ data using machine-learning selection (for example, Sánchez-Sáez et al., 2021), aiming to observe $\sim 60\%$ of sources from

a sample of $\sim 1.5 \times 10^6$ AGN with $r_{AB} \leq 21$. Our SED selection derives from DELVE-DR2, VHS-DR6, VIKING-DR2, and catWISE2020 data using SED-fitting techniques (for example, Assef et al., 2010; Boquien et al., 2019), aiming for $\sim 30\%$ coverage from a target pool of $\sim 1.8 \times 10^6$ AGN with $r_{AB} \leq 23$. We augment these samples with $\sim 10\,000$ multi-wavelength selected AGN in four 4MOST/LSST deep-drilling fields (DDFs) and $\sim 150\,000$ host-dominated AGN or unique BH-related phenomena selected using the LSST’s unparalleled variability constraints during its first few years of operation (see below). The resulting spectroscopic observations will characterise a large, representative population of relatively unobscured (i.e., potentially reddened), lower- M_{BH} , low- M_{BH}/M_{host} -ratio, and/or lower- L/L_{Edd} AGN out to $z \sim 0.5-1$, that have yet to be well sampled by any other method, owing to weaker emission and host domination.

Specific scientific goals

BH accretion rate (BHAR) and M_{BH} densities, evolution and host synergies. The moderately accreting AGN sample to be probed by ChANGES ($10^{-4} < L/L_{Edd} < 10^{-1}$; see Figure 1) comprises $\sim 50-80\%$ of the estimated total mass accretion onto BHs in type 1 and mildly obscured AGN and strongly complements other 4MOST AGN samples. The sample will be used to characterise the low- L/L_{Edd} and low-mass contributions to the BHAR and M_{BH} density distributions and push several landmark $z \leq 0.1$ constraints out to $z \sim 0.5-1$, as functions of several, potentially interdependent, driving parameters (for example redshift, M_{BH} , L/L_{Edd} , M_* , SFR, morphology, gas content, M_{halo} , and environment). We aim to assess in better detail where

and how lower-mass BH growth occurs (as input for the next-generation Event Horizon Telescope, Athena, and LISA), and quantify the role of downsizing and feedback processes in the establishment of AGN scaling relations.

Novel time-domain spectral synergies.

AGN vary on nearly all timescales. Our experimental design will yield 4MOST spectra for up to $\sim 1.2 \times 10^6$ AGN, which when combined with intensively sampled LSST multi-colour light curves will: 1) relate their variability and SED/spectral properties; 2) enable precision measurement of continuum lags for type 1 AGN; 3) gain insight into the unobservable far-UV regime based on the emission-line strengths of high ionisation species; and 4) extend our database of labelled systems to optimise the LSST’s photometric classification and redshifts. We seek to observe $\sim 20\%$ of the variability-selected AGN sample (all with $r_{AB} < 19$ and 50% with $19 < r_{AB} < 20$) at least twice, to systematically study spectral variations in tandem with the LSST’s unprecedented optical monitoring. Our large samples will cover a broad span of AGN physical (z , M_{BH} , L/L_{Edd}) and variability (amplitude and characteristic timescale of their light curves) parameter spaces, allowing examination of how AGN spectral properties vary across these parameters and how they comply with standard accretion disc predictions. Differences for low- M_{BH} vs. low- L/L_{Edd} AGN may probe when and how AGN transition to advection-dominated accretion flows.

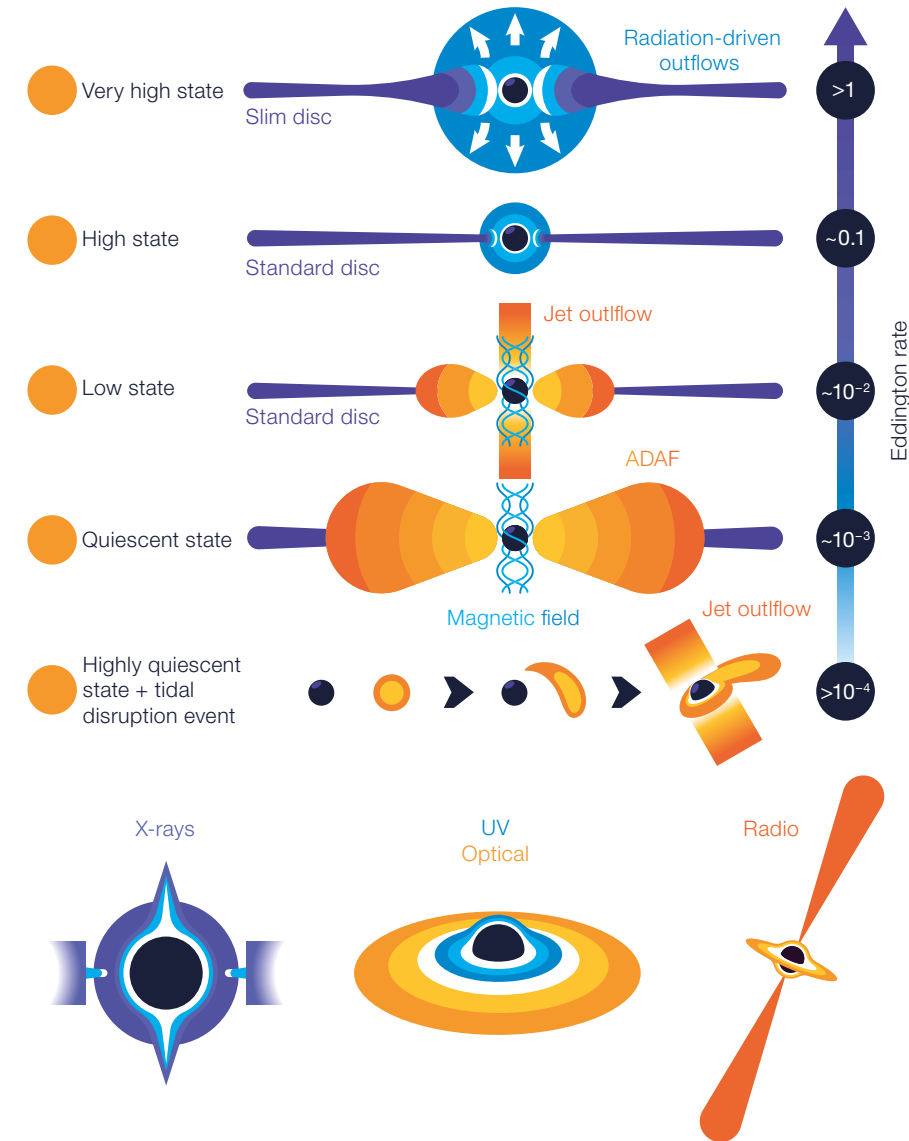
Completeness and obscured fraction corrections. Although the optical-MIR selection of ChANGES will cover a wide parameter space, it will still suffer from various forms of incompleteness (for example, ability to recover redshifts,

detect spectral features, discern AGN types in severely host-dominated sources) and be biased against heavily obscured AGN. To correct for these, ChANGES will carry out deeper observations in the DDF regions for both optical variability+SED selected AGN (HSC/VST/DES) to assess completeness and obscured AGN samples from X-rays (XMM-SERVS), MIR (SERVS) and radio (MIGHTEE/EMU) to estimate obscured fractions as functions of, for example, z , M_{BH} , L/L_{Edd} , M_* .

Changing-type/EVAGN. Current samples of extreme variability AGN (EVAGN; $\Delta m/\Delta t > 1 \text{ mag yr}^{-1}$) number in the thousands (for example, Luo, Shen & Yang, 2020; López-Navas et al. 2023), with the LSST expected to uncover orders of magnitude more. ChANGES will prioritise up to $\sim 100\,000$ such targets for single (and when feasible, multi-epoch) spectra to establish an unprecedented sample for studies of detailed accretion physics and constraints on ‘changing-type’ AGN (Graham et al., 2020). The latter can be compared to a well-characterised search for changing-type AGN among $\geq 200\,000$ targets with high-signal-to-noise multi-epoch splits from ChANGES’ Time-Domain Spectral Synergy campaign to establish absolute rates.

Tidal disruption events (TDEs). TDEs provide important constraints on the physics and demographics of quiescent SMBHs and their hosts, but only ~ 60 have been well characterised to date (for example, Gezari, 2021). The LSST is expected to find ~ 6000 TDEs a year to $z \sim 0.5$ ($r_{\text{AB}} \sim 23.5 \text{ mag}$), providing much larger samples with which to understand their demographics and triggering. ChANGES aims to prioritise ~ 1000 high-confidence TDEs below $z \sim 0.2$ for direct confirmation and characterise $\sim 15\,000$ TDE hosts (measuring velocity dispersions for a brighter subset). Of particular interest will be IMBH-TDEs from compact stars and white dwarfs, which should be less luminous and shorter than TDEs from SMBHs.

High-redshift AGN. Moderate- L_{bol} AGN at $z > 4$ are a key population for constraining BH formation models and early evolution (Volonteri et al., 2017). Yet the current $z > 4$ QSO luminosity function is



pinned down by just a few hundred objects at $-24 < M_{1450} < -30$ (for example, McGreer et al., 2018), leaving the faint-end slope and evolution highly uncertain; uncertainties rise further beyond $z \sim 5$, since classical colour selection techniques break down because of confusion with stars. ChANGES will target $\sim 12\,000$ $z > 4$ candidates, selected via optical-MIR photometry and/or variability, to improve statistics particularly for fainter AGN.

Lensed AGN. The LSST will discover thousands of strongly lensed QSOs out to high redshift, enabling novel constraints on, for example, accretion processes,

Figure 1. The distinct types of accreting SMBHs we expect to detect with 4MOST-ChANGES (super L/L_{Edd} , high- L/L_{Edd} , low- L/L_{Edd} , quiescent + TDE). Credits: J. Utreras/F. Bauer (CATA)

evolution, the initial mass function, cosmology (addressing early vs. late H_0 ‘tension’) and the inner structure of high- z AGN. However, an essential first step for most lensed-AGN-enabled science cases is measurement of both source and lens redshifts. ChANGES aims to spectroscopically confirm ~ 1500 QSOs and lens galaxies, dramatically increasing the number of confirmed QSO lenses in the southern hemisphere.

Intervening quasar absorption-line systems (QALs). QALs are powerful probes of the neutral gas content and metal inflow–outflow in galaxies over cosmic time. Past spectroscopic surveys have provided unprecedented QAL statistics but may potentially be biased against the most gas-rich systems as a result of the blue QSO colour selection (for example, Krogager et al., 2019). The low spectral resolution has also limited the accuracy of metal column densities, which are sensitive tracers of galaxy conditions and cosmic chemical evolution. ChANGES QSOs will be much less biased, providing an unprecedented sample of QALs covering key absorption lines (H α , CIV, SiIV, SIII, CII, OI, MgII, and NaI).

Spectral success criteria and figure of merit

The wide-area surveys aim for signal-to-noise $\geq 10 \text{ \AA}^{-1}$ in one $\sim 1000\text{-\AA}$ blue, green or red window for $r_{\text{AB}} \leq 21$ targets to constrain AGN and host properties (weak lines, stellar continua, etc.), and signal-to-noise $\geq 1 \text{ \AA}^{-1}$ among fainter targets to constrain redshifts only. Within the DDFs, we extend these $\sim 1 \text{ mag}$ deeper. We anticipate a spectroscopic success rate of $\sim 80\%$ for most subsurveys (dropping to $\sim 50\%$ for $z > 5$ AGN). Our overall figure of merit is a weighted combination of each subsurvey, based on achieving the specified completeness limits for the target numbers indicated.

Acknowledgements

This work was funded by: ANID Millennium Science Initiative ICN12_009 (FEB, TA, LHG), CATA-BASAL

FB210003 (FEB, ET, TA, RJA, FB, MB, CR), FONDECYT Regular 1190818 (ET, FEB), 1200495 (FEB, ET), 1230345 (CR), 1201748 (PL), and 1191124 (RJA); RScF 19-12-00281 (IC, KG, IK, VT).

References

- Aird, J. et al. 2015, MNRAS, 451, 1892
 Assef, R. J. et al. 2010, ApJ, 713, 970
 Boquien, M. et al. 2019, A&A, 622, 103
 De Cicco, D. et al. 2021, A&A, 645, A103
 Flesch, E. W. 2021, arXiv:2105.12985
 Gezari, S. 2021, ARA&A, 59, 21
 Graham, M. J. et al. 2020, MNRAS, 491, 4925
 Greene, J. E., Strader, J. & Ho, L. C. 2020, ARA&A, 58, 257
 Krogager, J.-K. et al. 2019, MNRAS, 486, 4377
 López-Navas, E. et al. 2023, MNRAS, 518, 1531
 Luo, Y., Shen, Y. & Yang, Q. 2020, MNRAS, 494, 3686
 McGreer, I. D. et al. 2018, AJ, 155, 131
 Pâris, I. et al. 2018, A&A, 613, A51
 Peters, C. M. et al. 2015, ApJ, 811, 95
 Sánchez-Sáez, P. et al. 2019, ApJS, 242, 10
 Sánchez-Sáez, P. et al. 2021, AJ, 161, 141
 Tie, S. S. et al. 2017, AJ, 153, 107
 Volonteri, M. et al. 2017, ApJ, 849, 155



The Next-Generation Transit Survey (NGTS) is located at ESO's Paranal Observatory in northern Chile. This project is searching for transiting exoplanets — planets that pass in front of their parent star and hence produce a slight dimming of the star's light that can be detected by sensitive

instruments. The telescopes focus on discovering Neptune-sized and smaller planets, with diameters between two and eight times that of Earth. This image shows the NGTS enclosure in the day. The VISTA (right) and VLT (left) domes can also be seen on the horizon.

The 4MOST–Gaia Purely Astrometric Quasar Survey (4G-PAQS)

Jens-Kristian Krogager¹
 Karen M. Leighly²
 Johan Peter Uldall Fynbo^{3,4}
 Kasper Elm Heintz^{3,4}
 Sergei Balashev⁵
 Franz Erik Bauer^{6,7}
 Trystyn Berg^{5,8}
 Hyunseop Choi⁹
 Lise Bech Christensen^{3,4}
 Annalisa De Cia^{10,11}
 Sara Ellison¹²
 Stefan Geier^{13,14}
 Eilat Glikman¹⁵
 Neeraj Gupta¹⁶
 Christina Konstantopoulou¹⁰
 Daria Kosenko⁵
 Cédric Ledoux¹¹
 Sebastian López⁸
 Bo Milvang-Jensen^{3,4}
 Leah Morabito^{17,18}
 Palle Møller^{4,11}
 Pasquier Noterdaeme^{19,20}
 Max Pettini²¹
 Jason Xavier Prochaska^{22,23}
 Sandra Raimundo^{4,25,26}
 Johan Richard¹
 Raghunathan Srianand¹⁶
 Ksenia Telikova^{11,5}
 Donald Terndrup²⁷
 Todd M. Tripp²⁸
 Marianne Vestergaard^{4,24}
 Tayyaba Zafar²⁹

¹ CRAL, University Claude Bernard Lyon 1, ENS of Lyon, France

² Homer L. Dodge Department of Physics and Astronomy, The University of Oklahoma, USA

³ The Cosmic DAWN Center, Denmark

⁴ Niels Bohr Institute, University of Copenhagen, Denmark

⁵ Ioffe Institute, Saint Petersburg, Russia

⁶ Institute of Astrophysics and Centre for Astroengineering, Faculty of Physics, Pontifical Catholic University of Chile, Santiago, Chile

⁷ Millennium Institute of Astrophysics, Santiago, Chile

⁸ Department of Astronomy, University of Chile, Santiago, Chile

⁹ Department of Physics, University of Montreal, Canada

¹⁰ Department of Astronomy, University of Geneva, Switzerland

¹¹ ESO

¹² Department of Physics & Astronomy, University of Victoria, Canada

¹³ Gran Telescopio Canarias, La Palma, Spain

¹⁴ Canary Islands Institute of Astrophysics, Tenerife, Spain

¹⁵ Department of Physics, Middlebury College, USA

¹⁶ Inter-University Centre for Astronomy and Astrophysics, Pune, India

¹⁷ Centre for Extragalactic Astronomy, Department of Physics, Durham University, UK

¹⁸ Institute for Computational Cosmology, Department of Physics, Durham University, UK

¹⁹ Paris Institute of Astrophysics, France

²⁰ French-Chilean Laboratory for Astronomy, Santiago, Chile

²¹ Institute of Astronomy, University of Cambridge, UK

²² Department of Astronomy & Astrophysics, UCO/Lick Observatory, University of California, USA

²³ Kavli Institute for the Physics and Mathematics of the Universe, Kashiwa, Japan

²⁴ Dark Cosmology Centre, Niels Bohr Institute, University of Copenhagen, Denmark

²⁵ Department of Physics and Astronomy, University of California, Los Angeles, USA

²⁶ Department of Physics & Astronomy, University of Southampton, UK

²⁷ Department of Astronomy, The Ohio State University, USA

²⁸ Department of Astronomy, University of Massachusetts, USA

²⁹ Australian Astronomical Optics, Macquarie University, Australia

The 4MOST–Gaia Purely Astrometric Quasar Survey (4G-PAQS) will carry out the first large-scale, colour-independent quasar survey selected solely on the basis of astrometry from Gaia. Our main objective is to quantify the selection effects of current colour-selected samples. These colour-selected samples bias our view of the neutral gas and its chemical enrichment because of dust obscuration and reddening of optical colours. Moreover, the broad absorption-line outflows observed in quasars are under-represented by optical colour selection. 4G-PAQS will provide the first sample to overcome these challenges and will constrain the physical and chemical properties of gas in galaxies and quasars at cosmic noon.

Scientific context

Atomic and molecular gas in galaxies

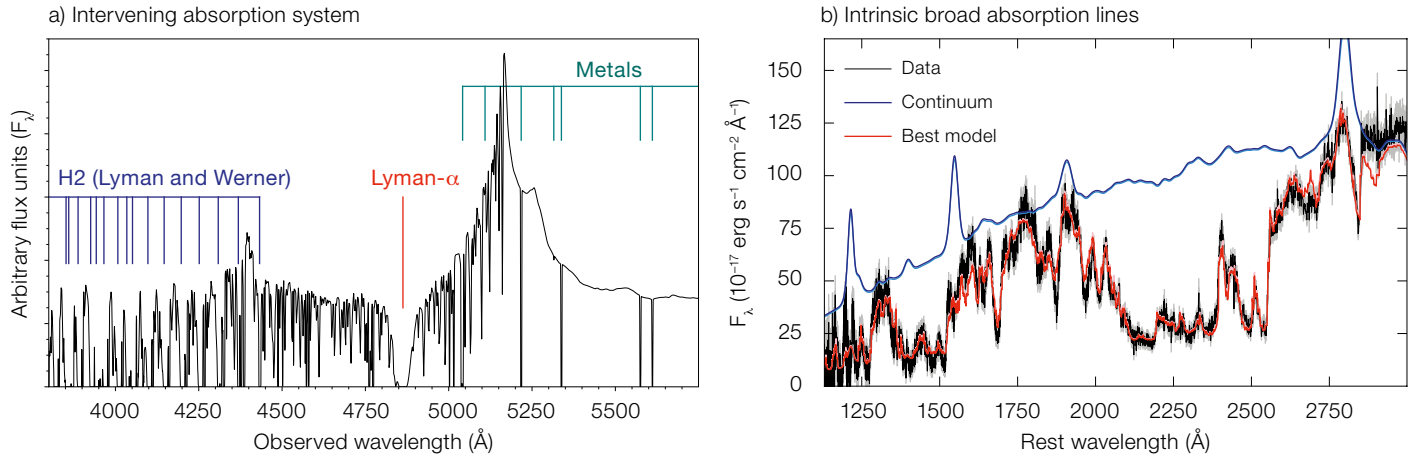
Studying HI absorption in spectra of luminous background sources such as quasars remains the best way to probe neutral hydrogen in individual galaxies beyond the local Universe ($z \geq 0.1$) until the advent of the Square Kilometre Array. Of particular interest for galaxy evolution studies are the so-called Damped Lyman- α Absorbers (DLAs; Wolfe, Gawiser & Prochaska, 2005), whose large HI column densities ($\log[N_{\text{HI}} \text{ cm}^{-2}] > 20.3$) arise in self-shielded, galactic environments. The neutral gas at even higher column densities ($\log[N_{\text{HI}} \text{ cm}^{-2}] \geq 21.5$) is sensitive to many physical processes, such as the formation of molecular hydrogen (H_2) and subsequently star formation (Bird et al., 2014; Noterdaeme et al., 2014).

Another important aspect of galaxy evolution is the buildup of metals over time and their redistribution in and around galaxies. Observations of DLAs offer a precise and model-independent way of measuring metallicities at high redshift through the numerous metal absorption lines observed in optical spectra of distant quasars (Prochaska et al., 2003; De Cia et al., 2018).

Owing to the cross-section selection of absorbers and the insensitivity of the Lyman- α transition to temperature, DLAs probe mostly the warm neutral medium ($T \sim 10^4 \text{ K}$). The cold neutral medium ($T \sim 100 \text{ K}$) is best traced by H_2 , found in only a few percent of the overall DLA population (Balashev & Noterdaeme, 2018). At high redshift, H_2 is directly detectable in optical spectra through Lyman and Werner bands in the rest-frame UV (900–1100 Å). The simulated quasar spectrum shown in Figure 1 (left panel) illustrates the molecular and atomic absorption features expected in our survey.

The impact of dust obscuration

If a significant amount of dust is present in the absorbing gas, the background quasar will appear fainter and redder than it is intrinsically. Quasars with dusty foreground systems are therefore more



likely to fall below the flux limit of optically selected spectroscopic surveys. Such quasar surveys will introduce a bias against dust-rich absorption systems (Pei, Fall & Bechtold, 1991). Since the amount of dust extinction scales with both metallicity and $N(\text{HI})$, the bias against dusty absorbers becomes a bias against high-metallicity and high- $N(\text{HI})$ systems (Pontzen & Pettini, 2009). Targeted searches for quasars reddened by foreground dusty absorbers have found many such cases (Krogager et al., 2015). The impact of dust bias in a purely flux-limited sample can be corrected using statistical modelling; however, current spectroscopic samples (such as SDSS) are also selected based on inhomogeneous optical and near-infrared colour criteria which are not easily corrected for.

Given the complex selection function of current quasar samples, the only way to make progress is by obtaining a reference sample of quasars and DLAs that is free from colour selection. Any foreground dust obscuration effects can then be corrected for in a statistical manner.

Quasar feedback at cosmic noon

Quasars may play an important role in shutting down star formation activity in galaxies and strong outflows are thought to be a key ingredient during quasar activity (Fabian et al., 2012). The broad absorption lines (BALs) observed in the rest-frame UV spectra of quasars are evidence for such powerful winds emerging from the central engine given their large,

blue-shifted velocities. These winds potentially contribute to the co-evolution of black holes and galaxies in a process known as quasar feedback (for example, Glikman et al., 2012 and references therein). Another important population of the overall quasar demographic is composed of intrinsically reddened quasars. These red quasars have moderate reddening ($E(B-V) \sim 0.25\text{--}1.5$ mag), such that their optical spectra are not fully dust obscured and still dominated by an AGN continuum and broad emission lines. Red quasars may represent a distinct evolutionary phase between a merger-driven starburst in a completely obscured AGN, and a normal, unreddened (i.e., blue) quasar (Urrutia, Lacy & Becker, 2008).

Large-scale optical surveys of quasars underestimate the fraction of both BAL quasars (BALQs) and red quasars as a result of the imposed optical-colour criteria (for example, Glikman et al., 2012; Fynbo et al., 2013). This is further supported by studies of radio-selected samples reporting larger numbers of reddened quasars (for example, White et al., 2003) and BALQs (Morabito et al., 2019). The colour-selection effects limit our understanding of the critical role that these objects play in the Universe.

Broad absorption lines and their link to red quasars

Low- and high-ionisation BALQs offer an array of absorption lines between 1020 and 3000 Å (rest-frame) that can be used to constrain the outflow properties (for

Figure 1. Noiseless mock 4MOST quasar spectrum featuring an intervening absorption system at $z = 3$ (left panel). The coloured marks indicate the absorption lines that allow us to quantify the chemical and physical properties of the absorbing gas: Lyman- α , H₂ lines and metal lines. The right-hand panel shows the best-fit synthetic BAL model to the SDSS spectrum of a FeLoBAL quasar allowing us to extract physical outflow parameters such as density, ionisation parameter and outflow velocity (Choi et al., 2020).

example, Leighly et al., 2018). The BAL outflow velocity is observed to correlate with luminosity and because of the strong dependence of outflow energy on velocity (outflow kinetic luminosity, $L_{\text{kin}} \propto v^3$), luminous quasars are potentially the strongest sources of feedback among BALQs.

FeLoBAL quasars — a subset of low-ionisation BALQs — have a myriad of absorption lines from Fe⁺ in their near-UV spectra (see Figure 1, right panel), and therefore they can be studied over a wide redshift range from 0.8 to 4. This range includes the cosmic noon, where feedback may have been especially impactful. Sixty percent of red quasars show BALs in their spectra, nearly all of which are low-ionisation BALs or FeLoBALs.

Specific scientific goals

The goal of 4G-PAQS is to obtain a colour-unbiased reference sample of quasars and their foreground absorbers. With this core sample of quasars, we will address the scientific goals set out below.

The unbiased cosmic mass density of metals from $2 < z < 3$

It has been shown that DLAs trace a significant fraction of metals over cosmic time, reaching $\sim 100\%$ of the inferred metal mass, $\Omega_{\text{Met, TOT}}$, at $z = 4$ (Péroux & Howk, 2020). However, this fraction is observed to decrease with decreasing redshift, based on optically selected samples. The colour-selection criteria of current optical quasar samples introduce a redshift dependence on the dust bias (Krogager et al., 2019) that directly affects the measured cosmic mass density of metals, Ω_{Met} . While Ω_{Met} at $z = 3$ may be underestimated by a factor of around two, this increases to a factor of around three at $z = 2$. Such a redshift-dependent bias would counteract the observed decrease in $\Omega_{\text{Met}} / \Omega_{\text{Met, TOT}}$. Our aim with this survey is to constrain Ω_{Met} as a function of redshift from an unbiased sample of nearly 2000 high-redshift DLAs.

The unbiased absorption cross-section of HI and H₂ at $z > 2$

Current numerical simulations are still unable to reproduce the observed redshift evolution of the HI absorption cross-section as inferred by the so-called line incidence, dn/dz (Bird et al., 2014; Hassan et al., 2020). If a dust bias is present in current observations, it is important to correct for this before drawing conclusions about feedback mechanisms in simulations. Moreover, simulations are only recently starting to resolve the cold (H₂) and warm (HI) neutral media in cosmological volumes (for example, Nickerson, Teyssier & Rosdahl, 2019; Feldmann et al., 2022). Hence, constraining the dn/dz of H₂ and HI in an unbiased sample will provide the first comparison to these new simulations.

What is the true number of BALQs?

Another core goal of 4G-PAQS is to quantify the unbiased, intrinsic fraction of BALQs and the physical conditions of the outflowing material over the redshift range $0.8 < z < 4$. The fraction of BALQs depends on the sample selection: Hewett & Foltz (2003) infer a fraction of 20% in

optically selected samples, but it may be as large as 40%, depending on the source luminosity (Bruni et al., 2019). There is further observational evidence that BALQs are 3.5 times as common at $z = 4$ as at $z = 2$ (Allen et al., 2011). This may be evidence that black hole feedback evolves, something that may be important for constraining feedback models, if the fraction of quasars that have BALs reflects the global covering fraction of the outflowing gas.

What are the gas properties of BAL outflows?

We aim to characterise the physical properties of the outflow in each quasar to obtain better insight into the potential interrelation between individual quasar subtypes (low-ionisation versus high-ionisation BALs and red quasars). This may provide a basis for understanding the link, if present, between each quasar subtype and different galaxy merger stages. We will use our novel spectral synthesis software SimBAL (Leighly et al., 2018) on the sample of BALQs to trace the outflow properties and feedback over cosmic time. An example of the spectral fitting is presented in Figure 1. Depending on the absorption lines present, we can obtain excellent constraints on the physical properties of the winds (ionisation parameter, density) which in turn yield measurements of the outflow properties (location, mass outflow rate, kinetic luminosity; Choi et al., 2020).

What is the true number of red quasars?

We aim to constrain black hole masses and accretion rates and determine the properties and representative fractions of the overall quasar population (red, blue and BAL sub-types). Intrinsically reddened quasars make up $\sim 20\text{--}30\%$ of quasars (Glikman et al., 2012). However, current representative samples are small (~ 150 objects), which makes it difficult to study any redshift evolution of the red quasar population. Since the red quasar phenomenon may be linked to an evolutionary phase with higher accretion rates (Kim et al., 2015), measuring the black

hole masses and accretion rates in a representative, unbiased sample will be crucial for quantifying any redshift evolution. If the red quasar phenomenon is an evolutionary phase, then determining their fraction as a function of redshift would constrain the duration of that phase.

Identifying rare quasars

Lastly, our purely astrometric selection with no assumptions about spectral shape will have significant potential to discover outlying and rare objects that may be overlooked otherwise (Hall et al., 2002; Geier et al., 2019). Our survey aims to identify rare quasars in a representative sample and to quantify the prevalence of such rare objects.

Target selection and survey area

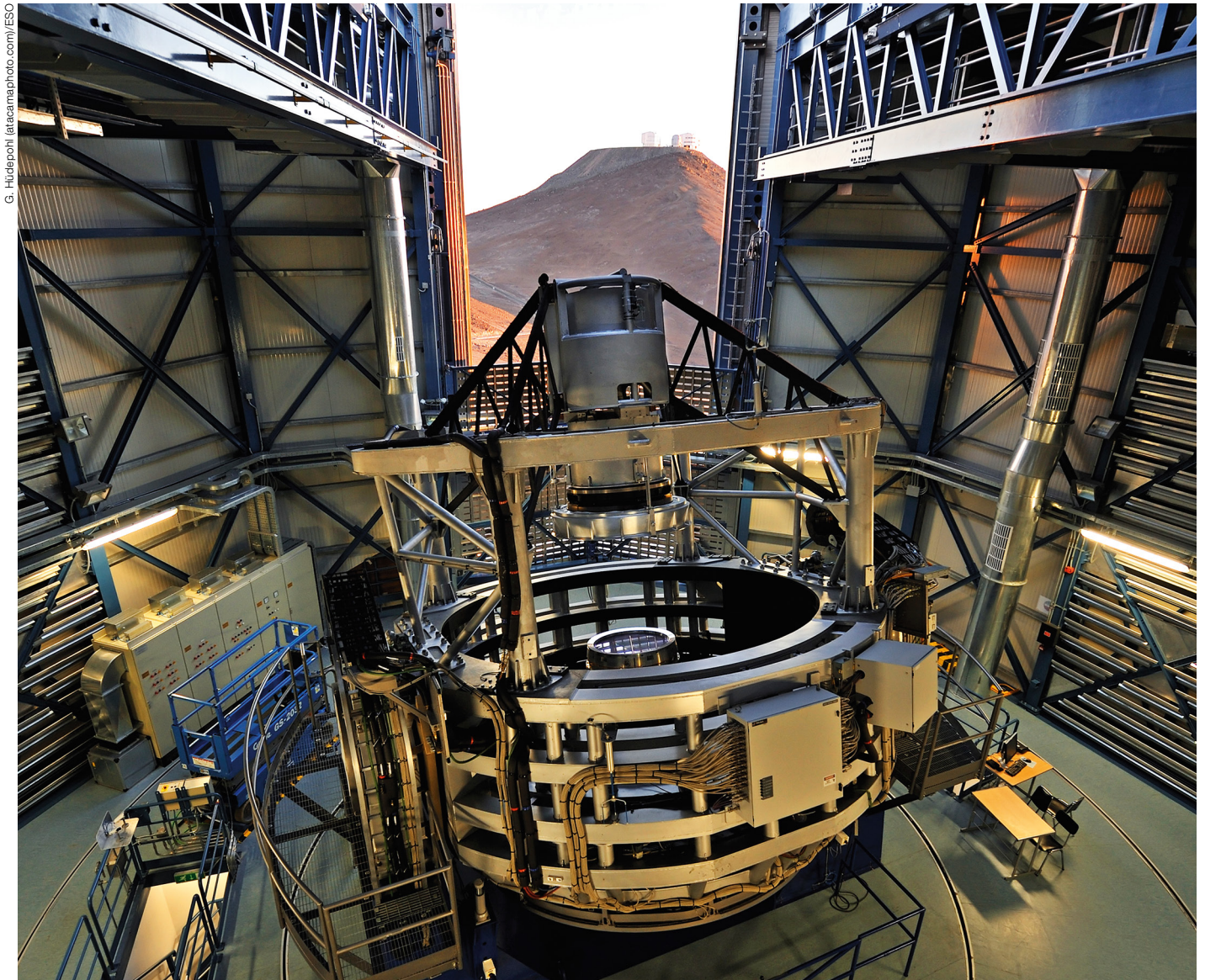
Candidate quasars for 4G-PAQS are selected purely on the basis that quasars are stationary sources on the sky (Heintz et al., 2018). We select sources from the Gaia catalog with proper motions and parallaxes consistent with zero at the 2σ level down to a limit of $G < 20.5$ mag. The completeness of our survey is therefore limited only by the fibre allocation efficiency (up to $\sim 80\%$). However, since the fibre allocation does not depend on the colour of the targets, this lower completeness will not introduce any selection bias.

Since the number of stationary sources in the Gaia catalogue increases drastically when observing close to the Galactic plane, we have limited our survey area to high Galactic latitudes, $b < -60$ deg. Based on a pilot study carried out at the North Galactic Pole (Heintz et al., 2020), we have estimated the stellar contamination to be around 40% over the entire survey area.

In total, 4G-PAQS will obtain a colour-unbiased sample of $\sim 100\,000$ quasars with no prior selection on the basis of redshift or spectral shape. Our sample will therefore be purely flux limited. To reach the above scientific goals, we will obtain spectra with a signal to noise ratio of at least 5 \AA^{-1} over $7700\text{--}8500 \text{ \AA}$.

References

- Allen, J. T. et al. 2011, MNRAS, 410, 860
Balashev, S. A. & Noterdaeme, P. 2018, MNRAS, 478, 7
Bird, S. et al. 2014, MNRAS, 445, 2313
Bruni, G. et al. 2019, A&A, 630, A111
Choi, H. et al. 2020, ApJ, 891, 53
De Cia, A. et al. 2018, A&A, 611, A76
Fabian, A. C. 2012, ARA&A, 50, 455
Feldmann, R. et al. 2022, arXiv:2205.15325
Fynbo, J. P. U. et al. 2013, ApJS, 204, 6
Geier, S. J. et al. 2019, A&A, 625, L9
Glikman, E. et al. 2012, ApJ, 757, 51
Hall, P. B. et al. 2002, ApJS, 141, 267
Hassan, S. et al. 2020, MNRAS, 492, 2835
Heintz, K. E. et al. 2018, A&A, 615, L8
Heintz, K. E. et al. 2020, A&A, 644, A17
Hewett, P. C. & Foltz, C. B. 2003, AJ, 125, 1784
Kim, D. et al. 2015, ApJ, 812, 66
Krogager, J.-K. et al. 2015, ApJS, 217, 5
Krogager, J.-K. et al. 2019, MNRAS, 486, 4377
Leighly, K. M. et al. 2018, ApJ, 866, 7
Morabito, L. K. et al. 2019, A&A, 622, A15
Nickerson, S., Teyssier, R. & Rosdahl, J. 2019, MNRAS, 484, 1238
Noterdaeme, P. et al. 2014, A&A, 566, A24
Pei, Y. C., Fall, S. M. & Bechtold, J. 1991, ApJ, 378, 6
Péroux, C. & Howk, J. C. 2020, ARA&A, 58, 363
Pontzen, A. & Pettini, M. 2009, MNRAS, 393, 557
Prochaska, J. X. et al. 2003, ApJ, 595, L9
Urrutia, T., Lacy, M. & Becker, R. H. 2008, ApJ, 674, 80
White, R. L. et al. 2003, AJ, 126, 706
Wolfe, A. M., Gawiser, E. & Prochaska, J. X. 2005, ARA&A, 43, 861



This spectacular view of the VISTA telescope was taken from the roof of the building during the opening of the enclosure at sunset. The VLT is visible on the neighbouring mountain. VISTA is the largest

survey telescope in the world and it is dedicated to mapping the sky at near-infrared wavelengths. Its primary mirror is 4.1 metres in diameter and is the most highly curved of its size. The extremely high

curvature reduces the focal length, making the structure of the telescope extremely compact. VISTA can map large areas of the sky quickly and deeply.

Transform our Understanding of the Baryon Cycle with High-Resolution Quasar Spectroscopy (ByCycle)

Celine Peroux^{1,2}
 Andrea Merloni³
 Joe Liske⁴
 Mara Salvato³
 Ramona Augustin⁵
 Fabian Balzer³
 Maria-Rosa Cioni⁶
 Johan Comparat³
 Simon Driver⁷
 Alejandra Fresco³
 Antonella Garzilli⁸
 Aleksandra Hamanowicz⁵
 Anne Klitsch⁹
 Jean-Paul Kneib⁸
 Jens-Kristian Krogager¹⁰
 Dylan Nelson¹¹
 Johan Richard¹⁰
 Patricia Schady¹²
 Yue Shen¹³
 Roland Szakacs¹
 Simon Weng¹
 Qian Yang¹⁴
 and the ByCycle team

¹ ESO

² Marseille Astrophysics Laboratory, France

³ Max Planck Institute for Extraterrestrial Physics, Garching, Germany

⁴ University of Hamburg, Germany

⁵ Space Telescope Science Institute, USA

⁶ Leibniz Institute for Astrophysics, Potsdam, Germany

⁷ International Centre for Radio Astronomy Research/University of Western Australia

⁸ École Polytechnique Fédérale, Lausanne, Switzerland

⁹ Dark Cosmology Center, Denmark

¹⁰ CRAL, University Claude Bernard Lyon 1, ENS of Lyon, France

¹¹ University of Heidelberg, Germany

¹² University of Bath, UK

¹³ University of Illinois Urbana-Champaign, USA

¹⁴ Center for Astrophysics Harvard & Smithsonian, USA

The term baryons refers to the normal matter of the Universe. Surprisingly, only a minority of this normal matter (< 10%) can be probed by observations of starlight from galaxies. The ByCycle project aims to study the remaining majority of the baryons traced by the intergalactic gas. To this end, ByCycle will use the

powerful synergy of absorption and emission diagnostics by observing a large sample of background quasars to probe the circumgalactic medium of foreground objects in the same sky regions. The objective of the 2.8-million fibre-hour ByCycle project is ultimately to characterise the physical processes by which gas changes phases and travels into, through, and out of galaxies. Such a study is essential to our understanding of the growth of structure in the Universe.

Scientific context

Astronomers now know the basic constituents of the present Universe: 73% dark energy, 23% dark matter, and 4% baryons. The term baryons is used to refer to the normal matter of the Universe. One of the great successes of the last decades is the excellent agreement between estimates of the total comoving baryon density from Cosmic Microwave Background (CMB) anisotropies (Planck Collaboration et al., 2016), primordial nucleosynthesis (Cooke, Pettini & Steidel, 2018) and fast radio burst dispersion measures (Macquart et al., 2020). However unlocking the physics of the normal matter continues to represent a most intriguing enigma in astrophysics and cosmology. Indeed, although the amount of matter bound in stars grows with time, only a minority of the baryonic material is found there; even today, > 90% of the baryons are found in the gaseous phase of the Universe. Notably, progress in determining the baryons' location and physical state will have an impact beyond understanding the evolution of star formation and galaxies. Indeed, the survival of satellite sub-halos in cosmological hydrodynamical simulations generating orders of magnitude more dwarf galaxies than observed — the 'missing satellites problem' — relates to our capacity to accurately model galactic feedback. Furthermore, baryonic effects impact the dark matter distribution and thus the inference of cosmological parameters from weak lensing surveys (Semboloni et al., 2011; Chisari et al., 2018; Foreman et al., 2020).

From the Big Bang onwards, the baryons collapse with dark matter to form the cosmic web, galaxies, stars and, ultimately,

the planets that we observe. Baryons from the cosmic web accrete onto galaxies and cool into a phase which fuels star formation, which in turn expels material in powerful outflows. The result is a multi-phase medium of pristine and enriched material that lies in the immediate surroundings of galaxies, the so-called circumgalactic medium. More globally, the cosmic baryon cycle describes these processes of motion and phase transformation of the baryons (Tacconi, Genzel & Sternberg, 2020; Peroux & Howk, 2020; Walter et al., 2020).

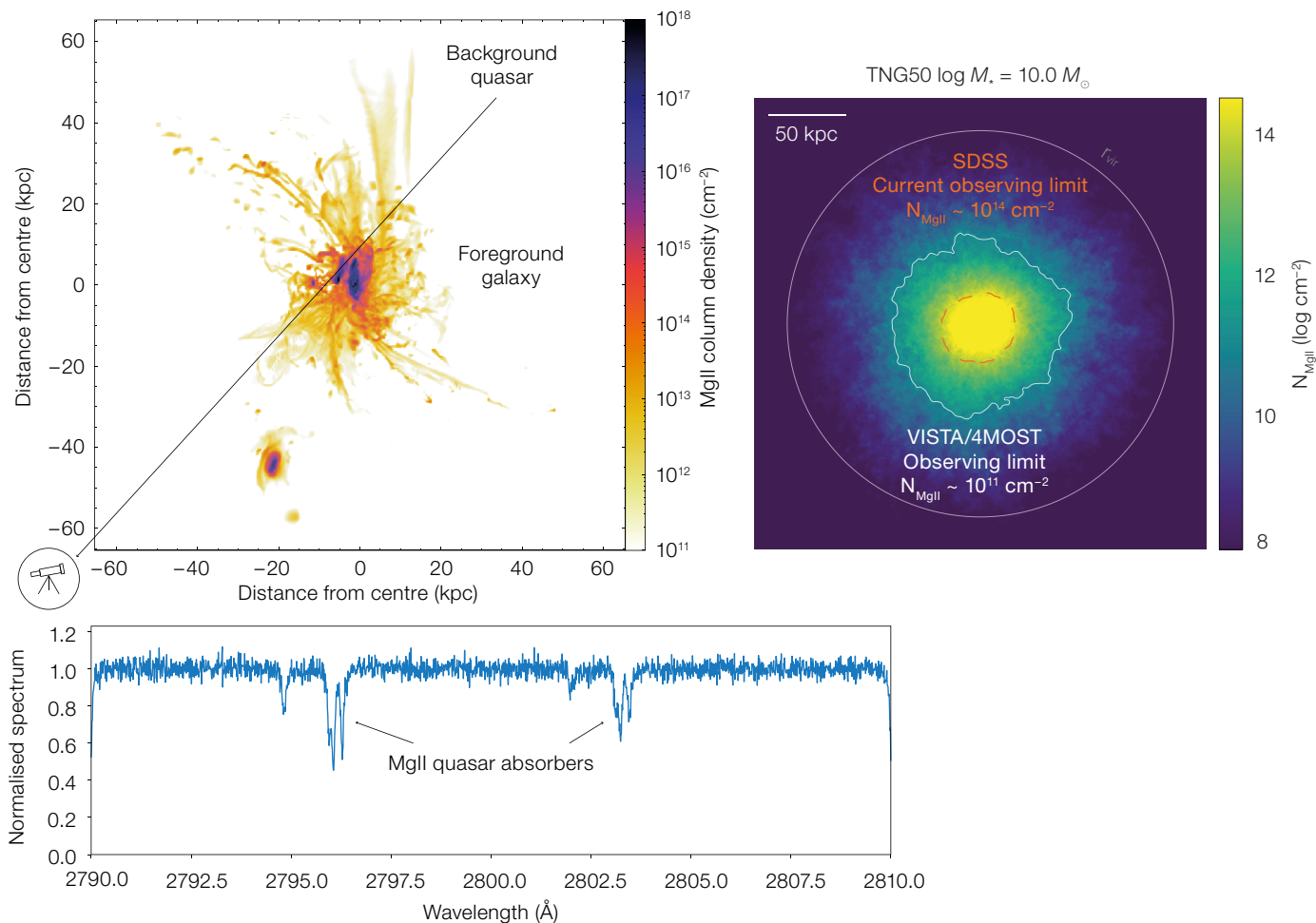
Specific scientific goals

Baryons as a function of time: a census of the cosmic metals

Characterising the relationship between stars, gas and metals is a critical component of understanding the cosmic baryon cycle. Observations of the evolution of metals are key to constraining this global picture of the evolution of the Universe. The early accounting of the total metal budget by Pettini (1999) found an order of magnitude shortfall in the comoving density of observed metals compared with those expected to be produced by the stellar content of the Universe (Madau & Dickinson, 2014; Bouwens et al., 2020; Zavala et al., 2021). The ByCycle project will observe hundreds of thousands of high-redshift quasar spectra with 4MOST at high resolution, providing a robust picture of the metal content of the baryons in the Universe over much of its history.

Baryons as a function of space: characterising the circumgalactic medium

Ultimately, a detailed map of the cool gas component around galaxies will characterise the dominant baryon reservoir associated with forming galaxies, as well as providing constraints on gas flows that are an essential part of the current galaxy formation paradigm (Chen et al., 2021). Recent findings indicate that the circumgalactic medium is a major reservoir of heavy elements with a mass rivaling, and possibly exceeding, that of the galaxies themselves (Peeples et al., 2014). Hence, the gas around galaxies holds valuable



clues to the fueling of star formation and feedback processes. The ByCycle project¹ aims to characterise the circumgalactic medium gas and metals of 1.5 million galaxies, active galactic nuclei, groups and clusters.

Building a sizeable legacy sample

Today, the circumgalactic medium is best probed by the powerful technique of examining the gas in absorption against background sources (such as quasars or gamma-ray bursts) whose lines of sight pass through an identified foreground galaxy's halo. The absorption lines offer the most compelling way to study the distribution, chemical properties and mass budget of the mixed halo gas by probing matter at different densities, metallicities and temperatures (Figure 1, left panels). In these quasar absorbers, the minimum

column density, which is tightly correlated to the volumetric gas density that can be detected (Rahmati et al., 2013), is set by the apparent brightness of the background sources and thus the detection efficiency is independent of the redshift of the foreground host galaxy. Figure 1 (right panel) illustrates the three orders of magnitude gain in magnesium (MgII) column density that will be reached with the ByCycle survey compared to what is available today. We will use the powerful synergy of absorption and traditional emission diagnostics by observing one million background quasars and 1.5 million foreground objects in the same sky regions with 4MOST.

The high-redshift element of ByCycle focuses on several dozen thousand strong Lyman- α absorbers tracing both neutral and ionised gas observed over a large area. The ByCycle high-redshift quasars will be used to probe the

Figure 1. Top left panel: Schematic view of the observational setup. Absorption lines detected against bright background quasars observed with 4MOST high-resolution fibres offer a unique opportunity to study the distribution and chemical properties of the circumgalactic medium gas of foreground galaxies observed with 4MOST low-resolution fibres. The top panel shows results from zoom-in FOGGIE² simulations with exquisite resolution (~ 0.1 kpc scales) in the circumgalactic medium of galaxies (Peebles et al., 2019; Augustin et al., 2021). The ByCycle project is designed to probe the whole range of MgII column densities displayed. The bottom left panel presents a 4MOST normalised mock quasar spectrum with typical rest-frame MgII doublet lines. Right panel: Illustrative TNG50³ simulations of the circumgalactic metal distribution (Szakacs et al., 2023). This is a 2D stack of 200 $z = 0.5$ galaxies like the ones probed by ByCycle. The red contour illustrates the current MgII column density detection limit from SDSS (Anand, Nelson & Kauffmann, 2021), while the white contours correspond to the MgII column density limit of ByCycle. The white circle shows the r_{200} radius, the Virial radius assuming a critical overdensity constant of 200. The ByCycle project will provide an improvement of three orders of magnitude in the MgII column density probed in the extended circumgalactic medium of galaxies, thanks to its large multiplexing capability and spectral resolution of $R = 20\,000$.

Lyman- α absorbers tracing the neutral gas phase and its metal content with the goal of providing a modern metal census. The metal content of gas traced by Lyman- α absorbers will be modelled with the column density of metal ions through Voigt-profile fitting (for example, Quiret et al., 2016). We will determine the dust-corrected and ionised-gas metallicity by performing a full photoionisation modelling (Hamanowicz et al., 2020) informed by the presence of elements with various degrees of ionisation. By counting the number of detected systems of various strengths, we will provide a robust estimate of the number density per unit redshift of strong Lyman- α absorbers which will allow us to calculate their gas mass content, Ω_{gas} . This quantity is also critical for estimates of the meta-galactic ultraviolet background used in radiative transfer models of the high-redshift Universe (Kollmeier et al., 2014; Fumagalli et al., 2017). With the measurements of the metallicity and gas mass, we will directly test whether the strong Lyman- α quasar absorbers at intermediate redshifts do indeed contain the reservoir of missing metals. This novel census of the metal mass density will provide a new perspective on the missing metals problem and existing tensions with models (Yates, Perox & Nelson, 2021).

With the low-redshift part of the ByCycle project, we will crosscorrelate quasar absorbers with galaxies detected in emission in the same fields. The primary targets are magnesium (MgII) quasar absorbers, that trace cooler gas at 10^4 K and whose doublet nature makes their signature in quasar spectra unambiguous. The strong complementarity of absorption and emission diagnostics will be used to characterise the low-density gas which is key to our understanding of galaxy formation and evolution. We will gather a sample of 1 million $z > 0.55$ quasar spectra, exploring the low-density gas traced by 250 000 MgII absorbers. The physical properties of the metal absorbers will be crosscorrelated with up to a million foreground galaxy spectra observed in the same fields (Driver et al., 2019; Richard et al., 2019). An additional 600 000 active galactic nuclei and 20 000 groups and clusters are ideally suited to probing the rarer, denser foreground objects (Merloni et al., 2019);

Finoguenov et al., 2019). These observations will be stacked to measure the radial profile of both Lyman- α gas and metals as a function of galactocentric radii (see left panels of Figure 1 and Turner et al., 2017; Chen et al., 2021). Specifically, we will quantify the covering fraction of the neutral gas and numerous ion species (including MgII and CIV) as a function of impact parameter. We will compute the number density of metal absorbers down to small rest-frame equivalent width, thus probing the most diffuse and extended gas. Together these measurements will put direct limits on the clumpiness of the medium and provide new constraints on the scales of metal mixing in the circumgalactic medium (Nelson et al., 2020; Augustin et al., 2021). These quantities relate directly to the missing satellites problem (Byrohl et al., 2021; Mitchell & Schaye, 2022). Furthermore, these findings will put new constraints on state-of-the-art cosmological hydrodynamic simulations with increased spatial resolution in the circumgalactic medium regions that aim to characterise the physical properties of the gas (van de Voort et al., 2019; Peebles et al., 2019). We will further assess the strength of the absorbers by computing the optical depth of the metal doublets for different phases of the gas from cold, at temperature $T = 10^4$ K (MgII), to warm, at $T = 10^5$ K (CIV). We will locate the gas spatially and in velocity space with respect to the associated foreground galaxies (Turner et al., 2014; Chen et al., 2021). In so doing, we will probe the net effect of inflow and outflow interactions, revealing recycled gas and the history of circumgalactic medium metal enrichment. We will constrain the source of ionisation, the dynamical state of the circumgalactic medium gas and hence the total baryonic content of galaxy halos. We stress that baryonic effects have a significant impact on the distribution of matter, which needs to be incorporated into ongoing and future weak lensing experiments.

Target selection and survey area

The ByCycle survey strategy requires an *a priori* knowledge that the quasar's redshift is greater than $z = 0.55$ to ensure the detection of intervening absorbers along its line of sight within the 4MOST wave-

length coverage. To assess both the nature and redshift of a large sample of targets we revert to a prior, likelihood, and posterior probability in a Bayesian analysis (see Yang & Shen, 2023). The selection algorithm assigns probabilities for quasars, galaxies and stars, and simultaneously calculates photometric redshifts (Salvato, Ilbert & Hoyle, 2019) for all extragalactic sources. We make use of the latest Gaia release (DR3) to classify known stars as well as the most recent DESI Legacy Imaging Survey⁴ (DR10) in concert to estimate photometric redshifts. The comparison of the results with available quasar spectroscopic redshifts confirms that the resulting sample has both high completeness and high purity, securing the requirement of $z > 0.55$. This computation results in a total of 3.2 million quasars within the 4MOST project footprint (for example, with declination $< +5$ deg). To ease scheduling, the ByCycle survey provides targets to choose from a more extended catalogue of sources. In addition, the ByCycle survey has no requirement on completeness, cadence of observations or selection function. Instead, the strategy aims at maximising the number of low- and high-spectral-fibre pairs.

A key component of ByCycle is the sharing of the focal plane with other low-redshift extragalactic surveys. Indeed, ByCycle will combine high-resolution fibre observations of bright background quasars with low-resolution fibre observations of foreground galaxies, active galactic nuclei, groups and clusters that are in the same field. The ByCycle survey comprises both a deep and a wide component. The former is driven by the deep observations that will be carried out by low-resolution galaxy surveys in five distinct cosmological fields. The latter extends to an area designed in synergy with other efforts to cover $> 15\,000$ deg².

In summary, the 2.8-million fibre-hour ByCycle survey will use the powerful synergy of absorption and emission diagnostics by observing a sizeable sample of background quasars and foreground galaxies in the same fields. At high redshift, we will build an unprecedented catalogue of Lyman- α absorbers, measuring their dust-free and ionisation-corrected metallicity to reappraise the missing

metals problem. At late times, we will crosscorrelate high-resolution fibre observations of the quasars with low-resolution spectra of 1.5 million foreground objects (including galaxies) over the same area. From stacked observations, we will measure the radial profile, covering fraction and optical depth of the neutral hydrogen and metals in their circumgalactic medium. Together, these results will provide a robust census of the cosmic metals and refine our view of the circumgalactic medium. This long-lasting legacy dataset will bring high-resolution quasar spectroscopy to a new level — an increase of three orders of magnitude over currently available samples.

Acknowledgements

This work benefited from computing time on the supercomputers at the Max Planck Computing and Data Facility (MPCDF).

References

- Anand, A., Nelson, D. & Kauffmann, G. 2021, *MNRAS*, 504, 65
- Augustin, R. et al. 2021, *MNRAS*, 505, 6195
- Bouwens, R. et al. 2020, *ApJ*, 902, 112
- Byrohl, C. et al. 2021, *MNRAS*, 506, 5129
- Chen, Y. et al. 2021, *MNRAS*, 508, 19
- Chisari, N. E. et al. 2018, *MNRAS*, 480, 3962
- Cooke, R. J., Pettini, M. & Steidel, C. C. 2018, *ApJ*, 855, 102
- Driver, S. P. et al. 2019, *The Messenger*, 175, 46
- Foreman, S. et al. 2020, *MNRAS*, 498, 2887
- Finoguenov, A. 2019, *The Messenger*, 175, 39
- Fumagalli, M. 2017, *MNRAS*, 467, 4802
- Hamanowicz, A. et al. 2020, *MNRAS*, 492, 2347
- Kollmeier, J. A. et al. 2014, *ApJL*, 789, L32
- Quirot, S. et al. 2016, *MNRAS*, 458, 4074
- Macquart, J.-P. et al. 2020, *Nature*, 581, 391
- Madau, P. & Dickinson, M. 2014, *ARA&A*, 52, 415
- Merloni, A. et al. 2019, *The Messenger*, 175, 42
- Mitchell, P. D. & Schaye, J. 2022, *MNRAS*, 511, 2600
- Nelson, D. et al. 2020, *MNRAS*, 489, 2391
- Peeples, M. S. et al. 2014, *ApJ*, 786, 54
- Peeples, M. S. et al. 2019, *ApJ*, 873, 129
- Peroux, C. & Howk, J. C. 2020, *ARA&A*, 58, 363
- Pettini, M. 1999, in *Chemical Evolution from Zero to High Redshift*, ed. Walsh, J. R. & Rosa, M. R. (Berlin: Springer-Verlag), 233

- Planck Collaboration et al. 2016, *A&A*, 594, A13
- Rahmati, A. et al. 2013, *MNRAS*, 430, 2427
- Richard, J. 2019, *The Messenger*, 175, 50
- Salvato, M., Ilbert, O. & Hoyle, B. 2019, *Nature Astronomy*, 3, 212
- Semboloni, E. et al. 2011, *MNRAS*, 417, 2020
- Szakacs, R. et al. 2023, submitted to *MNRAS*
- Tacconi, L. J., Genzel, R. & Sternberg, A. 2020, *ARA&A*, 58, 157
- Turner, M. L. et al. 2014, *MNRAS*, 445, 794
- Turner, M. L. et al. 2017, *MNRAS*, 471, 690
- van de Voort, F. et al. 2019, *MNRAS*, 482, L85
- Yang, Q. & Shen, Y. 2023, *ApJS*, 264, 9
- Yates, R. M., Peroux, C. & Nelson, D. 2021, *MNRAS*, 508, 3535
- Walter, F. et al. 2020, *ApJ*, 902, 111
- Zavala, J. A. et al. 2021, *ApJ*, 909, 165

Links

- ¹ ByCycle project webpage: <http://www.eso.org/~cperoux/ByCycle.html>
- ² FOGGIE webpage: <https://foggie.science/>
- ³ IllustrisTNG simulation project webpage: <https://www.tng-project.org>
- ⁴ DESI Legacy Imaging Surveys: <https://www.legacysurvey.org/>

C. Durany/ESO



This picture shows the grand skies of the Chajnantor plateau in the Chilean Atacama desert. The rare sight of clouds in this typically dry and arid region

creates a dramatic display of reds and blues, as well as a sun pillar — an optical phenomenon caused by ice crystals in the atmosphere — that emanates from

the Sun in line with a telescope. This large antenna is a part of the Atacama Large Millimeter/submillimeter Array (ALMA), which is co-owned by ESO.

The 4MOST Hemisphere Survey of the Nearby Universe (4HS)

Edward N. Taylor¹
 Michelle Cluver²
 Eric Bell³
 Jarle Brinchmann⁴
 Matthew Colless⁵
 H el ene Courtois⁶
 Henk Hoekstra⁷
 Sheila Kannappan⁸
 Claudia Lagos^{9,10,11}
 Jochen Liske¹²
 Elmo Tempel¹³
 Cullan Howlett¹⁴
 Sean McGee¹⁵
 Khaled Said¹⁴
 Rosalind Skelton¹⁶
 Madusha Gunawardhana¹⁷
 Sabine Bellstedt⁹
 Leslie Hunt¹⁸
 Thomas Jarrett¹⁹
 Chris Lidman⁵
 John Lucey²⁰
 Shadab Alam²¹
 Maciej Bilicki²²
 Anna de Graaff²³
 Wojciech Hellwing²²
 Sarah Leslie⁷
 Ilani Loubser²⁴
 Lucia Marchetti^{19,25}
 Michael Maseda²⁶
 Moses Mogotsj¹⁶
 Peder Norberg²⁰
 Alessandro Sonnenfeld²⁷
 Jenny G. Sorce^{28,29,30}
 and the 4HS Team

- ¹ Centre for Astrophysics and Supercomputing, Swinburne University of Technology, Melbourne, Australia
² Department of Physics and Astronomy, University of the Western Cape, South Africa
³ Department of Astronomy, University of Michigan, USA
⁴ Institute of Astrophysics and Space Science, University of Porto, Portugal
⁵ Research School of Astronomy & Astrophysics, Australian National University, Canberra, Australia
⁶ Lyon Institute of Physics of the 2 Infinities, University of Lyon, France
⁷ Leiden Observatory, Leiden University, the Netherlands
⁸ Department of Physics and Astronomy, The University of North Carolina at Chapel Hill, USA
⁹ International Centre for Radio Astronomy Research, University of Western Australia, Perth, Australia

- ¹⁰ ARC Centre of Excellence for All Sky Astrophysics in 3 Dimensions, Australia
¹¹ Cosmic Dawn Center, Denmark
¹² Hamburg Observatory, University of Hamburg, Germany
¹³ Tartu Observatory, University of Tartu, Estonia
¹⁴ School of Mathematics and Physics, University of Queensland, Brisbane, Australia
¹⁵ School of Physics and Astronomy, University of Birmingham, UK
¹⁶ South African Astronomical Observatory, Cape Town, South Africa
¹⁷ Sydney Institute for Astronomy, School of Physics, University of Sydney, Australia
¹⁸ INAF–Arcetri Astronomical Observatory, Florence, Italy
¹⁹ Department of Astronomy, University of Cape Town, South Africa
²⁰ Department of Physics, Durham University, UK
²¹ Tata Institute of Fundamental Research, Mumbai, India
²² Center for Theoretical Physics, Polish Academy of Sciences, Warsaw, Poland
²³ Max Planck Institute for Astronomy, Heidelberg, Germany
²⁴ Centre for Space Research, North West University, Potchefstroom, South Africa
²⁵ INAF–Institute for Radio Astronomy, Bologna, Italy
²⁶ Department of Astronomy, University of Wisconsin–Madison, USA
²⁷ Department of Astronomy, School of Physics and Astronomy, Shanghai Jiao Tong University, China
²⁸ University of Lille, CNRS, France
²⁹ Institute of Space Astrophysics, University of Paris-Saclay, CNRS, Orsay, France
³⁰ Leibniz Institute for Astrophysics, Potsdam, Germany

The 4MOST Hemisphere Survey (4HS) will obtain uniform spectroscopy and redshifts for approximately six million galaxies over $\sim 2\pi$ steradians, and with high and unbiased completeness for $z < 0.15$. 4HS aims to 1) complete the map of mass and motion in the Local Volume, 2) map the influence of environment on galaxy evolution through overwhelming statistics, and 3) define the local ($z < 0.15$) galaxy reference sample for the era of LSST, Euclid, and ASKAP/MeerKAT/SKA. The

result is a dataset with exceptional and long-lasting legacy value.

Scientific context

Census-class surveys of the low- z galaxy population are central to the study of galaxy formation and evolution in at least three ways. First, empirical mappings of demographic distributions and scaling relations at $z \sim 0$ are vital in the calibration and/or validation of numerical simulations and theoretical models. Second, local samples provide the essential $t \sim 0$ reference point to anchor evolutionary studies over higher redshifts. Third, statistically representative samples are critical as control groups for studies of interesting or unusual classes or populations, for example group and cluster populations, radio- or HI-selected samples, transient hosts, etc.

The last decades have shown how low- z science is driven by — or can be limited by — the availability of spectroscopic redshifts and high-quality multiwavelength imaging over wide areas. Imagine a Universe in which we have eRosita, LSST, VISTA-VHS, Euclid, Roman, WISE, SKA, and LIGO/LISA, but where low- z science in the south is limited to 6dFGS (Colless et al., 2001; $K_{AB} < 14.5$), WAVES (~ 1000 deg²; Driver et al., 2019) and/or the margins of DESI-BGS (Hahn et al., 2022).

In this context, the 4MOST Hemisphere Survey (4HS) addresses an urgent need for uniform, wide-area, local-Universe spectroscopy in the southern hemisphere, to support low- z science with flagship European and global facilities. Accordingly, 4HS is designed to provide the best possible description of the low- z galaxy population in the southern Universe, with particular emphasis on science activities that absolutely require spectroscopy and/or spectroscopic (as opposed to photometric) redshifts.

In particular, 4HS takes full advantage of the unique capabilities of the 4MOST facility and consortium structure to achieve high and unbiased spectroscopic completeness for low- z galaxies over the widest possible area. Sharing the focal plane enables 4HS to efficiently obtain high completeness, and stellar partners enable us to press into the historic Zone

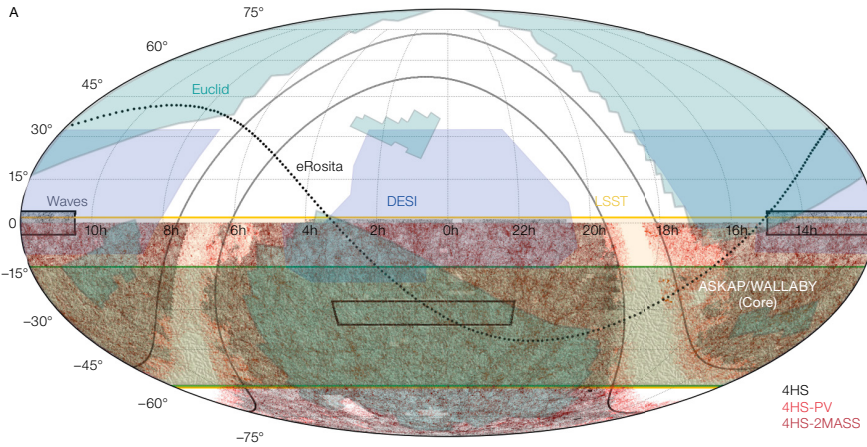
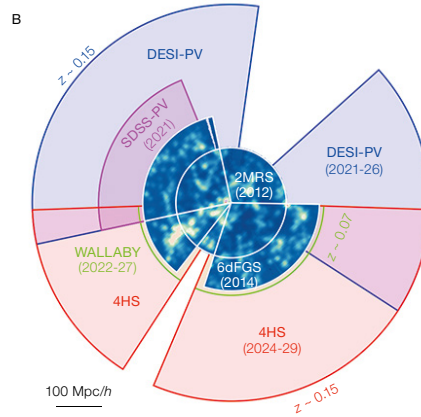


Figure 1. A: 4HS in the context of wide-field surveys, including ASKAP-WALLABY, VRO-LSST, and Euclid. The points show our preliminary input catalogue, based on a reanalysis of archival VISTA imaging. The main, PV, and 2MASS XSC sub-surveys are shown in black, red, and dark red, respectively. Note how 4MOST enables us to operate efficiently even deep into the historic Zone of Avoidance for PV science. B: 4HS in the context of major PV cosmology surveys. We stress that having overlapping samples is critical for controlling systematics between different surveys/teams. On its own, 4HS will be the largest southern PV experiment by a factor of about 10 in volume, and about 50 in the number of galaxies, and the largest globally by $\sim 30\%$ in area and a factor of two in number. Together with DESI-PV, 4HS will complete the map of the cosmic density and velocity fields in the Local Volume.



of Avoidance. (Equally, 4HS supports stellar halo science around the Galactic caps and the Sagittarius stream.) As well as extending samples and areas for other participating extragalactic surveys, shared observing costs for common targets means that 4HS carries efficiency dividends within the 4MOST consortium amounting to $\sim 25\text{--}30\%$.

Specific scientific goals

The key science goals for 4HS are set out below.

Map the mass, motion, and gravitational growth of structure in the southern Universe

4HS will measure velocity dispersions to enable distance and peculiar velocity (PV) determinations from the Fundamental Plane (FP) for up to $\sim 650\,000$ early-type galaxies at $z < 0.12$. (The soft limit of

$z \sim 0.12$ represents the limit of where the uncertainties in FP-derived distances, which scale with redshift, begin to blow up.) The unique contribution of 4HS will be to map the cosmic velocity field to distances of ~ 500 Mpc, covering virtually the full southern extent of the Local Volume, and including the most massive cosmological structures (i.e., Laniakea, Shapley, Vela, etc.) that are found in the south. When combined with the cosmological density field (as traced by galaxy positions), this provides a snapshot of the cosmic web in formation via gravitational collapse. 4HS will map the late-time (< 3 Gyr) evolution of the growth rate of structure through 5–10% precision measurements of the parameter combination $f(z)\sigma_8$ which is composed of the cosmological growth rate and mass clustering parameters, in each of six independent redshift bins over the interval $0 < z < 0.3$. The relation between the cosmic density and velocity fields also represents a direct measurement of gravitation on the largest scales

($>> 10$ Mpc): when combined with Planck data, 4HS will provide a $\sim 5\%$ measurement of the gravitational growth index, γ , to directly test general relativity and modified/alternative theories of gravity.

Map the demographic trends across the $z < 0.15$ galaxy population as a function of local and large-scale environment

That galaxy populations vary with environment is well established (for example, the morphology-density relation, group/cluster conformity, etc.), but the challenge remains to disentangle the mechanisms and effects that produce the observed trends. This multidimensional problem will only be resolved with overwhelming statistics. With high and unbiased completeness for a large statistical sample of $z < 0.15$ galaxies, 4HS will deliver the comprehensive suite of environment metrics (for example, local density, halo mass, situation with respect to group/void/filament/node, etc.) that is needed to advance the field. Further, 4HS will identify $> 60\,000$ galaxy groups, including $\sim 30\,000$ in the low-to-intermediate mass range ($10^{11}\text{--}10^{13} M_\odot$; multiplicities in the range 1–10) where group and galaxy properties seem to be most sensitive to the relative strengths of interacting processes (for example, Davies et al., 2019). Thus 4HS is designed to provide a solid empirical basis to describe exactly how environment influences galaxy properties, in order to challenge and constrain the next generations of hydrodynamical simulations, and so to resolve the environmental processes/effects that most influence galaxy formation and evolution.

Establish the benchmark local galaxy reference sample for the next generation of wide-area surveys and large/high-resolution simulations

With an increase in statistical power of about seven over the Sloan Digital Sky Survey and about 65 over the Galaxy And Mass Assembly (GAMA) survey, 4HS will establish the definitive benchmark sample of galaxies at $z < 0.15$, including $\sim 400\,000$ galaxies in the $8.5 < \log M_* < 9.5$ dwarf regime, all the way up to the very rarest and most massive galaxies. Relative to DESI-BGS, the southern advantage gives

4HS access to areas covered by LSST, ALMA, and ASKAP/MeerKAT/SKA, plus extensive overlap with eRosita, and with Euclid in the South Galactic Cap, to add to existing data from all of GALEX, VISTA-VHS, and WISE. Following the successful model of GAMA (Driver et al., 2022), and together with 4MOST partners including WAVES and CHANCES, 4HS is the keystone galaxy redshift survey necessary to establish a truly transformational laboratory for empirical studies of galaxy formation and evolution with comprehensive, panchromatic vision across the entire baryon cycle.

Target selection and survey area

The 4HS input catalogue is derived from a reanalysis of *JK* imaging from the VISTA Hemisphere Survey (VHS) plus several other programmes to fill gaps as far as possible. For target characterisation (for example, masses, star formation rates, etc.), we currently include optical imaging from Pan-STARRS1 where available ($\text{Dec} > -30^\circ$). We plan to extend to infrared imaging from WISE in the next year, and then to LSST optical and Euclid infrared imaging as they become available. Our photometric pipeline is built around the Scarlet deblender (Melchior et al., 2018) to obtain robust and signal-to-noise (S/N)-optimised extended source photometry. We are committed to releasing this new photometry as a public resource before the start of 4MOST survey operations.

The main 4HS sample is selected as $J_{\text{AB}} < 18$ and $(J-K) < 0.45$ (foreground corrected; AB), with a notional mean target density of $\sim 325 \text{ deg}^{-2}$. *J*-band selection is a nearly optimal basis for pre-selecting stellar-mass-limited samples: 4HS is volume limited for $\log M_* > 9.3/10.0/10.3$ and $z < 0.05/0.10/0.15$. As a means to pre-select $z < 0.15$ galaxies with near total completeness, our simple $(J-K)$ colour selection is maximally transparent, and is only marginally less efficient than a photometric *z* selection. For star/galaxy separation, we use a combination of both colour and resolved-ness in the VISTA imaging, with the opportunity to include information from Gaia. To cover the widest possible area, the main survey footprint is defined as the area where $E(B-V) < 0.3$ in the Planck dust map; including

the two WAVES-Wide fields this gives a total area of $\sim 18\,000 \text{ deg}^2$.

Our observing strategy is to obtain approximately uniform spectroscopic depth for all targets, equivalent to ~ 18 minutes integration in nominally grey conditions. This strategy guarantees $> 98\%$ redshift success per observation for our $z < 0.15$ targets. Further, we expect $S/N \geq 12$ for a high fraction ($> 80\%$) of $\log M_* > 10$ early-type galaxies at $z \leq 0.12$ to enable the velocity dispersion measurements that underpin our PV cosmology aims. Having roughly uniform spectral data quality brings other significant science benefits: for example, easy-to-characterise sensitivity limits for emission-line science (star formation rates, metallicities, emission-line diagnostics, etc.), and additional science opportunities using high-S/N subsets of the data (beyond our key PV cosmology science goals, including Galactic/Magellanic dust attenuation, etc.).

For PV cosmology, more than completeness, the object is to span the largest possible area/volume. To this end, we define a PV subsample as $J_{\text{AB}} < 16.5$ and $0 < (J-K) < 0.3$ ($\sim 65 \text{ deg}^{-2}$), which extends beyond the footprint of the main survey to $E(B-V) < 1.5$, for a total of $\sim 19\,890 \text{ deg}^{-2}$. Our goal with this sub-survey is to capture those early-type galaxies at $z < 0.12$ for which we can obtain useful velocity dispersion measurements. As a means of pre-selecting suitable FP targets from the main sample, this selection is $\sim 60\text{--}65\%$ complete and $\sim 30\text{--}35\%$ reliable. In contrast to the main sample, the *J*-magnitude selection for this sub-survey is applied to magnitudes as observed (i.e., without foreground correction), to focus on targets where we can get sufficient S/N for a velocity dispersion measurement to ≤ 0.1 dex. We anticipate this sub-survey will provide about an additional 30 000 useful PV measurements over and above the main sample, extending our area/volume for PV science by $\sim 10\%$.

Further, we include the 2MASS Extended Source Catalogue (Jarrett et al., 2000) as a supplemental sample to push to very low Galactic latitudes towards the Galactic anticentre, through the Magellanic Clouds, and wherever there are gaps in the VISTA imaging.

Figure 1a shows a preliminary 4HS input catalogue in the context of other current and future wide-area surveys. We also emphasise 1) the strong synergies between 4HS and each of VRO-LSST, Euclid, and ASKAP-WALLABY, 2) the complementarity of 4HS in the south with DESI-BGS in the north, and 3) the lasting legacy value of uniform and highly complete spectroscopic redshifts across the hemisphere.

As a near-infrared-selected spectroscopic redshift survey of the southern hemisphere, 4HS is more than three magnitudes deeper than 6dFGS for a factor of > 50 increase in target density and number of redshifts. In combination with high-quality optical-to-infrared photometry from LSST, Roman, Euclid, VISTA, and WISE — plus eRosita X-ray and ultimately ASKAP/MeerKAT/SKA radio data — 4HS can equally be viewed as providing GAMA-like depth and panchromatic coverage over > 60 times the area, to establish an incredible legacy dataset.

As a PV cosmology survey, 4HS expands the current state of the art (for example, Qin et al., 2018; Kourkchi et al., 2022; Howlett et al., 2022) by factors of > 60 and > 10 in number and volume, respectively (see Figure 1b). More importantly than ‘factor of’ comparisons, in combination with DESI in the north, and with complementary data from ASKAP-WALLABY at lower redshifts, 4HS will complete the map of gravitational mass and motion in Local Volume.

Acknowledgements

We acknowledge the support of the 4MOST Consortium, and Astronomy Data and Computing Services, Australia.

References

- Colless, M. et al. 2001, MNRAS, 328, 1039
- Davies, L. J. M. et al. 2019, MNRAS, 483, 5444
- Driver, S. P. et al. 2022, MNRAS, 513, 439
- Driver, S. P. et al. 2019, The Messenger, 175, 46
- Hahn, C. et al. 2022, arXiv:2208.08512
- Howlett C. et al. 2022, MNRAS, 515, 953
- Jarrett T. H. et al. 2000, AJ, 119, 2498
- Kourkchi, E. et al. 2022, MNRAS, 511, 6160
- Qin, F. et al. 2018, MNRAS, 477, 5150
- Melchior, P. et al. 2018, Astronomy & Computing, 24, 129

The 4MOST Strong Lensing Spectroscopic Legacy Survey (4SLSLS)

Thomas E. Collett¹
 Alessandro Sonnenfeld²
 Chris Frohmaier³
 Karl Glazebrook⁴
 Dominique Sluse⁵
 Veronica Motta⁷
 Aprajita Verma⁸
 Timo Anguita⁹
 Leon Koopmans¹⁰
 Crescenzo Tortora¹¹
 Frederic Courbin¹²
 Remi Cabanac¹³
 Brenda Frye¹⁴
 Graham P. Smith¹⁵
 Jose Maria Diego¹⁶
 Bruno Alteiri¹⁷
 Sebastian Lopez¹⁸
 Chris Fassnacht¹⁹
 Asantha Cooray²⁰
 Ariel Goobar²¹
 Dan Ryczanowski¹⁵
 Stephen Serjeant²²
 Johan Richard²³
 Tommaso Treu²⁴
 Leonidas Moustakas²⁵
 Rui Li²⁶
 Colin Jacobs⁴
 Cameron Lemon¹²
 Lucia Marchetti²⁷
 Phillipa Hartley²⁸
 Eric Jullo²⁹
 Chien-Hsiu Lee³⁰
 Simon Birrer³¹
 Alexander Fritz³²
 James Nightingale³³
 Nicola Napolitano¹¹
 Andres Alejandro Plazas³⁴
 Sandor Kruk³⁵
 Chiara Spiniello⁸
 Claudio Grillo³⁶
 Sherry Suyu³⁷
 Anowar Shajib³⁸
 Georgios Vernardos¹²
 Simon Dye³⁹
 Tansu Daylan⁴⁰
 Jeffrey Newman⁴¹
 Stefan Schuldt³⁶

¹ University of Portsmouth, UK

² Shanghai Jiao Tong University, Shanghai, China

³ University of Southampton, UK

⁴ Swinburne University of Technology, Australia

⁵ University of Liège, Belgium

⁶ Paris Institute of Astrophysics & Marseille Astrophysics Laboratory, France

⁷ University of Valparaíso, Chile

⁸ University of Oxford, UK

⁹ Andres Bello University, Santiago, Chile

¹⁰ University of Groningen, the Netherlands

¹¹ INAF–Capodimonte Astronomical Observatory, Naples, Italy

¹² École Polytechnique Fédérale, Lausanne, Switzerland

¹³ Midi Pyrénées Observatory, Toulouse, France

¹⁴ University of Arizona, USA

¹⁵ University of Birmingham, UK

¹⁶ Cantabria Institute of Physics, Santander, Spain

¹⁷ ESA – European Space Astronomy Centre, Madrid, Spain

¹⁸ University of Chile, Santiago, Chile

¹⁹ University of California at Davis, USA

²⁰ University of California at Irvine, USA

²¹ Stockholm University, Sweden

²² The Open University, UK

²³ Lyon Astrophysics Research Centre, France

²⁴ University of California at Los Angeles, USA

²⁵ Jet Propulsion Laboratory, Pasadena, USA

²⁶ University of Chinese Academy of Sciences & National Astronomical Observatories, PR China

²⁷ University of Cape Town, South Africa

²⁸ Square Kilometre Array Observatory, UK

²⁹ Marseille Astrophysics Laboratory, France

³⁰ NSF's NOIRLab, USA

³¹ Stony Brook University, USA

³² Max Planck Institute for Extraterrestrial Physics, Garching, Germany

³³ Durham University, UK

³⁴ Princeton University, USA

³⁵ ESA – European Space Research and Technology Centre, Noordwijk, the Netherlands

³⁶ University of Milan, Italy

³⁷ Max Planck Institute for Astrophysics, Garching, Germany

³⁸ University of Chicago, USA

³⁹ University of Nottingham, UK

⁴⁰ Washington University in St. Louis, USA

⁴¹ University of Pittsburgh, USA

Almost all science that can be done with strong gravitational lenses requires knowledge of the lens and source redshifts. The 4MOST Strong Lensing Spectroscopic Legacy Survey (4SLSLS)

will follow up strong lens candidates discovered in the Euclid survey and the Legacy Survey of Space and Time. 4SLSLS will provide pairs of redshifts for 10 000 strong-lensing galaxies (lenses) and background galaxies (sources). Velocity dispersions will also be measured for 5000 lenses. This sample will enable discoveries about the evolution of galaxies, the study of intrinsically faint objects and of the cosmological model.

Scientific context

General Relativity (GR) is based on the principle that massive objects warp space-time. Because of this, light passing close to massive objects is deflected. If the surface mass density of the object is great enough, then multiple images of a single background source can form; this is the regime of strong gravitational lensing.

For each strong lens system, the images observed depend on the light profile of the background source, the mass and mass distribution of the foreground lens, the cosmological distances between observer, lens and source and the nature of gravity. Strong lenses are therefore sensitive probes of both astrophysics and cosmology. As such, strong lenses have been used to constrain the masses and density profiles of galaxies (Auger et al., 2010; Shajib et al., 2021), the dark subhalo and field-halo populations (Vegetti et al., 2014; Ritondale et al., 2019), cosmological parameters (Collett & Auger, 2014; Wong et al., 2020), the high-redshift luminosity function (Barone-Nugent et al., 2014), the nature of high-redshift sources (Newton et al., 2011) and the validity of GR (Schwab, Bolton & Rappaport, 2010; Collett et al., 2018). For many of these analyses, the shortage of suitable strong lenses is a major limiting factor.

To date, several hundred galaxy-galaxy strong lenses have been discovered in heterogeneous searches of photometric and spectroscopic survey data (Myers et al., 2003; Bolton et al., 2006; Gavazzi et al., 2012; Negrello et al., 2014; More et al., 2016; Hartley et al., 2017; Petrillo et al., 2019; Jacobs et al., 2019; Li et al., 2020). The reason known lenses are rare is because even the most massive galaxies

are only capable of deflecting light by an arcsecond or two. Only a small fraction of the sky has been observed to sufficient depth and with good enough image resolution to identify a typical Einstein ring. Several ongoing, and forthcoming, wide and deep sky surveys offer improved depth, area and resolution compared to existing data (Miyazaki et al., 2006; Ivezić et al., 2008; Laureijs et al., 2011). These surveys have the potential to increase the current galaxy-scale lens sample by orders of magnitude (Collett, 2015; Marshall, Blandford & Sako, 2005). Between Euclid and the Vera C. Rubin Observatory Legacy Survey of Space and Time (LSST), up to 300 000 lenses are discoverable. However, these surveys will not provide adequate redshift information for science: this is what 4SLSLS will deliver.

With a large increase in the known strong lens population, current work could be extended to new regimes, including lower lens masses, higher-redshift lenses and intrinsically fainter sources. A critical component of any results derived from this increased discovery space is the confirmation of any identified strong lens candidate with a spectroscopic redshift for the lens and the source behind it.

Spectroscopy is needed for two main reasons:

1. Features on the sky often look similar to strong lenses but are not. Ring galaxies, star-forming tidal features and interacting galaxies are often particularly hard to distinguish. Spectroscopy confirms that the putative lens is indeed closer than the putative arcs.
2. Strong lensing observables are naturally in angular units (Einstein radius, unlensed angular size of source, lens mass, etc). Converting them into physical quantities requires precise spectroscopic redshifts.

Specific scientific goals

The primary purpose of 4SLSLS is to enable the strong lensing community to exploit the large increase in sample sizes. Having a homogeneous sample of 10 000 lenses with a well understood selection function represents a huge step forward for the community. Here we

highlight three main science goals that are a priority for the project team.

Galaxy formation — the inner structure of lenses

Dark matter and baryons exist in comparable amounts within the Einstein radius (Auger et al., 2010) and as a result galaxy-scale lenses are well suited to the study of both components. Strong lensing is a particularly useful tool to simultaneously address questions related to the inner structure of massive galaxies.

What fraction of the cosmological baryon content is converted into stars?

Virtually all current measurements of galaxy stellar masses are obtained by converting observed luminosities into masses on the basis of synthetic stellar population models which have not been calibrated against model-independent stellar mass measurements. These models introduce a systematic uncertainty in the total baryonic mass locked in stars. The main uncertainty is the stellar initial mass function (IMF), the choice of which can plausibly vary the stellar mass-to-light ratio of a galaxy by a factor of two. Constraining stellar mass-to-light ratios of galaxies provides a unique way of gaining insight into the stellar IMF and the physics of star formation.

What is the inner density profile of the dark matter halo?

The determination of the inner dark matter density profile can provide unique constraints both on dark matter physics, for example by testing the self-interaction scenario (Elbert et al., 2018), and on baryonic physics: the dark matter distribution responds to processes such as adiabatic contraction from gas infall (Gnedin et al., 2011), feedback from the central supermassive black hole (Martizzi, Teyssier & Moore, 2013) and dynamical friction (Romano-Díaz et al., 2008). Cosmological hydrodynamical simulations generally predict, in the centres of massive galaxies, dark matter profiles steeper than the Navarro-Frenk-White model used to describe dark matter-only simulations

(Schaller et al., 2015; Xu et al., 2017; Peirani et al., 2017). Current strong lensing observations suggest a larger diversity in dark matter profiles (Oldham & Auger, 2018), although the number of galaxies for which such measurements are available is still very limited. Confirming or ruling out this tension can be very useful for improving the accuracy of the subgrid physics recipes adopted in simulations.

Strong lensing is one of the very few methods available for simultaneously constraining galaxy stellar masses and dark matter density profiles independently of a stellar population model. 4SLSLS will statistically combine strong lensing measurements from a large set of systems (for example, Sonnenfeld & Cautun, 2021). Our forecasts show that 4SLSLS will constrain the average stellar IMF normalisation of a sample of 5000 lenses with a precision of 5%, while measuring the average dark matter density slope with a precision of 0.1 (see Figure 1). With such precision, we will be able to settle the dark matter core vs. cusp issue in massive lens galaxies and put much tighter constraints on the stellar IMF of these objects than is currently possible. Moreover, by combining lensing constraints with 4SLSLS velocity dispersion measurements it will be possible to address additional questions, such as how the IMF varies as a function of galaxy properties and within each galaxy as a function of position (Sonnenfeld et al., 2018).

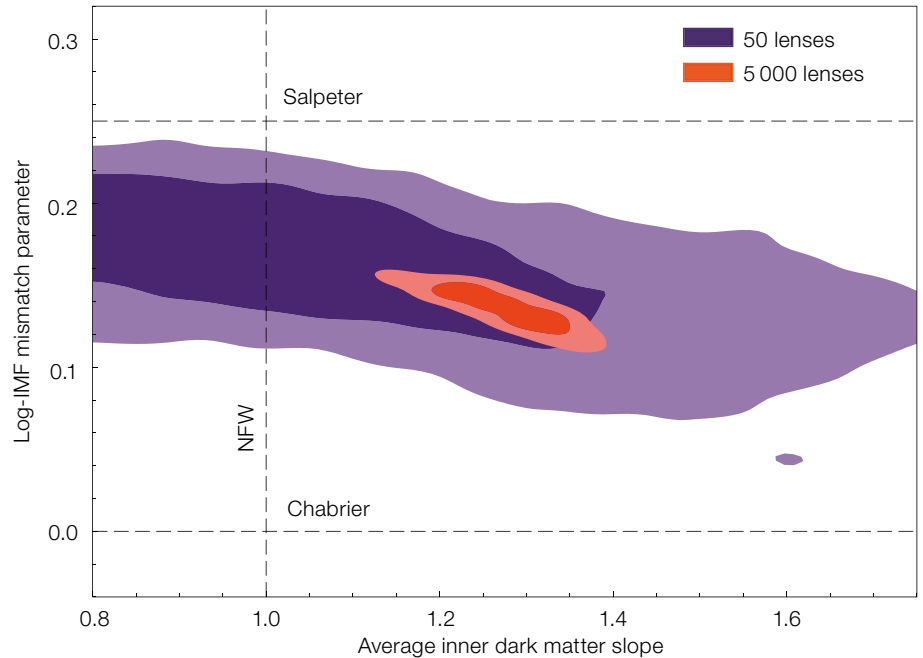
Probing the cosmological parameters with 4SLSLS

The Einstein radius of a strong lens is a function of lens mass and cosmological distances. Measuring cosmological distances as a function of redshift can teach us about the underlying cosmological model of the Universe, but doing this with strong lenses requires additional information to break the degeneracy between mass and distances. 4SLSLS will provide two pathways to break this degeneracy: directly by providing a lensing-independent measurement of the mass through velocity dispersions, and indirectly by confirming exotic strong lenses with information beyond a single Einstein radius. Grillo et al. (2018) showed that velocity dispersions can in principle be used to constrain the

dark energy content of the Universe. However, connecting the scales probed by unresolved kinematics with the Einstein radius requires a knowledge of the lens density profile. A large sample of lenses with sources at different redshifts is critical to inferring cosmological parameters and marginalising over any trends in the redshift evolution of lens density profiles. Forecast constraints show that constraints on Ω_M at the level of 5% can be derived with 5000 lenses. The assumption that GR holds over cosmological distances is a key aspect of Λ CDM, but GR is poorly tested on extragalactic length scales. In addition to probing cosmological parameters, the 5000 4SLS systems with velocity dispersions will test GR by comparing observed deflection angles to those predicted from the kinematic mass (Schwab, Bolton & Rappaport, 2010). 5000 lenses will constrain the amount of spatial curvature produced per unit mass to the 1% level, without assuming a fixed background cosmological model. This is 10 times better than any other extragalactic test of GR (Collett et al., 2018). 4SLS will also confirm a population of ~ 300 double-source plane lenses: in these systems the ratio of the Einstein radii is sensitive to cosmology (Collett et al., 2012), but not to the primary lens mass. After lens modelling of the Euclid data, these systems will yield an 8% constraint on the equation of state of dark energy, independent of any other dataset or a 4% constraint with a weakly informative prior from the distance to the CMB.

Using highly magnified sources to constrain intrinsically faint galaxy populations

The frontier of galaxy evolution is set by those galaxies at the limiting reach of the largest telescopes. Observations therefore benefit immensely from the flux amplification and spatial resolution enhancement provided by lensing magnification. The benefits brought by strong lens magnification to the study of high redshift sources were neatly demonstrated recently by Rigby et al. (2017). They showed that even HST-resolution imaging of unlensed $z = 2.5$ systems cannot come close to probing the intrinsic spatial scales that can be reached by strong lensing. Many studies have used



lens systems to probe the galaxy assembly and star formation. Observations of lensed sources have helped us to: understand the role of high-redshift mergers in galaxy formation (Wuyts et al., 2014); measure the size of star-forming clumps to connect them to kinematic stability (Livermore et al., 2015; Swinbank et al., 2015); spatially resolve star-forming clumps to constrain the physical properties of the ISM (Frye et al., 2012); establish the conditions in the ISM which regulate star-forming and starbursting activities (Dye et al., 2022); probe gas-phase metallicity to determine growth channels (Yuan et al., 2011; Jones et al., 2015; Wang et al., 2017); and identify and investigate massive, post-blue-nugget galaxies (Napolitano et al., 2020). High-resolution rest-frame-UV spectroscopy has studied outflow composition and energetics, probing the physics of feedback-driven outflows (Pettini et al., 2002; Frye, Broadhurst & Benítez, 2002; Yuan, Bu & Wu, 2012; Jones, Stark & Ellis, 2018). Today, the main limiting factors are sample size and heterogeneous selection functions. 4SLS will provide the first statistically large sample of spectroscopically confirmed intrinsically faint galaxies with well-defined selection functions. By virtue of the size of the 4SLS sample, prime sources for targeted follow-up (for example with adaptive-optics-fed 10-metre- &

Figure 1. Red contours: Forecast on the inference of the average inner slope of the dark matter density profile and the stellar IMF mismatch parameter (that is, the ratio between the true stellar mass of a galaxy and the stellar mass obtained from stellar population fitting assuming a Chabrier IMF) from the statistical combination of strong lensing data on a sample of 5000 4SLS lenses. Purple contours: forecast on a sample of 50 lenses, approximately the number of galaxy-scale strong lenses with currently available lens and source spectroscopic redshifts. Contour levels correspond to 68% and 95% enclosed probability regions.

ELT-class spectrographs) can be selected on the basis of source properties and redshifts. As a result, 4SLS will enable an unprecedented understanding of the nature of galaxies up to $z = 1.5$ at enhanced spatial resolution.

Target Selection and Survey area

The large number of strong lenses that will be discovered means that spectroscopic confirmation must move beyond one-by-one observations of individual sources. Already, most of the current Dark Energy Survey and Kilo-Degree Survey lenses do not have spectroscopic redshifts. To combat the expanding scale of the strong lens follow-up problem, 4SLS is the community's move to multi-object spectroscopy, albeit with sparse densities (~ 20 lenses per square degree

from Euclid and a further ~ 8 per square degree from the LSST; see Collett, 2015). By sharing the focal plane of a multi object spectrograph with larger surveys, strong lens redshifts can be obtained efficiently. 4SLSLS targets will be discovered across the LSST and Euclid Southern footprints. We will target lens candidates with a photometric redshift consistent with $z_s < 1.5$, where the OII doublet falls out of the 4MOST wavelength band. This represents about a third of the LSST and Euclid sample. All but the most massive 4SLSLS targets will be lens-source blends, with the fibre centred to maximise source flux.

Acknowledgements

TEC is funded by a Royal Society URF. This work is supported by the European Research Council grant 945536 LensEra. Data are available from the first author upon request. For the purpose of open access, the authors have applied a Creative Commons Attribution (CC BY) licence to any Author Accepted Manuscript version arising.

References

- Auger, M. W. et al. 2010, *ApJ*, 724, 511
 Barone-Nugent, R. L. et al. 2014, *ApJ*, 793, 17
 Bolton, A. S. et al. 2006, *ApJ*, 638, 703
 Collett, T. E. et al. 2012, *MNRAS*, 424, 2864
 Collett, T. E. 2015, *ApJ*, 811, 20
 Collett, T. E. & Auger, M. W. 2014, *MNRAS*, 443, 969
 Collett, T. E. et al. 2018, *Sci*, 360, 1342
 Dye, S. et al. 2022, *MNRAS*, 510, 3734
 Elbert, O. D. et al. 2018, *ApJ*, 853, 109
 Frye, B., Broadhurst, T. & Benítez, N. 2002, *ApJ*, 568, 558
 Frye, B. et al. 2012, *ApJ*, 754, 17
 Gavazzi, R. et al. 2012, *ApJ*, 761, 170
 Gnedin, O. Y. et al. 2011, *arXiv:1108.5736*
 Grillo, C. et al. 2018, *ApJ*, 860, 94
 Hartley, P. et al. 2017, *MNRAS*, 471, 3378
 Ivezić, Z. et al. 2008, *SerAJ*, 176, 1
 Jacobs, C. et al. 2019, *ApJS*, 243, 17
 Jones, T. et al. 2015, *AJ*, 149, 107
 Jones, T., Stark, D. P. & Ellis, R. S. 2018, *ApJ*, 863, 191
 Laureijs, R. et al. 2011, *arXiv:1110.3193*
 Li, R. et al. 2020, *ApJ*, 899, 30
 Livermore, R. C. et al. 2015, *MNRAS*, 450, 1812
 Marshall, P., Blandford, R. & Sako, M. 2005, *NewAR*, 49, 387
 Martizzi, D., Teysier, R. & Moore, B. 2013, *MNRAS*, 432, 1947
 Miyazaki, S. et al. 2006, *SPIE*, 6269, 62690B
 More, A. et al. 2016, *MNRAS*, 455, 1191
 Myers, S. T. et al. 2003, *MNRAS*, 341, 1
 Napolitano, N. R. et al. 2020, *ApJL*, 904, L31
 Negrello, M. et al. 2014, *MNRAS*, 440, 1999
 Newton, E. R. et al. 2011, *ApJ*, 734, 104
 Oldham, L. J. & Auger, M. W. 2018, *MNRAS*, 476, 133
 Peirani, S. et al. 2017, *MNRAS*, 472, 2153
 Petrillo, C. E. et al. 2019, *MNRAS*, 484, 3879
 Pettini, M. et al. 2002, *Ap&SS*, 281, 461
 Rigby, J. R. et al. 2017, *ApJ*, 843, 79
 Ritondale, E. et al. 2019, *MNRAS*, 485, 2179
 Romano-Díaz, E. et al. 2008, *ApJL*, 685, L105
 Schaller, M. et al. 2015, *MNRAS*, 451, 1247
 Schwab, J., Bolton, A. S. & Rappaport, S. A. 2010, *ApJ*, 708, 750
 Shajib, A. J. et al. 2021, *MNRAS*, 503, 2380
 Sonnenfeld, A. & Cautun, M. 2021, *A&A*, 651, A18
 Sonnenfeld, A. et al. 2018, *MNRAS*, 481, 164
 Swinbank, A. M. et al. 2015, *ApJL*, 806, L17
 Vegetti, S. et al. 2014, *MNRAS*, 442, 2017
 Wang, X. et al. 2017, *ApJ*, 837, 89
 Wong, K. C. et al. 2020, *MNRAS*, 498, 1420
 Wuyts, E. et al. 2014, *ApJ*, 781, 61
 Xu, D. et al. 2017, *MNRAS*, 469, 1824
 Yuan, F., Bu, D. & Wu, M. 2012, *ApJ*, 761, 130
 Yuan, T.-T. et al. 2011, *ApJL*, 732, L14

P. Horálek/ESO



This magnificent image shows ESO's Visible and Infrared Survey Telescope for Astronomy (VISTA), located at Paranal Observatory. The Milky Way galaxy sweeps behind the telescope with several nebulae visible, like the Gum Nebula and the Carina Nebula.



This wider coverage area reveals even more stars in the crowded neighbourhood surrounding the Carina nebula. Captured by VISTA, the world's largest infrared survey telescope, we witness the dramatic evolution of this living stellar city, where stars form and perish side by side.

Telescopes and Instrumentation



The Hunga Tonga–Hunga Ha’apai volcano erupted on 15 January 2022 and produced an explosion bigger than any other volcanic eruption so far in the 21st century. Huge quantities of particles, including dust and water vapour, were released into the atmosphere. This image depicts a stunning sunset — one of many — witnessed at Paranal Observatory ever since. Information about the various effects this volcanic eruption has had on observations at Paranal Observatory is presented on p. 58.

SPEED – Get Ready for the (PCS) Rush Hour

Patrice Martinez¹
Mathilde Beaulieu¹
Carole Gouvret¹
Alain Spang¹
Aurelie Marcotto¹

¹ Lagrange Laboratory, Côte d'Azur Observatory, Côte d'Azur University, CNRS, Nice, France

The Segmented Pupil Experiment for Exoplanet Detection (SPEED) optical test bed is now ready for operation. SPEED is dedicated to high-contrast imaging at short angular separations with segmented telescopes. Its optical design allows a wide range of applications and the immediate goal is to demonstrate a high-contrast dark hole close to the stellar vicinity. This will be achieved by a combination of optimal wavefront shaping architecture, small inner working angle coronagraphy, and efficient complex field sensor for fine cophasing and dark hole generation.

Science case and challenges

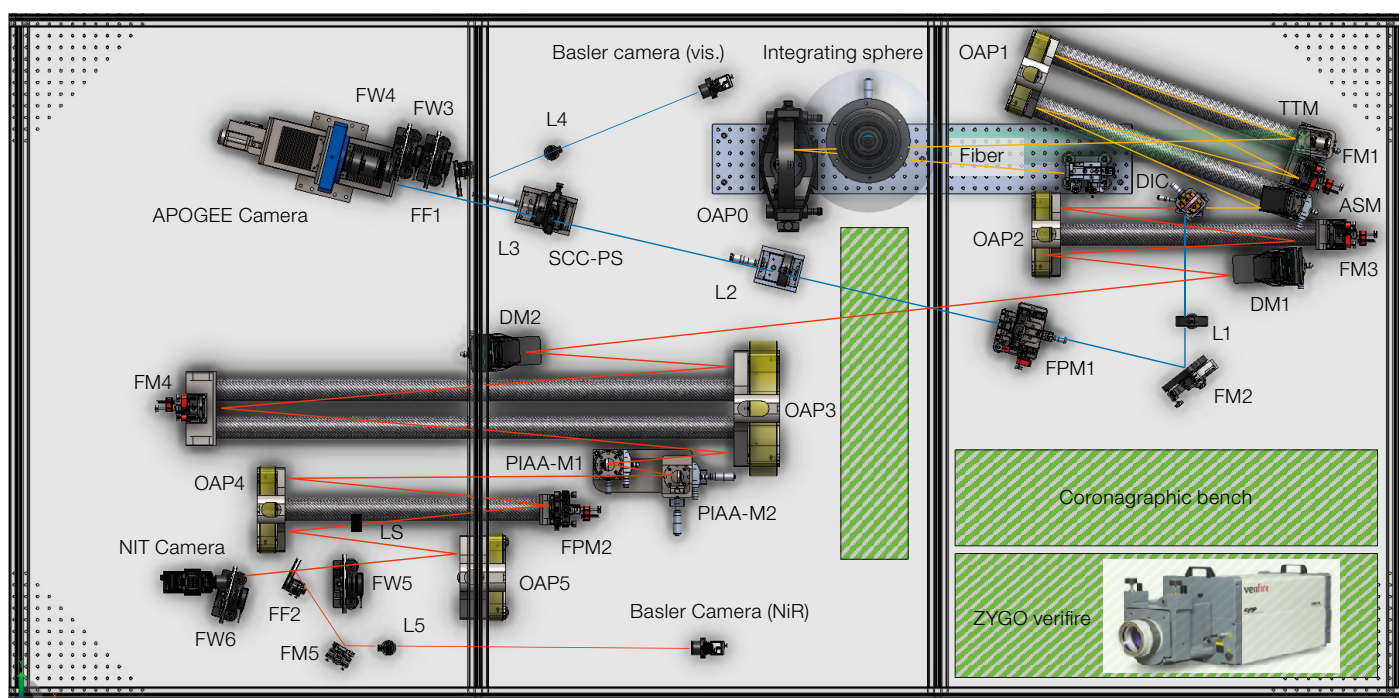
Direct observation of exoplanets is challenging but essential to the study and

understanding of the properties of exoplanets' atmospheres, for which few data are available. The majority of exoplanets so far known were discovered by indirect methods and, despite the progress with the second generation of high-contrast imaging (HCI) instrumentation, direct imaging detections remain marginal (~ 1%). Directly imaging and characterising a fairly large number of exoplanets requires an optimal combination of telescope and instrument to provide extremely high contrast, very good sensitivity, and exquisite image quality and stability. Among the target stars, low-mass M-stars are particularly attractive because of the considerable number they represent within 20 light-years of the Sun, and because they are arguably the most common environment with the potential to harbour life. Observing habitable planets around nearby M-stars is of the greatest scientific importance but represents an extreme instrumental challenge. The Planetary Camera and Spectrograph (PCS; Kasper et al., 2021) for ESO's Extremely Large Telescope (ELT) must provide an imaging contrast of 10^{-8} at 15 milliarcseconds angular separation from the star (1.5 to $2 \lambda/D$ in the near-infrared) and 10^{-9} at 100 milliarcseconds and beyond. A promising path to reach these capabilities is a combination of

extreme adaptive optics (XAO) supported by a second-stage AO to reduce the temporal delay, an HCI system, and high-dispersion spectroscopy (HDS). Various activities are under way in the community on these topics, for example SPHERE+ (Boccaletti et al., 2020), HiRISE (Vigan et al., 2018), RISTRETTO (Blind et al., 2022), KPIC (Mawet et al., 2018), MagAO-X (Males et al., 2018), SCEXAO (Lozi et al., 2018) as well as many laboratory-based developments¹.

In this context, the Segmented Pupil Experiment for Exoplanet Detection (SPEED)² facility offers an ad hoc environment to improve HCI considering the ELT pupil fragmentation and to assess the impact on control and control stability of quasi-static speckles. SPEED is positioned within a three-body problem:

Figure 1. 3D CAO view of the SPEED test-bed. Colour code: telescope simulator and common path (yellow), visible path (blue) and near-infrared path (red). Abbreviations: TTM – tip/tilt mirror, OAP – off-axis parabola, ASM – active segmented mirror, DM – deformable mirror, FM – flat mirror, DIC – dichroic, L – lens, SCC-PS – self-coherent camera-phasing sensor, FPM – focal plane mask, PIAA-M1 & PIAA-M2 – phase induced amplitude apodisation mirror 1 & 2, LS – Lyot stop, APOGEE – visible camera, NIT – near-infrared camera, Basler – pupil camera (visible and NiR), FF – flip-flop mirror, FW – filter wheel.



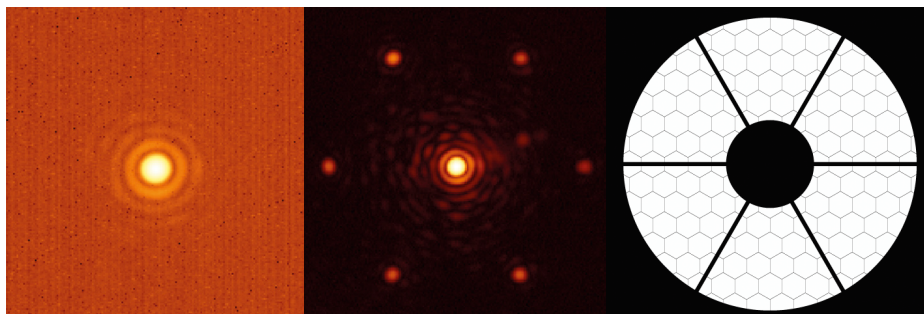


Figure 2. From left to right: near-infrared arm (H band, $1.65\ \mu\text{m}$, Strehl ratio = 98%) point spread function image; visible arm ($650\ \text{nm}$, Strehl ratio = 93%) point spread function; and an image illustrating the telescope pupil.

improving, at the HCI system level, the contrast (deeper), and the angular separation (closer), to access new scientific targets (fainter). Integrated into an ISO7 clean room at the Lagrange Laboratory of Côte d'Azur University, SPEED will be an optimal cocoon for studying coronagraphy, control and shaping of the wavefront, and fine correction of cophasing error by considering the effects, disturbances, and instabilities generated by pupil fragmentation. Active control and temporal stability of residual wavefront errors is one pillar to consider for improving detection yields and getting access to object classes with masses ideally down to exo-Earths. The bench is now completed and is entering a period of intense exploitation before being made available to the community.

Concept and design choices

SPEED, as depicted in Figure 1, combines a light source module, a telescope simulator (orange line), and a dichroic reflecting in the visible light to cophasing optics (blue line) and transmitting the near-infrared light (red line) towards wavefront shaping, coronagraphy, and the science camera. The common path includes all the optics needed to feed the beam to the cophasing and science paths. The telescope simulator consists of the combination of an active segmented mirror (ASM) with 163 segments controlled in piston and tip-tilt, and a physical mask magnetically fixed on the structure of the tip-tilt mirror (TTM; for beam stability

control) to simulate the presence of a large central obscuration and secondary support structures mimicking the ELT pupil (see Figure 2, right panel). The cophasing unit (blue line) is based on image-plane analysis using the Self-Coherent Camera Phasing Sensor (SCC-PS; Janin-Potiron et al., 2016) and Fast-Modulated Self-Coherent Camera (FM-SCC; Martinez, 2019). The near-infrared path (H band, red line) includes a wavefront control and shaping module made of two Kilo-C deformable mirrors (DM) of 952 actuators (DM1 and DM2) separated by free-space propagation. Both DMs are out-of-pupil planes, enabling efficient correction of phase and amplitude errors (Beaulieu et al., 2017). The coronagraph, a Phase Induced Amplitude Apodisation Complex Mask Coronagraph (Guyon et al., 2014), or an Apodised Pupil Complex Mask Coronagraph (APCMC), offers high throughput and close to $\sim \lambda/D$ inner working angle (IWA). A FM-SCC is being integrated into the near-infrared arm of the bench at the Lyot Stop (LS) plane. The bench rests on a 1.5×2.4 metre table with active vibration isolation supports. The area where the table is installed is isolated from building vibrations.

SPEED incorporates a lot of devices: four detectors, two webcams, three lamps, ~ 25 motorised functions, five sensors, 12 piezo actuators, two shutters, three DMs, one TTM, amongst others. We select reflective optics for the whole design, except for the phasing unit arm. Super-polished off-axis parabolas (OAP) are employed to minimise optical aberrations down to 3 nm RMS over a 10-mm beam diameter surface with power spectral density (PSD) following a f^{-3} power law. We operate the bench completely covered with protection panels forming a nearly closed box to minimise internal

turbulence and optimise stability. The instrument boasts five observing modes: three engineering modes enabling pupil control and monitoring in the near and visible arms, a science observing mode for monitoring and correcting in close loop the alignment of the telescope primary mirror segments (fine cophasing optics), and a science observation mode for real-time coronagraphic and dark hole observations. The bench also accommodates on its table a separated coronagraphic test bed (Figure 1, hatched area) for controlling the performance of the coronagraph focal plane masks before inserting them into the SPEED optical path. In addition, we use a ZYGO interferometer for metrological and alignment purposes.

Along with the evolution of the architectural design, a simulation model tool through an end-to-end simulator (e2e) was developed for specifications, performance control, evaluation, and analysis (Beaulieu et al., 2017, 2020). The SPEED e2e is a high-fidelity performance, design analysis and verification tool that incorporates Fresnel diffraction propagation using PROPER (Krist et al., 2007) combined with a realistic system model, and up-to-date optical bench design. It considers simulated wavefront sensing and control, including as-built optics with measured wavefront errors, and guarantees that the simulator is in step with the SPEED bench optical contrast design. A by-product of the SPEED e2e is to simulate and test hardware parts or pieces of algorithms that the bench itself does not yet support.

Our wavefront-shaping architecture for high-contrast imaging at short separations consists of a pair of out-of-pupil DMs separated by 1.7 m (DM1 is at 0.2 m and DM2 is at 1.5 m from the pupil). It was determined based on significant efforts in complex modelling by considering the intrinsic properties of the optics setup, including polishing frequency distribution, relative beam size, the distance between optics, DM optical location (in a collimated beam — out-of-pupil plane or in a pupil plane — versus converging beam) and separation, DM properties (actuator number, etc.). High-contrast imaging at short separations with multi-DM architecture requires large DM separations, and exhibits a significant

performance dependence on the DM location, on the amount of aberrations and the power spectral density (PSD) power law and on the dark hole size. It is not impacted by highly aberrated optics as long as they are located in a collimated beam (cophasing errors, deformable mirrors windows, dichroic), but it is affected by finite DM stroke, adjacent non-functional actuators, phase errors on the coronagraph or near the focal plane, and optics aberrations downstream of the coronagraph.

Calibration and instrument control

Non-common-path aberrations (NCPA) are present to some extent in all high-contrast imaging data, and contribute additional speckle noise which is strongest at small angular separations and thus detrimental to coronagraphic performance. For SPEED, these aberrations are typically estimated to contribute an average wavefront error of approximately 40 nm RMS. An offline differential optical transfer function (Codona et al., 2013) compensation procedure has been operated to further reduce these NCPAs to 28 nm RMS using the ASM for the correction. This is an impressive result, considering that the ASM is segmented and that the main contributor to the wavefront error budget is the ASM itself with 30 nm RMS wavefront error (mostly dominated by segment focus and astigmatism errors that the ASM cannot correct for). The optical quality of the SPEED test bed near-infrared arm is, without correction of the NCPA, of the order of $\sim 96\%$ Strehl ratio at 1650 nm. Correcting for NCPA improved the Strehl ratio to a very high $\sim 98\%$, i.e., $\lambda/40$ RMS at 1650 nm (Figure 2, left panel). The final near-infrared point spread function image demonstrates exquisite image quality. The optical quality of the SPEED test bed visible arm is, without correction of NCPA, of the order of $\sim 86\%$ a Strehl ratio at 650 nm and drops to $\sim 93\%$ with NCPA correction (Figure 2, middle panel).

The SPEED test bed, being more complex than a simple laboratory test bench but less demanding than an on-sky instrument at a telescope, requires a specific and adapted system and software control development that enable the

bench to operate efficiently and safely (Martinez et al., 2022a). The bench is controlled through a dedicated control network that interconnects three workstations and uses the instrument software (SPEED control software, SCS) that enables control of all the sub-systems consistently and reliably. The SCS is in charge of controlling all the bench functions, coordinating the execution of actions, implementing all observation, calibration, and safety procedures, and providing a quick look for monitoring the status of ongoing observations and conditions. Interactions with external parties such as the building centralised technical management, internal and external network, as well as a backup system, are also incorporated. We enforce a great deal of error checking at compile-time and at run-time through a crash log diary and command feedback window (CFW) and CFW log file so that there are various recordings of what has happened. We pay close attention to implementing any non-trivial functionality in such a way that it can be tested without the need to start the entire software or a substantial part of it that belongs to hardware and in particular sensitive hardware. For that reason, the SCS includes an emulator mode that allows diagnostic or implementation and testing, connecting only emulated hardware if needed. The safety of hardware is a priority and consists in protecting every piece of hardware from damage using a series of safeguards within the code. We implement an additional layer of security on top of the security sometimes offered by hardware controllers. Operational conditions, such as environmental conditions, are of concern because they may prohibit the use of specific hardware. They are therefore constantly tracked and verified. We also avoid conflict of use and manage error codes or status codes to track anomalies and leave the hardware in a safe state.

Roadmap for the next years

The SPEED test bed is aligned, completed, and ready for exploitation. It saw first light in the visible in 2020 and the near-infrared in summer 2022 (Martinez et al., 2022b). In the coming years we plan to (1) support and validate the high-level primary objectives defined in

our top-level requirements, (2) initiate an upgrade programme of the bench towards a more representative environment of the ELT, including for instance an XAO residual turbulence generator using phase screens or a spatial light modulator, (3) make the bench available to the community as a representative environment with unique capabilities for testing hardware and algorithms given the PCS instrument. Ultimately, this laboratory experience will help refine computational models, leading to performance and tolerance predictions for future instrument architectures.

Acknowledgements

The activities outlined in this paper are partially funded by the European Union as part of the FEDER program, by the French government, and by the Region Alpes Côte d'Azur. The project also benefits from funding support from the French national space agency (CNES), the University of Côte D'Azur (UCA), Côte d'Azur Observatory (OCA), and Lagrange Laboratory. We thank the director of the Lagrange Laboratory, Philippe Stee, for his constant support of the project.

References

- Beaulieu, M. et al. 2017, MNRAS, 469, 218
- Beaulieu, M. et al. 2020, MNRAS, 498, 3914
- Blind, N. et al. 2022, Proc. SPIE, 12185, 1218573
- Boccaletti, A. et al. 2020, arXiv:2003.05714
- Codona, J. L. et al. 2013, Opt. Eng., 52, 097105
- Guyon, O. et al. 2014, ApJ, 780, 171
- Janin-Potiron, P. et al. 2016, A&A, 592, A110
- Kasper, M. et al. 2021, The Messenger, 182, 38
- Krist, J. E. et al. 2007, Proc. SPIE, 6675, 66750P
- Lozi, J. et al. 2018, Proc. SPIE, 10703, 1070359
- Males, J. R. et al. 2018, Proc. SPIE, 10703, 1070309
- Martinez, P. 2019, A&A, 629, L10
- Martinez, P. et al. 2022a, Proc. SPIE, 12184, 121843W
- Martinez, P. et al. 2022b, Proc. SPIE, 12184, 121843Y
- Mawet, D. et al. 2018, Proc. SPIE, 10703, 1070306
- Vigan, A. et al. 2018, Proc. SPIE 10702, 1070236

Links

- ¹ Website of the community of adaptive optics and high-contrast test-beds: <https://sites.google.com/view/highcontrastlabs/home?authuser=0>
- ² SPEED project website: <https://lagrange.oca.eu/en/lag-speed-home>

Effects of the Hunga Tonga–Hunga Ha‘apai Volcanic Eruption on Observations at Paranal Observatory

Robert J. De Rosa¹
 Angel Otarola¹
 Thomas Szeifert¹
 Jonathan Smoker^{1,2}
 Fernando Selman¹
 Andrea Mehner¹
 Fuyan Bian¹
 Elyar Sedaghati¹
 Julia Victoria Seidel¹
 Alain Smette¹
 Willem-Jan de Wit¹

¹ ESO

² UK Astronomy Technology Centre,
 Royal Observatory, Edinburgh, UK

The Hunga Tonga–Hunga Ha‘apai volcano erupted on 15 January 2022 with an energy equivalent to around 61 megatons of TNT. The explosion was bigger than any other volcanic eruption so far in the 21st century. Huge quantities of particles, including dust and water vapour, were released into the atmosphere. We present the results of a preliminary study of the effects of the explosion on observations taken at Paranal Observatory using a range of instruments. These effects were not immediately transitory in nature, and a year later stunning sunsets are still being seen at Paranal.

Introduction

Many astronomers were likely unaware of the impact of volcanic eruptions on astronomical observations when the Hunga Tonga–Hunga Ha‘apai (HTHH) volcano erupted in January 2022. The release of sulphur dioxide (SO₂) by such eruptions can have a significant effect on the atmospheric transmission and on Earth’s

climate. When injected into the stratosphere, SO₂ is transformed into sulphuric acid (H₂SO₄) by the photochemical effect in the presence of water vapour. While Earth’s surface effectively cools because the Sun’s short wavelength radiation is scattered by the sulphate aerosols in the stratosphere, heat radiation from Earth’s surface is efficiently absorbed by the same particles, resulting in an altered weather pattern and climate. The sulphate aerosol particles in the stratosphere circulate globally and are only removed by precipitation on timescales of several years.

In terms of the energy released, the world’s biggest volcanic incident in the past 1300 years was the eruption of Mount Tambora, in what is now Indonesia, in April 1815. In addition to the immediate and direct destruction, a huge dust cloud entered the stratosphere, which disrupted weather systems in 1816 and for the following three years in the northern hemisphere. The year 1816 was the second-coldest year on record since the Middle Ages and is known as the ‘year without a summer’. The change in climate was followed by famine, disease, poverty and civil unrest, with many social and political consequences (D’Arcy Wood, 2014; Behringer, 2019). The years after the Tambora eruption also sparked the imaginations of artists (for example Mary Shelley’s Frankenstein, the dark poetry of Lord Byron, paintings by J. M. W. Turner and Caspar David Friedrich, and music by Beethoven and Schubert)^{1,2}. Interestingly, the link between climate change in

the 1810s and the volcanic eruption of Tambora was not recognised at the time. This connection was only realised after the eruption of the Krakatoa in Indonesia in 1883 (Royal Society, 1888), at a time when news could be quickly reported via telegraphy across the world.

The eruption of the Hunga Tonga–Hunga Ha‘apai volcano

The submarine HTHH volcano in the South Pacific erupted violently on 15 January 2022. An ash plume shot 57 km into the mesosphere, shockwaves rippled through the atmosphere, and the eruption triggered a tsunami with heights of more than 19 m above sea level³, causing massive infrastructure destruction on the nearby islands and the death of four people in Tonga and two in Peru. The energetic output from the volcano has been estimated to be approximately 61 megatons of TNT equivalent (Diaz & Rigby, 2022). Ocean floor maps showed that the volcano spewed out at least 9.5 km³ of material in total⁴. By comparison, the 1815 eruption of Tambora in Indonesia ejected more than 100 km³ of erupted material, the 1883 eruption of Krakatoa in Indonesia 25 km³, the 1991 eruption at Mount Pinatubo in the Philippines 5.5 km³, and the CE 79 eruption of Mount Vesuvius 4 km³. In the case of HTHH, 1.9 km³ of material ended up in the atmosphere, which caused the stunning sunsets observed from Paranal following the eruption.

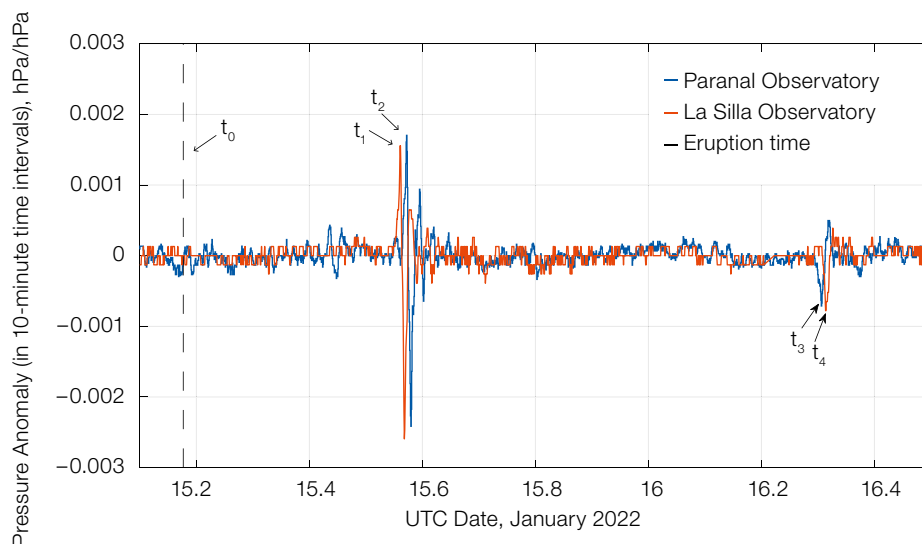


Figure 1. Atmospheric pressure anomaly. Observations on Paranal and La Silla of the pressure wave caused by the HTHH volcanic eruption. The indicated time stamps are: t_0 = eruption moment (2022-01-15 04:14:45 UT), t_1 = arrival of the front edge of the pressure wave at La Silla Observatory (2022-01-15 13:28:42 UT), t_2 = arrival of the front edge of the pressure wave at Paranal Observatory (2022-01-15 13:43:49 UT), t_3 = arrival of the far edge of the pressure wave at Paranal Observatory (2022-01-16 07:45:32 UT), t_4 = arrival of the far edge of the pressure wave at La Silla Observatory (2022-01-16 07:20:13 UT).

Conclusions drawn in the work of Legras et al. (2022) and references therein describe the following picture that characterises the event: a) the eruption was intense with a large injection of water vapour into the stratosphere; b) the zonal atmospheric circulation spread the plume across all longitudes in less than one month; c) after six months the plume, mainly sulphates and water vapour, had spread in the 35°S–20°N latitude range, in two plumes separated in latitude; d) satellite observations of the plume in the optical and millimetre spectral bands and the observed sedimentation rate seem to show the sulphate aerosol particles reached a size of about 1.0 and 1.4 μm in diameter. The size evolution of the particles has been explained by hygroscopic growth during the first phase (up to about April), followed by coagulation (in the period April–May) and then decay by evaporation in the later stage which is dominated by evaporation as a result of dry air and a more diluted plume.

Detection of the atmospheric shockwave at La Silla and Paranal Observatories

The shockwave from the eruption was detected at various weather stations around the world (Harrison, 2022). Figure 1 shows the pressure anomaly caused by the shockwave passing over both Paranal and La Silla in Chile, a distance exceeding 10 000 km from the eruption. From the geodetic distances between the volcano site and the ESO observatories, and the elapsed times for the arrival of the atmospheric pressure wavefronts we were able to compute the average speed of the pressure wave to be approximately 307 m s^{-1} . Moreover, the ESO weather stations show both the arrival of the front edge and the far edge of the pressure wave. The front edge is the part of the shockwave that propagated from the location of the volcano towards the East in the direction of Chile. The far edge is the part of the shockwave that propagated in the opposite direction, around the planet, before reaching the observatory sites. The amplitude of the pressure anomaly for the far-edge wave is down to 30% of that of the front-edge wave, an indication of the loss of energy as the shockwave propagated away from the main event.

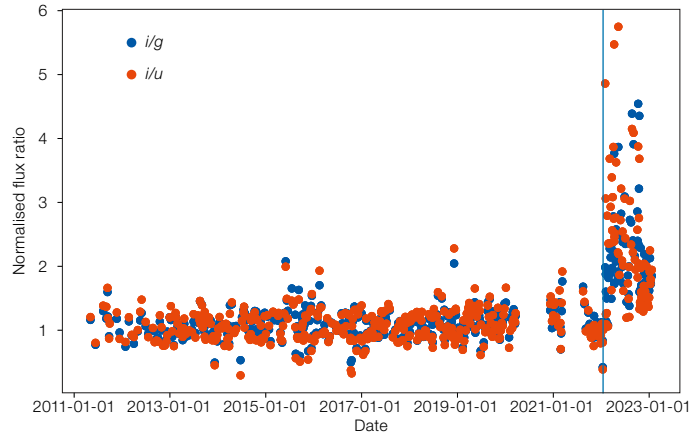


Figure 2. Flux ratio for *i/g* (blue symbols) and *i/u* (red symbols) sky flatfields taken with OmegaCAM at the VLT Survey Telescope as a function of time. Observations in the different bands were taken simultaneously with the mosaic filter and are normalised to the pre-explosion ratio. The vertical line indicates the date of the volcanic eruption.

Effects on Paranal

Sky flatfields

Particles of volcanic dust in the atmosphere can cause spectacular sunsets, which have been captured in paintings, for example by the artists J. M. W. Turner and Caspar David Friedrich, after the Tambora eruption in 1815. Following the eruption of the HTHH volcano, there was some awareness of this effect on Paranal, because of publications of several post-eruption standard-star observations on La Silla (Rufener, 1986a,b; Grothues & Goehermann, 1992; Burki et al., 1995a,b). In the aftermath of the HTHH eruption, the colour of the Paranal sunset was very different from what we were used to seeing in the previous years.

During normal operations at Paranal, sky flatfields are taken on a regular basis to calibrate scientific data and to monitor the instrument health. Figure 2 shows the normalised flux ratio against time for optical flatfields taken at twilight using the segmented filter of the OmegaCAM camera at the Very Large Telescope (VLT) Survey Telescope, where images are taken simultaneously with the *ugri* SDSS filters. A few days after the volcanic eruption, the ratio of the *i* (770 nm) and both the *u* (350 nm) and *g* (480 nm) flatfields increased by a factor of five, indicating a significant reddening of the twilight sky, and these have still not returned to the pre-explosion values one year later. These measurements are consistent with perceived changes of the colour of sunsets seen at Paranal. Dome flatfields obtained with the same filters do not

show any change in the flux ratio, indicating that the observed effect is atmospheric and not instrumental.

A similar effect was seen in the sky flats taken with the VIRCAM camera at the Visible and Infrared Survey Telescope for Astronomy (VISTA) where the ratio of the K_s (2146 nm) to Y (1021 nm) twilight flats increased after the explosion. A sudden change in the decay time of the twilight was also observed in near-infrared data from the HAWK-I instrument at the VLT. Figure 3 shows the count rate during twilight with the K_s filter as a function of the elevation of the Sun, before and after the volcanic eruption.

Model of the observed changes in the HAWK-I twilight sky brightness

The change in the decay time of the sky brightness in the HAWK-I twilight flatfields can be explained by a 36-km-high column of dust in the line of site of the telescope, which became the dominant source of reflection rather than the molecular gas in the troposphere before the eruption. The decay of the reflected light observed in the twilight sky flats can be explained by the rising of the Earth shadow, as illustrated in Figure 4, where the Rayleigh scattering region is shown in blue, and the stratospheric layer with the red circle. Twilight ends when the Earth shadow reaches the upper boundary of the stratospheric layer of dust. From this, the height of the volcanic dust plume can be estimated as 36 km in March 2022 compared to the 57-km height of the dust dome above the volcano immediately

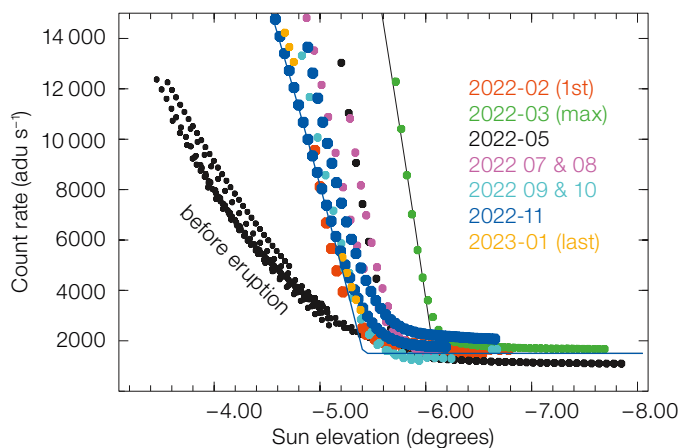


Figure 3. Decay of the twilight flux in near-infrared light (K_s) observed with HAWK-I as a function of the elevation of the Sun below the horizon. The green line is a model for March 2022, which estimates a column height of the volcanic dust plume of 36 km. The blue line indicates a model for November 2022, which estimates a height of 29 km and 0.6 times less reflected light per meter of illuminated column height.

after outburst (Proud, Prata & Schmauß, 2022). In observations obtained in November 2022, the flatter twilight flat-field decay time indicates a decreasing density of the dust in the stratosphere and a reduction in the height of the dust layer down to 29 km, indicated by the later onset of the infrared twilight and illustrated in Figure 3.

Atmospheric extinction and zero points

The atmospheric extinction is an important parameter for photometric measurements. Besides seasonal and other long-term variations, significant increases of the extinction coefficients can be caused by major volcanic eruptions that inject large amounts of aerosols into the stratosphere at altitudes between 20 and 30 km. These aerosols are distributed over wide areas of Earth’s atmosphere by jetstreams and can influence astronomical observations at great distances (for example, Moreno & Stock, 1964; Rufener, 1986a,b; Grothues & Gochermann, 1992; Burki et al., 1995a,b).

Long-term variations of the extinction caused by the volcanic eruptions of El Chichón in Mexico in 1982 and the Pinatubo eruption in the Philippines in 1991 were observed extensively at La Silla (Rufener, 1986a,b; Grothues & Gochermann, 1992; Burki et al., 1995a,b). The stratospheric load due to the eruption of El Chichón was estimated to be about 8 megatons of SO_2 and the Pinatubo eruption emitted about 20 megatons of SO_2 into the atmosphere. The increase of the extinction in both events

was very sudden — roughly 150 days (El Chichón) and 100 days (Pinatubo) after the eruptions. The removal of the volcanic aerosols from the atmosphere lasted at least 1000 days. Aerosols from different volcanoes are very different; for example, Pinatubo produced a flatter extinction curve than El Chichón.

To search for the possible effect of the aerosols injected into the upper atmosphere by the eruption of the HTHH volcano, we analysed the extinction measurements obtained from the observation of standard stars utilising the FORS2 imager at the VLT on Paranal. Data from the wide-field imager OmegaCAM were also included in the analysis, although in this case we do not measure the atmospheric extinction, assuming instead a constant value. Hence, a variation in extinction is observed as a change in zero point which we monitor for each detector and filter; an increase in atmospheric extinction should appear as a reduction in the zero point of similar magnitude.

The corrected extinction data for four FORS2 filters and only for stable night transparency conditions are plotted in Figure 5. They were obtained as a part of the QC1 quality control process⁵ following the method developed for the FORS Absolute Photometry project⁶, as described by Freudling et al. (2007). The data, for filters b_{HIGH} (440 nm), v_{HIGH} (557 nm), R_{SPECIAL} (655 nm) and I_{Bessel} (768 nm), cover the period from 1 January 2021 until the end of December 2022. The date of the eruption is shown with a vertical line. The increase in extinction

that could be attributed to an increase in aerosol content in the stratosphere (at 25–27 km altitude) from the volcano is not significant compared to the seasonal variability in the sky extinction. The seasonal variability is due to the change in the atmospheric absolute humidity and barely visible cirrus condition induced by the altiplanic winter. The OmegaCAM data show an analogous seasonal variability.

Water vapour

The HTHH explosion released substantial amounts of water vapour into the stratosphere (Millán et al., 2022; Legras et al., 2022). The work of Legras et al. (2022), with data from the satellite-borne Microwave Limb Sounder (MLS) instrument, shows the eruption of the volcano injected a plume of water vapour of up to 25 ppmv concentration in the layer between 20 and 30 km above sea level. This is five times more than the background water vapour level at that altitude for the tropical latitude of the Paranal Observatory.

At the time of the volcanic eruption, two water vapour radiometers were in operation at Paranal (LHATPRO; Kerber et al., 2012). Unfortunately, the increase in water vapour at such high altitudes is not detectable at ground level using the LHATPRO. This is because the water vapour emission in the stratosphere gets attenuated by absorption along the long

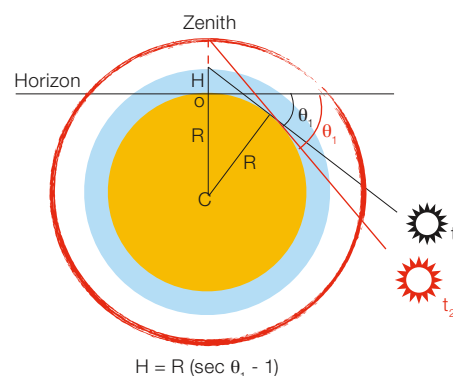
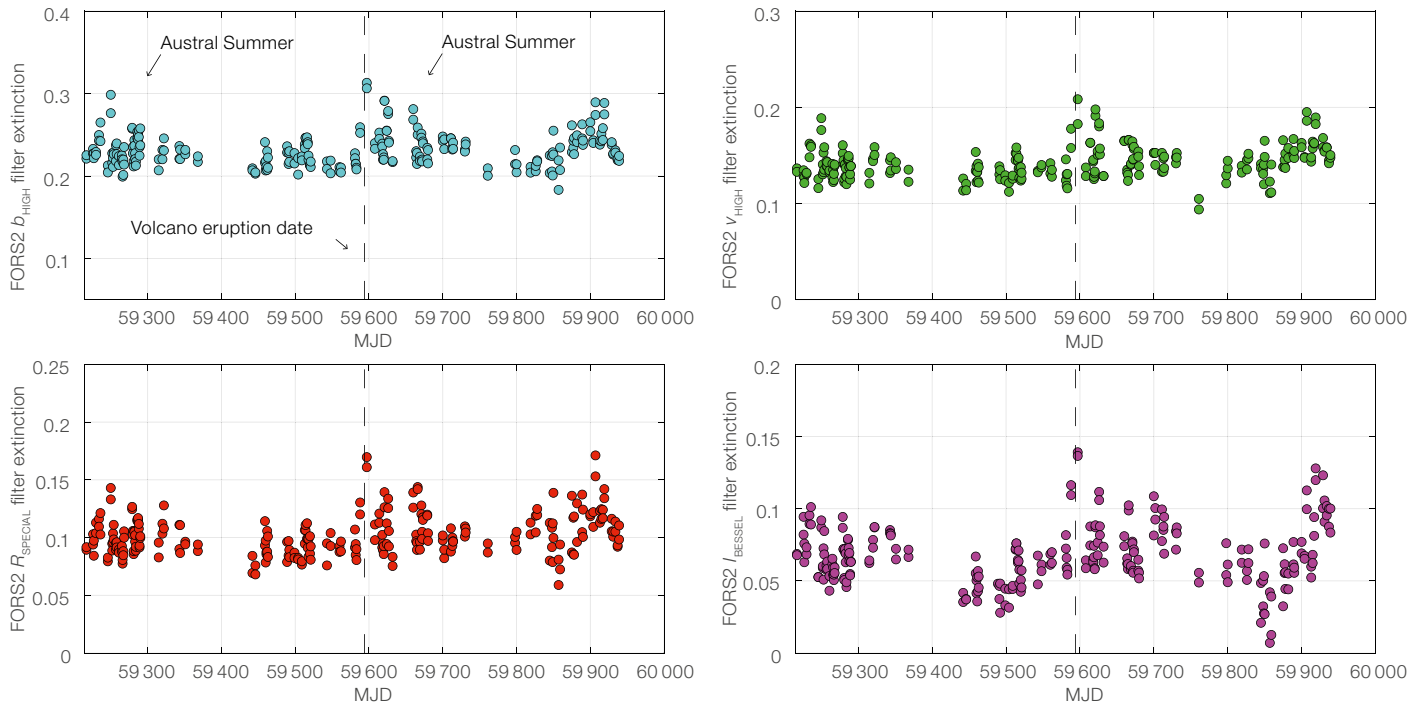


Figure 4. Schematic diagram (not to scale) of our model to explain the sky brightness variations during twilight caused by scattering from aerosols at different altitudes within the stratosphere. The Sun at time t_2 only illuminates the higher regions in the stratosphere when observing the zenith from position O.



path to the LHATPRO detector on Earth's surface. We computed the atmospheric brightness temperature using the atmospheric model *am* (Paine, 2022) and find that a change in brightness temperature at the peak of the 183 GHz water vapour line induced by a 25 ppmv water vapour layer, with respect to the background condition, is only around 0.07%, corresponding to a change of 0.04% in precipitable water vapour, which is well below the daily temporal variability of water vapour at Paranal.

Conclusions

The HTHH volcanic eruption had several observable effects at Paranal Observatory, located more than 10 000 km away from the eruption site. These included measurements of the shockwave and a striking change in the colour of the sky visible in routine calibration sky flats taken during twilight at optical and infrared wavelengths. The detection of variations in the extinction, observed via standard star observations, is harder to assess since the volcanic eruption took place during the austral summer. This is a period when we observe a natural variability and increase of the atmospheric extinction owing to an increase in humidity

and barely visible cirrus, induced by the altiplanic winter atmospheric condition. The detection of the increase in water vapour, injected by the volcano in the stratospheric level, was not possible because of the low sensitivity of our water vapour radiometers to emission from such a high altitude. A more detailed analysis of the data is ongoing to determine the composition of the aerosols and to monitor the longer-term effects of the explosion on astronomical observations. Given the intensity of the eruption and the large amount of water vapour injected in the stratosphere, it is believed the effects will last for several years.

References

- Behringer, W. 2019, *Tambora and the Year without a Summer: How a Volcano Plunged the World into Crisis* (Medford, MA: Polity Press)
- Burki, G. et al. 1995a, *The Messenger*, 80, 34
- Burki, G. et al. 1995b, *A&AS*, 112, 383
- D'Arcy Wood, G. 2014, *Tambora: The Eruption That Changed the World* (Princeton: Princeton University Press)
- Diaz, J. S. & Rigby, S. E. 2022, *Shock Waves*, 32, 553
- Freudling, W. et al. 2007, *The Messenger*, 128, 13
- Grothues, H.-G. & Gochermann, J. 1992, *The Messenger*, 68, 43
- Harrison, G. 2022, *Weather*, 77, 87
- Kerber, F. et al. 2012, *Proc. SPIE*, 8446, 84463N
- Legras, B. et al. 2022, *Atmos. Chem. Phys.*, 22, 14957
- Millán, L. et al. 2022, *Geophys. Res. Lett.*, 49, 99381
- Moreno, H. & Stock, J. 1964, *PASP*, 76, 55

Figure 5. FORS2 extinction time series⁵ between 1 January 2021 and 30 December 2022. The vertical line in each subplot shows the date of the eruption. (top-left) b_{HIGH} filter, (top-right) v_{HIGH} filter, (bottom-left) R_{SPECIAL} filter, (bottom-right) I_{BESSEL} filter.

- Proud, S. R., Prata, A. T. & Schmauß, S. 2022, *Science*, 378, 554
- Royal Society 1888, *The Eruption of Krakatoa: And Subsequent Phenomena* (London, Trübner & Company)
- Rufener, F. 1986a, *The Messenger*, 44, 32
- Rufener, F. 1986b, *A&A*, 165, 275
- Paine, S. 2022, *The am atmospheric model (v. 12.2)*, <https://doi.org/10.5281/zenodo.6774376>

Links

- Ian Ritchie's website: <https://www.ianritchie.org/the-year-without-a-summer>
- The Guardian website: <https://www.theguardian.com/music/2016/jun/16/1816-year-without-summer-dark-masterpieces-beethoven-schubert-shelley>
- The BBC website: <https://www.bbc.com/news/science-environment-61567521>
- National Institute of Water and Atmospheric Research website: <https://niwa.co.nz/news/tonga-eruption-confirmed-as-largest-ever-recorded>
- FORS2 QC1 processed zeropoint and extinction data: http://archive.eso.org/qc1/qc1.cgi?action=qc1_browse_table&table=fors2_photometry
- See the section FORS2 *Absolute Photometry Project* at <https://www.eso.org/sci/facilities/paranal/instruments/fors/doc.html>

The IC4701 nebula is part of a rich and vast complex of dust and gas within which new stars spring to life. When stars are born, most of them are cooler, redder, and less massive than our own Sun. Hotter, more massive stars are much rarer, and they quickly burn through all their fuel and die. This makes these brilliant blue and massive stars, and their surrounding glowing gas, beacons of recent star formation.

The First Results of Distributed Peer Review at ESO Show Promising Outcomes

Tereza Jerabkova¹
 Ferdinando Patat¹
 Francesca Primas¹
 Dario Dorigo¹
 Fabio Sogni¹
 Lucas Astolfi¹
 Thomas Bierwirth¹
 Michael Prümm¹

¹ ESO

The European Southern Observatory (ESO) implemented a new paradigm called Distributed Peer Review (DPR) as part of its proposal evaluation process in Period 110. Under DPR, Principal Investigators who submit proposals agree to review a certain number of proposals submitted by their peers and accept that their own proposal(s) are reviewed by their peers who have also submitted proposals in the same cycle. This article presents a brief overview of the DPR process at ESO, and its outcomes based on data from periods 110 and 111.

DPR introduction and ESO DPR P110 and P111 overview

The Distributed Peer Review (DPR) paradigm should be seen not only as an innovative concept, but above all as a natural consequence of the increased number of proposals requiring review. Different opinions on whether the expert panel review model needed revision have been put forward more than once since its inception a couple of centuries back. However, the recently increased numbers of applications for observing time made this issue more pressing and challenging for all large astronomical facilities and their time allocation processes. To keep logistical aspects manageable and, at the same time, to ensure a high-quality proposal evaluation, peer review by standard expert panels has become a less and less viable option, calling for suitable and sustainable alternatives.

The DPR concept was first introduced and formalised by Merrifield & Saari (2009). The general idea underlying it is that submitted proposals are not reviewed by pre-selected expert panels

but rather by fellow PIs who have also applied for observing time, hence actually staying true to the very concept of peer review, in which the applicants and the referees are at the same level. Gemini Observatory pioneered the adoption of DPR for telescope time allocation in their Fast Turnaround channel in 2015 (Andersen, 2020). DPR was first considered at ESO following a report by the Time Allocation Working Group (Patat, 2018), which turned into a successful DPR experiment that was conducted on a voluntary basis alongside the panel review (Patat et al., 2019). DPR was deployed for ALMA time allocation in 2021 for Cycle 8 (Meyer et al., 2022), followed by ESO in 2022 for Period 110. In this article we present a statistical analysis of the first two semesters.

In P110 and P111 proposals requesting more than 16 hours of observing time and special programmes (for example, Targets of Opportunity, Calibration Proposals, and joint XMM-Newton proposals) were evaluated by expert panels and approved by the Observing Programmes Committee (OPC). The 16-hour limit was chosen to produce a balanced distribution between DPR and panels, effectively reducing the load on the panels by a factor of two, while leaving about 80% of the time under their control. The threshold value was defined in the Call for Proposals for the corresponding period, and it might be adjusted in future. The DPR channel evaluated 435 proposals distributed to 379 reviewers in P110 and 417 proposals with 362 reviewers in P111.

The DPR scheme was set up so that PIs (or delegated PIs) submitting proposals that qualified for DPR had to agree — at time of submission — to evaluate 10 proposals per submitted (DPR) proposal. They also had the option of selecting one of the proposal co-Is as the delegated DPR reviewer. Failing to do this by the set deadline would result in the automatic rejection of their proposal/s. This guaranteed that each proposal received 10 independent grades (from 1 to 5) and comments.

Expertise evaluation and proposal assignment

An important aspect of any peer review process is the set of criteria that are used

to assign proposals to the reviewers. The ESO DPR in P110 and P111 aimed for expert peer review in which proposals were assigned to reviewers with expertise as close as possible to the science case of the proposals. Thus, the expertise level for each proposal-reviewer pair needed to be evaluated and the assignment algorithm was then responsible for an optimal proposal distribution that maximised the match overall.

Reviewer-proposal expertise score

The Phase 1 tool (P1)¹ introduced by Primas et al. (2019) has revolutionised the way proposals are submitted to ESO. In order to submit a proposal, users must have a User Portal account, where they must provide information about their career stage, affiliation, and scientific expertise through keywords. These keywords are grouped into classes such as Cosmology, Galaxies and Galactic Nuclei, Interstellar Medium, Star Formation and Planetary Systems, and Stellar Evolution. Each proposal submitted through the P1 tool must include a subset of these keywords that describe the proposal's science scope (up to five and a minimum of three).

In each case, the keywords are specified by the applicant in decreasing order of relevance. This information is then used to compose a knowledge vector for each proposal and each reviewer. For each reviewer-proposal pair, it is then possible to compute the scalar product of their respective knowledge vectors, resulting in what we will refer to as the match score. In other words, the match score is a figure of merit describing how parallel the two vectors are. The match scores range from 0 (no match), through 1 (match within a science category), to 2 (perfect full match). This information provides essential input for the assignment process and is used to ensure that proposals are assigned in a controlled way to the most qualified reviewers.

Proposal-reviewer matching

The proposal assignment is a thorough and methodical process that takes into account various factors to ensure the best possible match between proposals

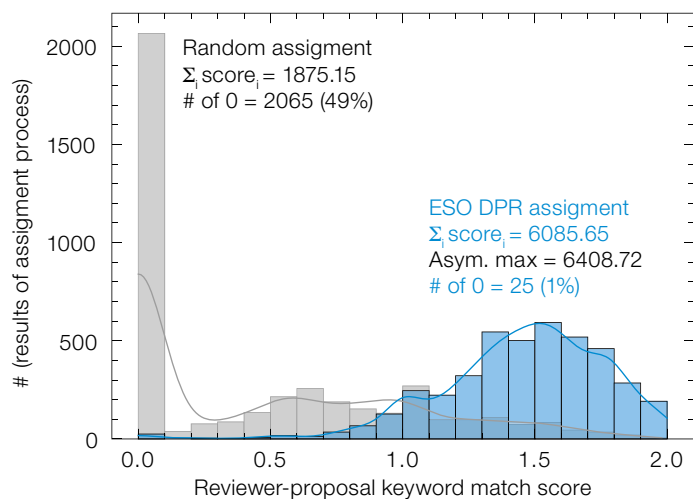


Figure 1. Example proposal assignment outcome in P111 (P110 provides quantitatively the same figure). The horizontal axis shows the match score, and the vertical axis shows the number of proposals assigned in each score bin. The blue histogram shows the assignment produced by the proposal_distributor. In grey, we show a random assignment that is representative of the overall score distribution.

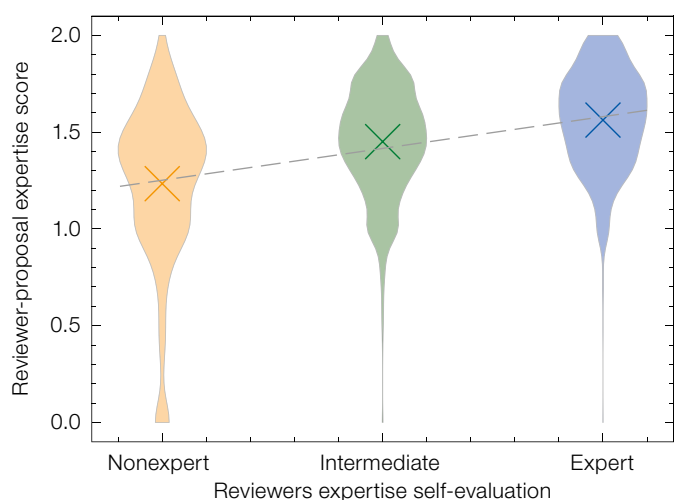


Figure 2. The reviewer-proposal match score calculated based on specified keywords compared to reviewers' expertise self-evaluation.

and reviewers. One of the key factors considered is the match score of each proposal-reviewer pair introduced above. To ensure fairness and consistency, ESO has specific rules for assigning proposals. For example, each reviewer is assigned a set number of proposals based on the number of submissions, and each proposal is assigned to a set number of reviewers. In addition, possible conflicts between reviewers, such as those arising from team or institute membership, are also considered, to avoid any potential bias. To manage the assignment process, ESO uses a java web-based tool called `proposal_distributor`, which employs an algorithm developed in-house to sort proposals based on their assignability. Proposals with the smallest pool of possible reviewers are given priority above the proposals with a larger number

of available experts. Reviewers are then assigned to proposals based on their expertise scores and the prior sorting. This process is repeated until all the assignment rules and constraints are met. The tool is designed to be efficient and transparent and ensures the best match between proposals and reviewers.

Figure 1 shows the proposal assignment outcome in blue. The shape of the distribution peaks towards high scores, showing the effectiveness of the assignment algorithm. This can be compared to the distribution of all scores, that is, the raw input for the assignment algorithm. For this we have plotted in grey a random assignment for the same number of proposals/referees. One straightforward way of quantifying the quality of the overall assignment outcome is to sum all their

match scores. A higher number means a better assignment in terms of expertise, while a null score means there are no common keywords for the reviewer-proposal pair. The final score value for the `proposal_distributor` is more than three times larger than in the case of the random assignment. Another comparison to gauge the performance of the matching algorithm can be made with the best distribution one can have with the available set of reviewers and proposals. To this end, for a given distribution of scores, one can construct a hypothetical asymptotic assignment which maximises the final score. This ideal proposal distribution takes the ten best assignments for each proposal, excluding conflicts, but ignoring the boundary constraint that each reviewer can have only 10 proposals to assess. This therefore represents an asymptotic, practically unachievable, upper limit for the match. The asymptotic score is a factor of 3.4 larger than the random assignment outcome and only a factor of 1.05 larger when compared to the `proposal_distributor`.

P110 und P111 summary

The DPR process in P110 and P111 ran smoothly, no technical issues were reported, and all reviewers delivered their evaluations on time. The final grade distribution was carefully analysed, showing that the DPR reviewers behaved statistically as panel members prior to the discussion phase. In addition, we did not detect any statistically significant systematic effects related to seniority or career stage. To produce the final proposal ranking list the DPR grades were normalised to have the same mean value and standard deviation as the grades awarded by the panels, adopting the same procedure in place for aligning the outcomes of individual panels.

Match scores and reviewers' self-evaluation

As discussed in the previous section, the match scores are a crucial ingredient of the DPR process. In the current system, we rely fully on the users and their input keywords, as specified in the ESO User Portal profiles and in the submitted pro-

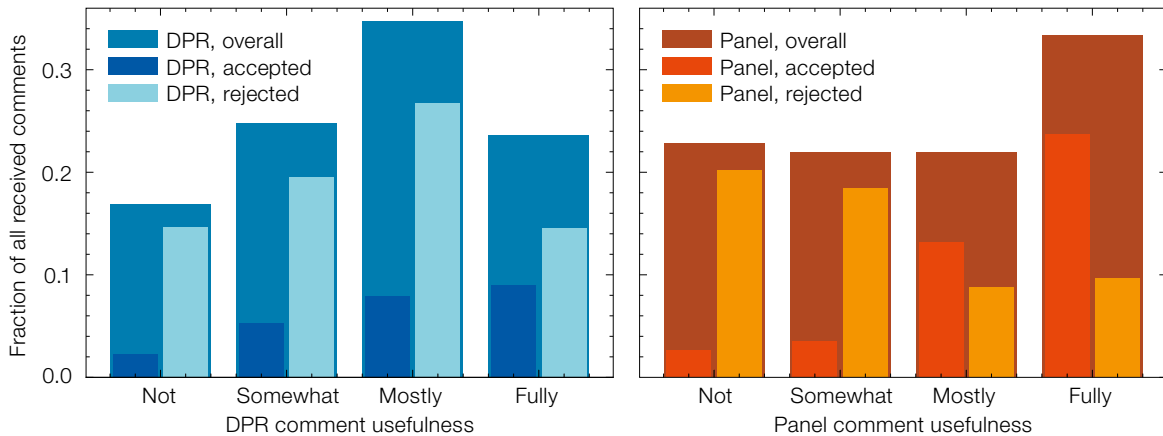


Figure 3. The comment usefulness as declared by PIs/dPIs in Period 110 for DPR (left) and panels (right).

posals. To monitor the performance of the algorithm, the DPR proposal evaluation interface requires each reviewer to express their self-evaluated expertise level (non-expert, intermediate, expert) for each proposal assigned to them. Figure 2 shows a comparison between the reviewer-proposal match score and the self-evaluated expertise level. For each self-evaluated expertise value, the match score distribution is plotted, with its mean value denoted by a cross. There is an overall trend, indicated by a dashed line fitted to the mean values, showing a positive correlation between the two indicators. Typically, low match scores are consistently evaluated as 'non-expert' by the users. However, several users categorised themselves as 'non-expert' while their match score was as high as 2, thus indicating a perfect keyword match (the same keywords specified in exactly the same order). These cases can have several possible explanations, such as incorrectly assigned keywords (either in the User Profile or in the proposal), keywords that were too broad, or subjective bias. In the data collected in P110, we noticed that early-career scientists were less likely to claim to be an expert, even in their own field. On the other hand, senior scientists, such as professors and staff astronomers, were more likely to claim to be an expert even in a field that is far from their declared expertise.

Feedback on the reviewers' proposal comments

In addition to grading proposals, both in DPR and panels, the reviewers are

responsible for providing useful feedback to the PIs. This feedback should clearly point out the strengths and weaknesses of the proposal and provide indications for improving it when applicable. For the first time in P110, we invited ESO PIs/dPIs to evaluate the usefulness of the received comments, on a voluntary basis. The PIs' response rate was the same for both the expert panels and DPR: around 30% provided their evaluation of the feedback they received. This fraction is not very satisfactory, and measures to increase it in future semesters are under discussion. However, the data already allow some basic analysis.

Figure 3 shows the distribution of the collected responses for DPR (left) and panels (right). These first results indicate a higher level of satisfaction for DPR. This becomes even more evident when looking only at the rejected proposals, which are arguably the most relevant cases for this specific aspect. While in the case of the panels most of the comments are judged as 'not' or 'somewhat' useful, an opposite trend is seen in the case of DPR. When considering this result, one must emphasise that the panels produce one single joint comment for each proposal, emerging from the discussion at the meeting, while in the case of DPR, each reviewer writes an independent evaluation, which is passed directly and unedited to the PI. Thus, in the case of DPR the feedback on the proposals captures more information, which is the likely explanation for the observed trend.

Summary and future prospects

DPR was deployed smoothly at ESO in periods P110 and P111, and the outcome is statistically comparable to that of the expert panels. The user feedback on the usefulness of the comments received by the PIs clearly favours DPR. In this respect, it is worth noticing that the decreasing level of user satisfaction with the feedback provided by the panels was one of the most quantitative drivers for considering DPR as a possible alternative to the classical paradigm. It is reassuring to see that DPR has improved this situation. At the same time, the data seem to indicate that, following the introduction of DPR, the level of satisfaction with the panels' feedback has increased, a beneficial result of the significant decrease in the number of proposals reviewed by each panel member.

As recommended by ESO's Scientific and Technical Committee, we will keep the same setup for P112 and P113, to collect more information under the same homogeneous conditions. Nevertheless, we are planning to further monitor and improve the process and to keep presenting our findings in order to remain as transparent as possible. More complex assignment algorithms are being tested (for example, Faez, Dickerson & Fuge, 2017; Stelmakh, Shah & Singh, 2018) and we are working on improving reviewer and proposal profiling via machine learning approaches (Patat et al., 2019; Kerzendorf et al., 2020). We are also looking into ways of increasing the rate of feedback return from the PIs, in order to have a larger statistical basis for future analyses.

As part of the development process, we organised the conference Peer-Review Under Review, held at ESO's Headquarters in Garching, Germany, on 6–10 February 2023, the outcome of which will be presented in a future Messenger article. The idea was to bring together not only the astronomers, but also representatives of the wider scientific community, in order to start a discussion about peer-review processes in general, and to identify ways to cope with a continuously growing scientific community and the appearance of intriguing new technologies.

Back in 1973, in his science fiction novel *Rendezvous with Rama*, Arthur C. Clarke wrote prophetically about an expert panel evaluating a proposal for a space mission: “Even by the twenty-second century, no way had yet been discovered of keeping

elderly and conservative scientists from occupying crucial administrative positions. Indeed, it was doubted if the problem ever would be solved.” The promising outcome of the deployment of DPR at ALMA and ESO indicates that this may indeed be one viable and valid alternative to the standard expert panel review process. For once, we might be ahead of science fiction.

Acknowledgements

The authors are grateful to ESO's Director General and Director for Science and to Markus Kissler-Patig for supporting this enterprise, which represents the most significant change in the proposal evaluation process at ESO since it was established. The support and the positive attitude shown by the Scientific Technical Committee, the Users Committee and the Observing Programmes Committee are also acknowledged. We would like to acknowledge the valuable assistance of OpenAI's language model, ChatGPT.

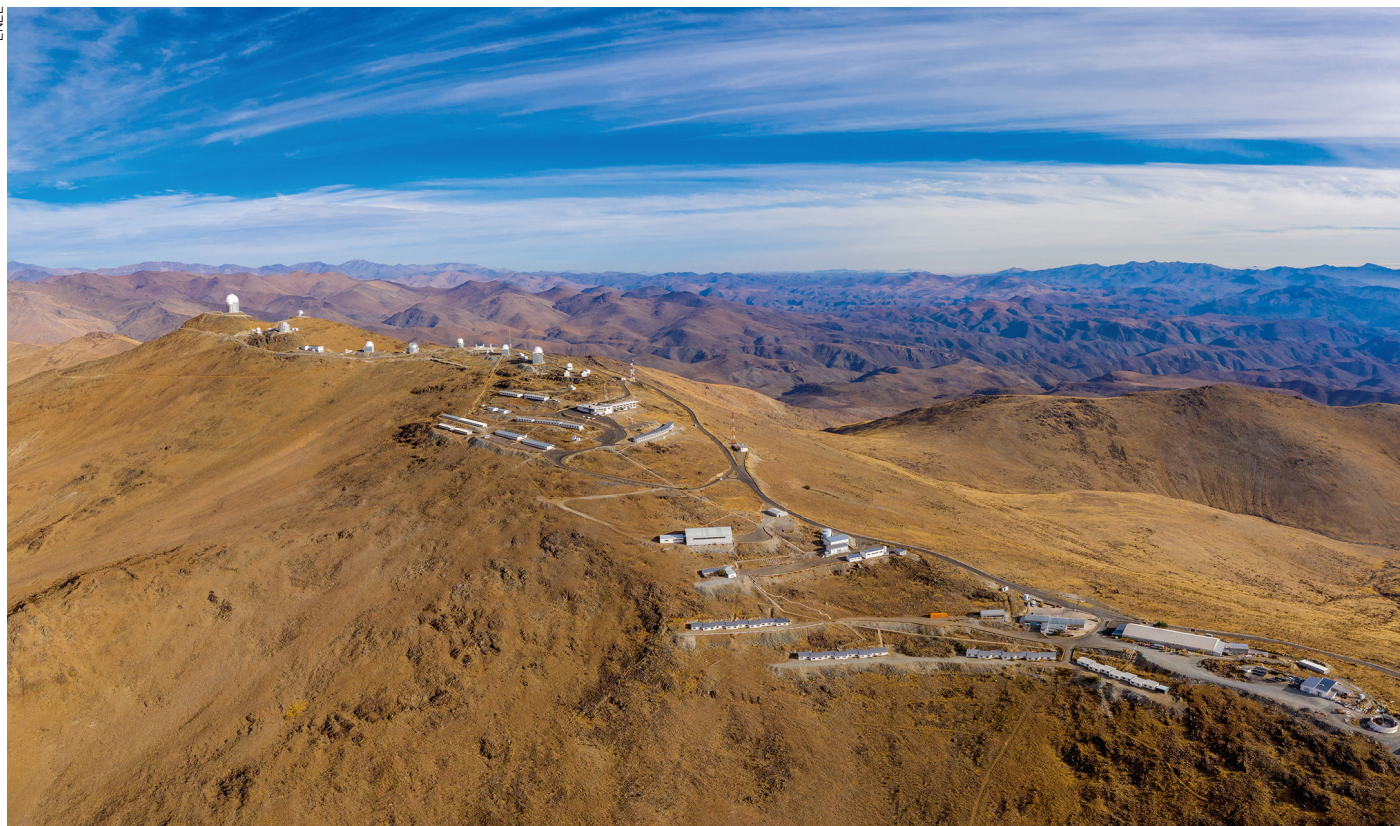
References

- Andersen, M. 2020, *Nature Astronomy*, 4, 646
 Faez, A., Dickerson, J. P. & Fuge, M. 2017, *Proceedings of the Twenty-Sixth International Joint Conference on Artificial Intelligence*, 35
 Kerzendorf, W. E. et al. 2020, *Nature Astronomy*, 4, 711
 Merrifield, M. R. & Saari, D. G. 2009, *A&G*, 50, 4.16
 Meyer, J. D. et al. 2022, *Bull. Am. Ast. Soc.*, in press
 Patat, F. 2018, *The Messenger*, 173, 7
 Patat, F. et al. 2019, *The Messenger*, 177, 3
 Primas, F. et al. 2019, *The Messenger*, 176, 41
 Stelmakh, I., Shah, N. B. & Singh, A. 2018, arXiv:1806.06237

Links

- ¹ The ESO P1 tool: <https://www.eso.org/sci/observing/phase1/p1intro.html>

ENEL



Located on the outskirts of the Chilean Atacama Desert, 600 km north of Santiago and at an altitude of 2400 metres, this seemingly tiny village in the

middle of a desert is in fact ESO's first observatory, La Silla Observatory.

Report on the IAU Hands-on Workshop

The VLTI High angular resolution Observations Workshop

held at ESO Vitacura, Santiago, Chile, 10–21 October 2022

Claudia Paladini¹
Konrad R. W. Tristram¹
Itziar de Gregorio-Monsalvo¹

¹ ESO

As part of the International Astronomical Union's Hands-On Workshops (I-HOW) initiative, ESO Chile organised the first international Very Large Telescope Interferometer (VLTI) workshop in Vitacura. The main goal was to train young scientists from Latin American countries in accessing, analysing and using VLTI archival data for their research projects. Through a series of lectures on interferometry and instrumentation, science, and soft skills, followed by practical hands-on sessions, the attendees were given the tools they needed to start using VLTI data for their own research. The workshop provided the perfect environment in which to build a network between VLTI specialists and future users and it furnished a great experience for all the participants, students, teachers and organisers alike.

The highest angular resolutions at optical and infrared wavelengths are reached not by large single-dish telescopes but by combining the light of multiple telescopes using long-baseline interferometry. With this technique, angular resolutions of milliarcseconds and below, as well as differential astrometry at tens of microarcseconds accuracy can be reached. Such high angular resolutions are required to study and understand various astrophysical objects and phenomena. Optical and infrared interferometry has thus provided fundamental contributions to different fields of astrophysics, ranging from the characterisation of planets to our understanding of the lives of stars, as well as the investigation of supermassive black holes and their surroundings.

Nevertheless, optical and infrared interferometry is not as widely used as it could be and it is often considered a complex observing technique to be employed only by specialists. To counter this perception and make the technique available to a wider community, special schools have been organised to train the



community in this observing technique, predominantly in Europe in the form of so-called Very Large Telescope Interferometer (VLTI) schools (for example, Garcia, 2009; Millour et al., 2021). The VLTI is the state-of-the-art infrared interferometer built and operated by the European Southern Observatory (ESO). With its second-generation instruments (PIONIER, GRAVITY, and MATISSE) and now undergoing an upgrade to extend its capabilities to faint sources (i.e., many more scientific topics and targets), the VLTI will play a key role in the era of ESO's Extremely Large Telescope and beyond. At the same time the VLTI has a vast unexplored science archive that calls for data mining, considering that a significant fraction of the publicly available archival data have not yet been published — a true treasure chest to be opened.

Enabling early-career astronomers from Latin America to use this archival data for their science was the main goal of the VLTI-HOW¹ (The VLTI High angular resolution Observations Workshop) held at ESO's Vitacura offices in Santiago, Chile between 10 and 21 October 2022. The workshop was the first of a new series of workshops hosted by the International Astronomical Union (IAU), the IAU Hands-On Workshops² (I-HOW). This IAU initiative aims to train young scientists in developing countries to access, analyse and use archival data for their

Figure 1. Workshop participants during lectures in the first week of the workshop.

research projects. The workshop was funded roughly half by ESO, and half by the Gordon and Betty Moore Foundation³ through the IAU. The school covered the board, lodging and social activities of the participants from outside Santiago for the duration of the school and provided support for travel expenses when needed. Participation in the school was in person, given the importance of the interaction between lecturers and students, not only during the lectures themselves but also informally during breaks, meals and other social activities.

Demographics

About 70 applications were received and from these a total of 37 students were selected based on academic and scientific merit. The number of students was limited to ensure a ratio of about three to five students per lecturer, especially during the hands-on activities. The countries represented by the participants were Chile (19, with 12 from Santiago and 7 from the regions), Brazil (4), Mexico (7), Argentina (2), Guatemala (1), Bolivia (1) and Colombia (3). Eight students were undergraduates, 23 postgraduates and four postdoc; one was a bachelor's student and one a senior researcher.



Figure 2. Workshop photo with all participants.

18 students identified themselves as female, 17 as male, and 2 as non-binary. Most of the students had no previous knowledge of interferometry. Despite the workshop's being in person, all the lectures were broadcast in real time via Teams and about 10 additional students joined the workshop lectures online.

Programme

The first week of the workshop was dedicated to lectures introducing the students to the basics of optical and infrared interferometry, the VLTI instruments, and the many tools commonly used for VLTI observation preparation and data reduction. Additionally, various scientific lectures were given covering different research areas where optical and infrared interferometry has made significant contributions, such as exoplanets, active galactic nuclei, massive young stellar objects, protoplanetary discs, stellar evolution, evolved massive stars and fundamental stellar parameters. The lectures were organised in two parts: first a general introduction to the scientific topic understandable by everyone, and then specific lectures presenting VLTI results on the given scientific topic. Several professors from Latin America were invited to give the general introductions, while the VLTI lectures were given by expert

interferometrists in the respective fields. In this way, the knowledge was also spread to more senior colleagues, and collaborations were fostered. The setup was very successful as some of the professors decided to stay on during the second week and join the practical sessions themselves. This enabled them to help the students with the scientific interpretation of the data.

The second week was dedicated to practical hands-on sessions. The students were divided into groups according to their scientific interests. Each team had a VLTI expert available to work with them as tutor during the entire week. On Monday, the students were assigned a scientific target observed with a specific VLTI instrument; they were shown how to browse the archive and how to download their data set, how to obtain and install the respective data reduction pipeline, and how to reduce the data. On Tuesday, they used the tools presented during the first week for model-fitting. Wednesday was dedicated to image reconstruction; the students attended a tutorial and then received a special data set suitable for image reconstruction. At the end of the day each group made a five-minute presentation of their results. On Thursday they continued working on their initial data set, finished any pending tasks, and prepared their final presentation which was given on Friday in front of the whole school. Students, lecturers and ESO

colleagues joined to listen to the various presentations.

The programme was organised to leave enough time for networking and for in-person interactions between students and lecturers during coffee breaks, lunches, and other activities: a welcome reception on the first day, a barbecue on the first Friday, an excursion on Saturday, and a wine and cheese reception on Wednesday of the second week. Several short talks during the first week were dedicated to soft-skills development such as unconscious bias, scientific writing, job hunting, career development, job applications and interviews, among others. Since the workshop was held at the ESO offices in Santiago and the telescopes were too far away to visit, a live connection with Paranal was hosted on Thursday of the second week. The students were shown the control room and could observe in real time during twilight. Calibrator observations were prepared by some students, and some volunteers reduced the data in real time. Moreover, during the second week the last hour of the day was dedicated to presenting various scientific profiles working at an observatory: the operator, the engineer working on the instruments, the astronomer. Special attention was paid to selecting the speakers so as to maintain the gender balance and also include women from Latin America to act as role models for the students.

The lecturers and tutors were highly impressed by the professionalism and commitment of the students. When polled after the workshop, the students were very satisfied with the quality of the lectures and the practice sessions. The hardest part for them was the data reduction, which also suffered from some hiccups with the network and the computer setups. But these issues were overcome and as a benefit many students returned with the relevant software packages and pipelines installed on their own hardware, ready to use for their own science after returning to their institutes.

The lecture presentations are being archived on the Zenodo open-access repository⁴. The I-HOW initiative will keep in touch with participants over the years,

forming a network of I-HOW alumni, to track their careers and offer possible follow-up activities. In conclusion, we are confident that the workshop reached its goal of providing the students with the skills and tools needed to explore and use archival VLTI data for their science. At the same time, the workshop has successfully contributed to the growth of the participants as scientists and provided room for networking, thus paving the way for (future) collaborations.

Acknowledgements

The organisers are grateful for the funding from ESO and the Gordon and Betty Moore Foundation through the IAU, without which the workshop would not have been possible. We are also very thankful for the support of the Jean-Marie Mariotti Centre⁵; their experience in carrying out VLTI-schools, and their tools

supporting the VLTI community over the years have been crucial for the success of the workshop. Finally, we thank our colleagues from the Chilean Astronomical Society (SOCHIAS) and ESO for their enthusiasm and support.

References

Garcia, P. 2009, *The Messenger*, 135, 50
Millour, F. et al. 2021, *The Messenger*, 185, 28

Links

- ¹ VLTI-HOW website: <https://www.eso.org/sci/meetings/2022/VLTI-How.html>
- ² IAU Hands-On Workshops: <https://www.iau.org/training/iau-hands-on-workshops/>
- ³ Gordon and Betty Moore Foundation: <https://www.moore.org/>
- ⁴ Presentations on Zenodo: <https://zenodo.org/communities/vltihow2022/>
- ⁵ Jean-Marie Mariotti Centre: <https://www.jmmc.fr/>



This picture shows a beautiful meeting between the Swedish-ESO Submillimetre Telescope (SEST) and the Milky Way, apparently almost touching each

other. This shot was taken at ESO's La Silla Observatory, located on the outskirts of the Chilean Atacama Desert, at an altitude of 2400 metres.

Fellows at ESO

Gabriela Calistro Rivera

Inspiring educational events and good science teachers can have a transformational impact on students' lives, and my story in astronomy is one of those examples.

One visit to a beautiful planetarium show ignited a spark, and thanks to a good physics teacher the spark turned into a passion. I come from Peru, one of the countries with the most beautiful and clearest skies in the world. However, socioeconomic limitations mean that opportunities to learn about the cosmos, like the ones I had abroad, are not broadly accessible. Working towards changing this, in addition to understanding how galaxies and black holes form and grow across cosmic history, are the goals of my work.

I was born in Huacho, a small fishermen's city a few hours away from Lima, the capital of Peru. At the age of seven, I moved to Lima, a large, vibrant and somewhat chaotic metropolis of around 10 million people. My parents, always prioritising high-quality education, sent me to the Peruvian–German school, where I was educated within a bilingual system with Peruvian and German teachers. In those years, my father, who had studied engineering, sometimes shared with me stories about the enigmatic physical phenomena he had heard of, such as black holes and special relativity. These stories awoke my curiosity about the cosmos from early on, although only in the background, as in most school years I was mainly interested in literature and arts.

In high school I visited Germany for the first time as an exchange student. During a weekend trip to Hamburg, I attended my first planetarium show. It was a show on the Hubble Deep Extragalactic Fields. This show left me in awe about the depth and richness of space, and the power of telescopes. At that point, I could have not imagined that those same images would be my work material one day. Motivated by this experience, once back at home I started paying more attention to physics classes and this was timely aligned with having a great physics teacher that year. In addition to lots of hands-on activities, the teacher motivated and reinforced my curiosity with extracurricular material,

introducing me to the first science magazines I read (*Spektrum der Wissenschaft*) and Physics TV shows (*Alpha Centauri*). Graduating from the German Abitur with a special interest in astrophysics, I then decided to study physics.

Since there is no astrophysics major in Peru, and physics research is extremely limited and well below the Latin American average, right after high school I left my country and moved to Germany to pursue my bachelor's degree in physics. This was possible thanks to a full scholarship from the German Academic Exchange Service (DAAD), given to high-school students selected among German schools from 120 different countries. The international environment I experienced in these meetings for the first time made me particularly fond of cultural diversity, which I cherish and have always looked for in my life. This is also one aspect I love about astronomy. In my career I have always worked in international institutes and, funnily, I now have an international family as well. My little Italian–Peruvian son born in Germany has just turned one year old.

I feel privileged to have worked in some of the main European hubs for astronomy during my career. Before coming to ESO, I did my bachelor studies in the University of Heidelberg, with a thesis project on cosmology at the Institute of Theoretical Astrophysics. For my master's, still in Heidelberg, I joined the Max Planck Institute for Astronomy to work this time on extragalactic observations. To expand the wavelength coverage of my work to the submillimetre and radio for my PhD, I moved to Leiden Observatory in the Netherlands. My PhD thesis focused on the panchromatic emission of star-forming galaxies and active galactic nuclei. As a student, I was able to participate in observing runs at La Silla and La Palma, and to give invited and contributed talks on my research at numerous conferences and institutions across the world.

One of these conferences, the Latin American Regional IAU Meeting in Colombia, was very special, as for the first time I met other Peruvian astronomers. Until this point in my career, I had not met colleagues from my own country, since we are not many and were all trained abroad. With these colleagues we



commented extensively on the large disadvantages that young people in our country are facing in terms of scientific education and the limited access to such an inspiring science as astronomy. These conversations made me realise that it was up to us, the very few national astronomers, to do something to change this situation. With this idea in mind, I started efforts to build up a network of Peruvian astronomers and have a better overview of the community. In 2018 the survey showed that there were around 25 Peruvian astronomers spread across the globe, including PhD students, post-docs and professors.

A few weeks before graduating with my PhD, I got the offer of an ESO Fellowship, one of the dream jobs I had been aspiring to since early in my career. I then spent the free months I had before the start of my appointment at ESO designing the CosmoAmautas programme, a programme which uses astronomy to support equitable scientific education in Peru. Finding like-minded Peruvian colleagues, we applied for an IAU Grant from the Office of Astronomy for Development. Three years after its conceptualisation, CosmoAmautas has now trained 120 teachers from half of the rural regions in Peru and opened 20 Astronomy Clubs in rural high schools. The combined results of this initiative have reached more than 7000 high-school students, in addition to mentoring as well undergraduate physics students, now doing their master's in Europe and the US.

ESO has been a great support to all my professional and personal goals. In addition to supporting my research work with a vibrant scientific atmosphere and collaborations, it has also given me the flexibility to dedicate some of my time to scientific education programmes, as part of the ESO Science Outreach Ambassadors that I co-organise. Additionally, as a fellow and huge fan and user of the ALMA Observatory, working as part of the ALMA Regional Center developing software to mine the ALMA archive and visiting the telescope have been incredible experiences. Astronomy is a unique and fascinating endeavour as it combines inspiring existential questions at its core, with exciting intellectual exercises and beautiful images in the day-to-day work. Additionally, it has the inspirational power to be used as a tool to pursue meaningful social change and improve overall scientific education, which I feel is an ideal complement to my research work. I thus feel very fortunate to be an astronomer and spend these years at ESO.

Michele Ginolfi

My younger self would have never imagined that one day I would travel around the world to discuss science with my colleagues and talk at international conferences, observe breathtaking night skies from the Atacama desert, or drive huge cars up to 5000 metres on the road to ALMA. But he dreamt of an adventurous life, and, well, an astronomer's life turns out to be quite adventurous. Come on, let's say it, among all scientists, we are what gets closest to James Bond; "A Martini, stirred not shaken", asks the astronomer at the bar.

But how did I become an astronomer?

You would expect the standard "Since I was a kid, I loved wondering about stars" or "I got inspired by that amazing book by Stephen Hawking". No, nothing like that. Mine was a rational choice, fully driven by Curiosity (note that I will be using a capital letter as if Curiosity was a person, a friend). I went to a high school that was very oriented towards classical and humanities studies. It was great. I loved studying literature, history, philosophy, and arts. But at the same time, I realised

that there was a whole portion of the world that I knew too little about. And I was curious about it. So at the time of choosing a university path, I thought I should go for science, trying to expand my comfort zone and broaden my vision of the world. Thus, physics looked like the most natural and stimulating choice, and now I can say that it was the best possible choice as I immediately fell in love with it. In particular, the branch of physics that fascinated me the most was astronomy, because of its unique property of containing a bit of everything else (for example, statistical and quantum mechanics, general relativity, thermodynamics, etc). Moreover, I love the fact that as an astronomer I am used to studying everyday natural phenomena that involve mechanisms working on extremely different scales (by many many orders of magnitude) in space, time, mass, etc. This helps me a lot in improving the way in which I look at the world.

After a BSc in physics and an MSc in astrophysics in Rome, I decided that becoming an astronomer would be a good way to satisfy Curiosity, and I started my PhD in Astronomy, Astrophysics and Space Science in Rome. I did a thesis on "The Baryon Cycle driving Galaxy

Evolution" under the supervision of Raffaella Schneider. Raffaella had the intuition that I would find my dimension by working with both theory and observations. I did not hesitate one second when she proposed that I explore the properties of the interstellar medium in local and distant galaxies by combining analyses of cosmological simulations with multi-wavelength observations. I spent part of my PhD at the University of Cambridge, working in Roberto Maiolino's group on ALMA data of molecular gas in distant galaxies, and MUSE observations of atomic gas surrounding bright quasars. Cambridge was magic. I could breathe science in the corridors of the astronomy buildings and at the same time enjoy the life of a graduate student in a vibrant city full of scholars.

After my PhD, towards the end of 2018, I moved to Geneva (Switzerland) to work as a postdoctoral researcher in the Astronomy Department at the University of Geneva, in Daniel Schaerer's group. I had the chance to work with amazing people. Interacting with them day by day, learning from them, and getting inspired by them, made me a better scientist and a better person. I consider the years spent in Geneva fundamental for my early



development as a scientist. In Geneva, I had the opportunity to work in the ALPINE collaboration, an ALMA large programme that observed the cold interstellar medium in more than a hundred galaxies at redshifts between four and six. ALPINE is a great team, and we have produced several important results. I arrived at ESO in November 2020. I wanted to become an independent scientist and the ESO Fellowship looked perfect. Now, after two years spent at ESO, I can confirm that the ESO Fellowship is the ideal position for young scientists to strengthen their scientific/human skills and improve as independent researchers, thanks to a rare combination of (i) proactive world-top scientific environment and (ii) the possibility of being involved in the functioning and the design of some among the most powerful current and future telescopes. What I like most about ESO is the privileged opportunity to see with my own eyes the full process beyond astronomical observations, starting from how they are conceived, up to how they are taken and distributed.

At ESO, I have been working on galactic feedback in distant galaxies and its impact on the chemical enrichment of the circumgalactic medium. For my functional work, I decided to split my duties into observations with APEX, and assistance in the development of a future exposure time calculator for ESO's Extremely Large Telescope. I learned so many things thanks to my functional duties! When I had the chance to travel several times to Chile to observe with APEX from Atacama, a dream came true. In those magnificent places, together with amazing colleagues, I lived moments that I will never forget and that remind me every day what beautiful work we do.

In November 2022 I started a new adventure in the beautiful city of Florence, where I will teach physics, astronomy, and data science at the university, and will continue my research on galaxy evolution.

I will do my best to share with students the beauty of understanding how the Universe works.

Julia Victoria Seidel

My journey to ESO can certainly be called the unconventional path within physics. If you look for the inspirational story of a small child with their first telescope, you will be sorely disappointed. But I hope it shows that astronomy has a vast reach and that your path does not have to be pre-determined at a certain age or career stage, but is in the end a rich canvas of serendipitous events meeting an open mind.

My personal journey starts in school in rural Germany, as the ever-curious — read annoying — student with a million questions and with every subject as 'my personal favourite'. I loved it all, biology, art, French, everything. But physics always held a special place. That intersection of the real world that can be explained with the hidden underlying language of maths seemed like magic to school-aged Julia. So much to my father's disappointment that I wasn't going to pursue the arts and my mother's utter shock, I decided that physics was my calling. More specifically, that particle physics and understanding what holds the world together was to be my way in life.

After two years of rigorous education in maths and physics in Germany, I decided that my life had become too confined and I switched to Paris to finish my bachelor's. In retrospect, this was the best decision I have ever taken. Suddenly I was part of a vibrant international research community in a city I fell in love with at first sight. It was that year that set me up for a job at CERN as a programmer soon after. While I loved my experience at CERN and the first cautious steps in the real-world job market, I soon realised that I was not done yet with education and that nuclear physics was confined to important, but few, open questions.

With that change in interest came a round of applications to various institutes worldwide for a master's position, with plenty of rejections. I had almost resigned myself to moving back to Germany to further my education when I got a place at Imperial College. So off I was to London. Little did I know just how expensive the city was and just at the dawn of Brexit my



supervisor came to me with the offer of a lifetime. Would I like to pursue a project on atmospheric physics for my thesis in Colombia? I don't think I can overstate just how elated I was. In that year in Bogota, I traced atmospheric dynamics above the rainforest to track explosions, learned Spanish, and saw more of life than I had in the previous 25 years. Two things became clear to me that year. I wanted to dedicate my life to understanding the climate and I wanted to live in South America again.

So, how did I end up in astronomy of all fields? Opportunity disguised itself as an outreach event while I was visiting friends in Switzerland. The topic: exoplanet atmospheres. And a year later I started my PhD on tracing atmospheric dynamics in exoplanet atmospheres, hoping to add my own piece of the puzzle of Earth's uniqueness in the Universe.

While in Geneva in David Ehrenreich's group, I got much more than I bargained for. What started out as the academic pursuit of understanding our atmosphere in the wider context of planetary studies soon became a fascination with astronomy as a whole. Geneva is one of the European instrumental powerhouses, involved in spectrograph design since the days of CORALIE all the way to ESO's

flagship high-resolution spectrograph ESPRESSO at the VLT in Paranal. As part of my PhD, I was sent to observe with the Swiss Euler telescope in La Silla in northern Chile and the first glimpse I got of the real night sky is something I will never forget. In the end, it was astronomy that led me to love the stars instead of the night sky leading me to astronomy. At the same time, I realised that astronomy is the gateway to STEM for the general public. This ambassadorial role in science communication is something I take very seriously, especially in the subfield of exoplanet studies. We are the bridge between climate science and sceptics to truly drive the most important message home: there is no Planet B.

Now, at ESO, all the different parts I loved most during the past years have come together: the night sky, studying our own atmosphere and exoplanets, a strong commitment to science education, and my personal love for South America.

I love working at an observatory — this bimodal world of extreme pressure observing and fixing problems on the fly to glimpse singular events in the sky but also experiencing the absolute silence and peace of the desert under the vast night sky is unlike any other job. I work with UT1 and UT2 of the VLT in Paranal and focus my work on the ESPRESSO spectrograph, the workhorse for my own science. In that context, I work with a mix of scientists, engineers, and operators, and not a day goes by when I don't learn something new.

I don't know what the future will hold, but I will always remember my time as a fellow as one of the big highlights of my career. I hope my path will somehow always link me to observatories, be it as an astronomer, a climate scientist, or a science communicator — opportunities present themselves to those welcoming them!

Michael Abdul-Masih

For me, astronomy was never part of 'the plan'. Growing up, I had always been interested in astronomy, but I never thought of it as a potential career option. Sure, being an astronaut would be super cool, but what kid doesn't want to be an astronaut

at some point? In my head, I always thought of astronomy in the same way that I thought of reading or playing video games: a hobby that I enjoyed in my free time, but not something that I would ever do professionally. It wasn't until the end of my bachelor's degree that I began to see astronomy as more than just a hobby.

From a young age my parents stoked my interest in space. My mom was an avid space fan and when she saw that I was also interested in it, she made sure that there were plenty of space-related activities for me to enjoy. I have fond memories of our family trip to Huntsville, Alabama where we spent a week at the US Space and Rocket Center attending space camp. But perhaps my favorite astronomy-related memory from childhood was setting up our hammock in the front yard so that we could watch the historic 2002 Leonid meteor shower in the early hours of the morning with a thermos full of hot chocolate to keep us warm.

Fast forward a few years to the end of high school; 'the plan' was in motion: I was going to be a medical doctor. I had just been accepted at Villanova University and it was time for me to choose what I would be studying for the next four years. There sitting at the top of the list of potential majors was Astronomy & Astrophysics. I distinctly remember the jolt of excitement when I saw that, but, alas, cooler minds

prevailed and I ended up selecting biochemistry as my major as it made much more sense for someone who was planning on attending medical school later. Nevertheless the thought of being able to take some astronomy classes remained at the back of my mind all summer.

By the time August rolled around, I had decided that I would see if I could take some astronomy classes to fill my elective slots. During my first week at Villanova, when we were selecting our classes for the semester, I went to speak with the head of the Astronomy Department to inquire about taking classes and by the end of the meeting I was signed up for my first astronomy class. I absolutely loved it! So much so, in fact, that I ended up taking another two classes the next semester and another one the following semester.

I couldn't get enough! It was around this time that I made my first big purchase with the money that I had been making from working at the ice cream shop on campus: an Orion Skyquest 8-inch Dobsonian telescope. I dragged all of my friends out at night to show them the moons of Jupiter, the rings of Saturn, the Orion Nebula, etc. It was also around this time that I had taken enough classes to have completed the astronomy minor. Instead of feeling proud of my accomplishment, I remember feeling incredibly sad at the thought of being finished with my astronomy journey.

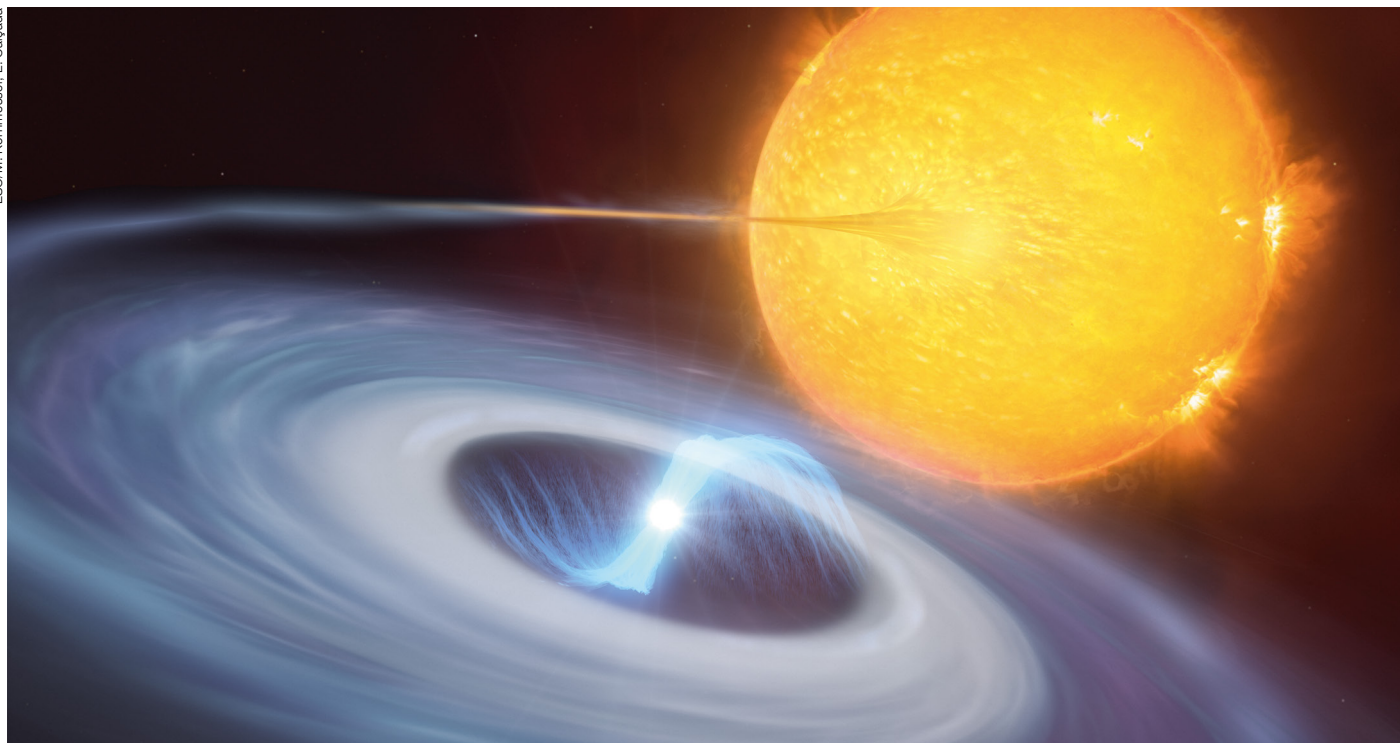


After quite a bit of moping, I decided I wasn't done and I that I would see if it was possible to continue. I spoke with the heads of both the Astronomy and Biochemistry departments and after a bit of finagling, I managed to come up with a schedule that would allow me to finish both the biochemistry major and an astronomy major on time. The day that I submitted the form to officially declare the astronomy major was one of the happiest of my life. The rest is history. During the final year of my bachelor's, I decided that I would try to continue in astronomy and applied for a few master's programmes. I was accepted at Rensselaer Polytechnic Institute and started in September and graduated with my master's a year and a half later. From there, I accepted a PhD position at KU Leuven, where I spent the next four years. I defended my thesis in 2020 and now I can say that I am officially a doctor, albeit a different doctor than I originally planned!

As with my life plan, my interests in astronomy have evolved quite a bit over the years. During my bachelor's, I was primarily interested in astrobiology and how life on other planets might look, bridging my interests in biochemistry and astronomy. By the time I was applying for my master's, I was more interested in planetary science and the detection of exoplanets. During my master's, however, I worked with eclipsing binaries and realised that I really enjoyed stellar astronomy. Continuing in that direction, my PhD focused on a particularly interesting class of eclipsing binaries known as overcontact binaries. The stars in these systems are so close to each other that they are actually touching and sharing material, making them roughly peanut shaped. Recently, my interests have broadened a bit and I have begun working on other classes of non-spherical stars such as rapidly rotating stars and semi-detached binaries.

Working at ESO has been a dream come true. When showing my friends the moons of Jupiter through my 8-inch telescope, I never imagined that 10 years later, I would get to point a telescope 40 times bigger at those same moons. I feel truly lucky to have the opportunity to work at one of the largest and most advanced observatories in the world. Being able to meet world-leading experts from around the world, getting to interact with new cutting edge instruments, and seeing how a world-class observatory operates behind the scenes has been an eye-opening experience. On a more personal level, working at ESO has only enhanced my love for astronomy and the night sky. I am still an avid stargazer and the night sky on a Moonless night at Paranal is unrivalled. From time to time, I will grab a mug of hot chocolate and go out to the platform in the hopes of catching a meteor or two. The only thing missing is a hammock.

ESO/M. Kornmesser, L. Calçada



This artist's impression shows a two-star system where micronovae may occur. The blue disc swirling around the bright white dwarf in the centre of the image is made up of material, mostly hydrogen, stolen from its companion star. Towards the centre of

the disc, the white dwarf uses its strong magnetic fields to funnel the hydrogen towards its poles. As the material falls on the hot surface of the star, it triggers a micronova explosion, contained by the magnetic fields at one of the white dwarf's poles.

Spectral Fidelity

Celebrating the HARPS spectrograph's 20 years
of operation, and its PI, Michel Mayor

ESO–INAF–UNIGE Joint Conference

4–8 September 2023
Firenze, Italy

<https://www.eso.org/sci/meetings/2023/fidelity.html>
spectralfidelity@eso.org

Scientific Organising Committee

Valentina D'Odorico
José Renan de Medeiros
Gayandhi De Silva
Debra Fischer
Matias Jones
Gaspare Lo Curto
Luca Pasquini (Co-Chair)
Francesco Pepe (Co-Chair)

Céline Peroux
Sofia Randich (Co-Chair)
Rafael Rebolo
Nicoletta Sanna
Nuno Santos
Rodolfo Smiljanic
Caroline Soubiran

Local Organising Committee

Patrizia Braschi
Francesco Guarneri
Louise Nielsen
Nicoletta Sanna
Rossella Spiga
Chantal Taçoy
Denisa Tako



INAF
ISTITUTO NAZIONALE
DI ASTROFISICA



PlanetS

ESO Conference, Garching, Germany
16–20 October 2023



A Decade of ESO Wide-field Imaging Surveys

Scientific Legacies and Benchmarks for Future Facilities

<https://www.eso.org/sci/meetings/2023/surveys.html>
surveys23@eso.org

Abstract deadline: 1 May 2023
Registration deadline: 1 September 2023

Scientific Organising Committee

Magda Arnaboldi (ESO)
Federica Bianco (University of Delaware)
María-Rosa Cioni (Leibniz-Institut für Astrophysik Potsdam)
Nick Cross (WFAU, Royal Observatory, Edinburgh)
Janet Drew (UCL, London)
Jim Dunlop (Institute for Astronomy, Edinburgh)
Annette Ferguson (Institute for Astronomy, Edinburgh)
Boris Häußler (co-chair, ESO)
Enrichetta Iodice (Astronomical Observatory of Capodimonte, Naples)
Konrad Kuijken (Universiteit Leiden)
Dante Minniti (Universidad Andrés Bello, Santiago)
Monika Petr-Gotzens (co-chair, ESO)

Local Organising Committee

Boris Häußler (ESO)
Maren Hempel (Universidad Andrés Bello, Santiago)
Michael Hilker (ESO)
Valentin Ivanov (chair, ESO)
Alonso Luna (ESO)
Monika Petr-Gotzens (ESO)
Emanuela Pompei (ESO)
Zdenek Prudil (ESO)
Marina Rejkuba (ESO)
Denisa Tako (ESO)

Images from top to bottom: VISTA image of the Fornax galaxy cluster, Credit: ESO/J. Emerson/VISTA. Acknowledgment: Cambridge Astronomical Survey Unit; The Helix Nebula in visible light, Credit: ESO; The Helix Nebula in infrared, Credit: ESO/VISTA/J. Emerson. Acknowledgment: Cambridge Astronomical Survey Unit; VST image of the Fornax galaxy cluster, Credit: ESO. Acknowledgment: Anello Grado and Luca Limatola